UNIVERSITÀ
DI SIENA
1240

UNIVERSITY OF SIENA

DEPARTMENT OF MEDICAL BIOTECHNOLOGIES

PhD COURSE IN MEDICAL BIOTECHNOLOGIES

COORDINATOR: PROF. LORENZO LEONCINI

XXXIV CYCLE

Mobile genetic elements carrying stress response systems, antibiotic resistance determinants, and catabolic pathways

Supervisor:

Prof. Gianni Pozzi

Co-supervisors:

Prof. Francesco Iannelli

Dr. Francesco Santoro

PhD candidate:

Valeria Fox

Academic year 2020–2021

Table of contents

Abstract

In the present thesis, I studied the activation of an SOS-like response in *Streptococcus pneumoniae* encoded by the *Streptococcus pyogenes* prophage φ1207.3. This system leads to the temporary activation of an hypermutable phenotype, which resulted in increased survival and increased mutation rate upon exposure to mitomycin C or UV-C light. Then, a different type of stress response, the Envelope Stress Response (ESR), was exploited as a strategy for sensitization of *Escherichia coli* to several antibiotics, by disbalancing five pathways, namely σ^E, Cpx, Rcs, Bae, and Psp. Disbalancing the Psp pathway increased *E. coli* susceptibility to some beta-lactam antibiotics. Prophage φ1207.3, carrying a two-genes macrolide efflux system, was originally described as an Integrative and Conjugative Element (ICE). In this thesis, φ1207.3 was transferred to the standard pneumococcal laboratory strain Rx1, for which the whole genome sequence was obtained. It was demonstrated that φ1207.3 is a functional phage of the Siphoviridae family, able to form mature phage particles. It was shown that φ1207.3 does not enter the lytic cycle, even upon induction with mitomycin C. Since φ1207.3 transfers through a mechanism requiring cell-to-cell contact resembling conjugation, the cellular localization of φ1207.3 was investigated. It was demonstrated that the number of φ1207.3 phage particles on the bacterial cells exceeds the number of phages in the culture supernatant by 3 orders of magnitude. φ1207.3 transfer to a variety of streptococcal species was obtained by setting up a mating protocol for the transfer of large mobile genetic elements. Tn*5253* is a composite ICE of *Streptococcus pneumoniae* carrying two elements: i) the ICE Tn*5251,* carrying the *tet*(M) tetracycline resistance gene, and ii) the Ωcat(pC194) not-conjugative element, harbouring the *cat* chloramphenicol resistance gene and able of intracellular transposition. The Tn*5253* chromosomal integration site (*att*B) was investigated in *S. pneumoniae* with different backgrounds and in other streptococcal and enterococcal species. Finally, during the sequencing of two *Mycobacterium chimaera* strains, it was reported the presence of an ICE carrying putative genes involved in the catabolic degradation of polycyclic aromatic hydrocarbons, important environmental pollutants.

CHAPTER 1 - General Introduction

1. Role of mobile genetic elements in shaping bacterial genome

Until the first half of the 20th century, genomes have been thought to be stable and fixed structures slowly evolving only due to mutations occurring randomly but at steady frequencies. It was with Barbara McClintock, and her experiments on maize, that the first evidence of the instability of genomes was provided, leading to the discovery of mobile genetic elements (MGEs), for which she was awarded the Nobel Prize in Physiology or Medicine in 1983. MGEs are segments of DNA that encode enzymes and proteins mediating their movement and all the MGEs of a cell are globally referred to as the mobilome[1]. In prokaryotes, MGEs movement is not primarily restricted within genomes as in the case of eukaryotes but can also occur between different genomes. This type of movement of genetic material is called Horizontal Gene transfer (HGT), as a juxtaposition with the standard vertical transmission from parental strains to their progeny. HGT can occur via at least three mechanisms: transformation (i.e., the uptake of extracellular free DNA), conjugation (frequently involving plasmids and Integrative Conjugative Elements (ICEs)) and transduction (promoted by bacteriophages)[2]. With the advance of genome sequencing technologies, it was discovered that different types of MGEs are present in all prokaryotic genomes, underlying their importance as an evolutionary force. HGT and MGEs, in fact, represent a primary source of diversity for prokaryotes, since they can have profound effects on bacterial evolution by different means, such as by broadening the gene repertoire by introducing novel genes or by disrupting existing genes[3–5]. These elements are important for the evolution of bacterial genomes and are responsible for the spread of virulence and antibiotic resistance genes (ARGs)[4]. Several mobile elements are involved in this spread and can be divided, based on their horizontal mobility mechanism, in those requiring and those not requiring cell-to-cell contact. The first category include plasmids and ICEs, recognized as key players in the spread of ARGs[6,7], which are transferred through conjugation. ICEs are usually found integrated in the host chromosome, encode the genes

necessary for their conjugation, integration and excision[5] and their size can reach up to hundreds of kilobases[8]. The latter category comprises natural transformation, and transduction through bacteriophages. Transduction can be generalized, when involves virtually any fragment of the bacterial genome, or specialized, when it is only restricted to few specific genes[7]. Bacteriophage's role in the spread of ARGs is a controversial matter. On one hand, the transfer of resistance determinants through phage transduction seems to be quantitatively less common than through conjugative elements[9], since it relies on mistakes happening during viral packaging resulting in the erroneous incorporation of bacterial DNA into the capsid. On the other hand, it is recognized that phages play an important role in the evolution of bacterial genome, as it has been estimated that up to 20% of total bacterial genomes have been acquired by phage-like elements[10]. Nonetheless, few cases of bacteriophages directly encoding ARGs in their genome have been reported. This usually happens when MGEs carrying resistance determinants invade bacteriophages or prophages. In the latter, the invasion may cause its inactivation, preventing the prophage to enter the lytic phase and to produce mature viral particles able to infect other bacterial cells[11]. Therefore, the importance of the contribution on ARGs spread of these lytically inactive prophages on ARGs spread is still not clear.

2. Bacterial responses to stress

During their lives, bacteria encounter various and fluctuating environments. In order to survive and adapt, they need to be able to sense and respond to rapidly changing conditions. This is of particular importance for pathogenic bacteria, which are subjected to challenging and extremely diverse conditions present within their hosts and also need to outlive the immune responses[12]. Therefore, bacteria have evolved different responses that are activated upon sensing environmental or intrinsic changes and comprise the modulation of their metabolism and gene expression. Depending on the response, this modulation is controlled by distinct regulators, which may generally be divided in groups and contains alternative sigma factors, gene repressors, small molecule effectors, and

inorganic molecules[13]. The different kinds of stress responses can display overlapping pathways and, even though at different extents, are often induced by the same environmental triggers. This allows bacteria to respond to a wide range of insults, like acidic pH, oxidative and nitrosative stress, envelope stress, DNA damage, nutrient limitation or starvation, oxygen limitation and toxic molecules[14].

2.1. DNA damage and SOS response

During their life, bacteria are constantly subjected to several types of stresses, both exogenous and endogenous, which threaten the integrity of their DNA. The efficient repair of these damages is essential for the survival of bacteria, as unrepaired DNA is likely to give rise to deleterious mutations and cell death. For these reasons, and in order to survive in various environmental conditions, bacteria have evolved several mechanisms for the repair of different kinds of DNA damages, which are activated or silenced, according to their needs. One of these mechanisms is an inducible system, which was discovered in *Escherichia coli* the 1970s[15] and was termed the 'SOS response'[16]. This response is activated by some bacteria upon exposure to stresses and DNA damage and comprises multiple factors and pathways, which are involved in DNA repair and maintenance, allowing for improved survival and continuous replication even upon extensive DNA damage. Depending on the extent of DNA damage, both error-free and error-prone factors are activated, the latter resulting in increased mutagenesis. Because of this potential mutagenic activity, the SOS response is tightly controlled and regulated. The regulation of the SOS response in *E.* coli is carried out by two key proteins: LexA (locus for X-ray sensitivity A) and RecA (recombinase A). In uninduced conditions, LexA forms homodimers through the CTD and binds through the helix-turn-helix of the NTD to specific operator sequence (SOS box) in the promoter region of the SOS genes, acting as a transcriptional repressor. In the presence of DNA damage and other stress signals, RecA binds the ssDNA and is converted to the activated form (RecA*), which is then able to stimulate the self-cleavage of LexA and other proteins, such as phage repressors[17]. This

autocleavage is carried out by the residues Ser119 and Lys156 of the CTD of LexA and occurs at a specific Ala84-Gly85 bond near the middle of the protein, which causes the inhibition of the activity of LexA[18], and the exposure of residues that cause LexA to be targeted by protease degradation. In this way, LexA pool starts to decrease, leading to the de-repression of the SOS genes, resulting in the activation of the SOS response. The activation of the SOS response hence results in the expression of the SOS regulon, which in *E. coli* comprises more than 50 genes with different functions and that are involved in several mechanisms, like induction of DNA repair, replication and recombination, and arrest of cell division. Expression of these genes does not occur at the same time and level, but is synchronized according to the DNA repair process and depends on the extent of the DNA damage and on the time it passed since the damage was detected[17,18]. The genes responsible for DNA repair, maintenance and replication and those involved in the cell division arrest are not the only ones controlled by LexA during the activation of the SOS response. LexA, indeed, is able to regulate the expression of a pool of genes involved in many bacterial processes, such as virulence, persistence, biofilm formation, as well as to induce prophage excision and horizontal gene transfer (HGT) events [19,20]. In fact, the SOS response activation results in the induction of many lysogenic prophages and virulence genes, like the CTX prophage induction with production of the cholerae toxin[21] and the expression of the Shiga toxin[22], but also the movement of pathogenicity island, like the SaPIbovI island of *S. aureus*[23]. Hence, in the context of mobile genetic elements spread, the SOS response plays a double role: it is activated by HGT, thus aiding the integration of the incoming DNA into the recipient genome, but at the same time it also induces HGT and transfer of genetic information. Moreover, by facilitating the movement of mobile genetic elements, it also contributes to the dissemination of antibiotic resistance determinants among bacteria, like the case of the integrative conjugative element SXT of *Vibrio cholera*, which carries genes conferring resistance to streptomycin, sulfamethoxazole, trimethoprim and chloramphenicol[24]. In a way, through the SOS response, bacteria are able to turn their exposure to adverse and stressful conditions in their favor: they are able to survive stressful conditions, change

and adapt to the new environments (through modification of their genome by increasing the rate of spontaneous mutations and genome rearrangements), and also share genetic information with other bacteria.

Apart from *E. coli*, different bacteria have been found to possess LexA or LexA functional homologues, suggesting that the SOS response might constitute a universal method for bacterial survival and adaptation[18,25]. Nonetheless, not all bacteria possess a 'canonical' SOS response, like in *E. coli*, but some display a different activation network, with the induction of genes implicated in different mechanisms, like in *Bacillus subtilis*, where the SOS response is responsible for the expression of different SOS genes, among which also a gene that codes for a cell-wall hydrolase, necessary for spore formation and dormancy[26]. Albeit the widespread diffusion of canonical and 'SOS-like' responses, some bacteria have been found to lack LexA and any kind of SOS response. This is the case of *Streptococcus pneumoniae*, which lacks an SOS response, but seems to exploit the genes involved in the competence for natural transformation to coordinate some of the same responses to DNA damage that are carried on by the SOS response in *E. coli*[27].

2.2. Envelope Stress Response

The Gram-negative bacterial envelope acts as a connection between the cell and the extracellular environment[12]. Its integrity is essential for bacterial viability as it represents one of the first line of defense against external insults, is responsible for the maintenance of cellular homeostasis, and is also the location of many essential metabolic processes. Different kind of insults, coming both from the external environmental space, like temperature, pH, antibiotics and other toxic compounds, and from intrinsic stressors, like translation stress, protein overexpression or mutations, can lead to impairment or destruction of the envelope[28]. Due to the importance of the envelope integrity, bacteria have evolved a wide range of responses able to maintain the envelope homeostasis and rapidly repair damages that may occur. These responses are part of a stress-response system, which comprise a wide range of pathways and are collectively known as the Envelope Stress Responses

(ESRs). The best characterized ESRs are: σ^E (envelope stress sigma factor) response, CpX (conjugative pilus expression) response, Rcs (regulator of capsule synthesis) response, Psp (phage shock protein) response and the Bae (bacterial adaptive) response. The σ^E response is activated in the presence of misfolded or mis-translocated outer membrane proteins (OMPs) within the outer membrane and the periplasmic space, and in the case of altered forms of lipopolysaccharide (LPS) production. Inducers of this response include different stress signals, like oxidative stress, heat shock, carbon starvation, biofilm formation, acid stress, ultraviolet A light (UVA) and hypo-osmotic stress[12,28,29]. The Cpx response is a widely conserved ESR in Gram-negative bacteria that is activated in response to a broad set of conditions, among which high pH, high salt concentration, alteration in the inner membrane lipid composition or in the peptidoglycan biosynthesis, adhesion to hydrophobic surfaces, antimicrobial peptides, changing osmolarity, and exposure to ethanol[12,28–30]. All these inducers are involved in protein misfolding in the inner membrane and periplasmatic space, in protein translocation defects and in the disruption of the inner membrane integrity in general. The Rcs response was first named based on its role in regulation of capsular biosynthesis[31], but it was then recognized to play a role in the presence of stress signals like alteration in the LPS charge and fluidity, changes in the peptidoglycan biosynthesis and defect in lipoprotein trafficking[28,31]. The Bae response is a stress response that is activated by and confer resistance to a variety of toxic compounds[32]. The stress signals responsible for the activation of this response include the exposure to toxic molecules like ethanol, indole, zinc, nickel, sodium chloride and tungstate, as well as pilin subunit overexposure[28]. Finally, the Psp response is an envelope stress response activated in the presence of severe damage to the inner membrane, which is usually also correlated to dissipation of the proton motive force (PMF) and change in the cell redox state. These kinds of damages are generally related to the phospholipids, which determine the physical and chemical properties of the membrane. The inducers of this response include infections by filamentous phages, extreme heat shock, ethanol and organic solvent exposure, disruption of protein secretion and localization of the OMPs at the inner membrane[28].

3. Mechanisms and spread of macrolide resistance in streptococci

3.1. Macrolides

Macrolides are a group of antibiotics mostly produced by *Streptomyces* and related species, closely related and characterized by a macrolactone ring, to which one or more sugars are attached through glycosidic bonds. These antibiotics are used as a major alternative to the use of penicillins and cephalosporins for the treatment of infections caused by a variety of bacteria, mostly Gram positive. Compounds belonging to this class of antibiotics can be divided, based on their macrolactone ring structure, in 14-membered lactones, like erythromycin and clarithromycin, 15-membered lactones, like azithromycin, and 16-membered lactones, like josamycin, spiramycin and tylosin. Macrolides bind to a specific site of the bacterial 50S ribosomal subunit, the nascent peptide exit tunnel (NPET), that is the way through which the synthesized protein leaves the ribosome, inhibiting the translocation step and thus causing the stop of the growing peptide chain synthesis[33]. They are considered to be bacteriostatic agents, but at high doses they can also be bactericidal.

3.2. Macrolide resistance in streptococci

The first macrolide, erythromycin, was introduced in the clinical practice in the 1950s. Since then, different bacteria have been found to be resistant to this class of antibiotics. Macrolide resistance generally arises in 3 ways in bacteria, (i) by target-site modification, with consequent prevention of the binding of the antibiotic to the ribosome, (ii) by active drug efflux through efflux pumps, and (iii) by drug inactivation, achieved through the production of different kinds of enzymes (such as esterases, lyases and phosphorylases)[34]. In streptococci, macrolide resistance started to arose upon extensive use of erythromycin as treatment for penicillin-resistant pneumococcal infections that developed in the 80s, and is mainly due to target-site modification and efflux pumps[35]. The first mechanism is given by the presence of erythromycin ribosomal methylase (*erm*) family genes,

which encode adenine-specific N-methyltransferases. These methylases add one or two methyl groups to a single adenine of the 23S rRNA, resulting in a conformational change that prevents antibiotic from binding. The *erm*(B) gene is the most common macrolide gene found in streptococci and is responsible for high level resistance to macrolides, with erythromycin MICs usually ≥ 256 μg/ml. Together with macrolide resistance, ribosome methylation by Erm(B) gene product also confers resistance to lincosamides and streptogamin B, giving rise to the so called MLSB phenotype[35]. Although the most widespread, *erm*(B) is not the only *erm* gene found in streptococci. The *erm*(TR) gene, grouped into the *erm*(A) gene class as it is closely related to *erm*(A) of *Staphylococcus aureus*[36], was detected first in *Streptococcus pyogenes*[37] and later in *Streptococcus pneumoniae*[38]. The second mechanism of macrolide resistance is due to the presence of efflux genes which confer the M phenotype, characterized by low level resistance to 14- and 15-membered macrolides but not to lincosamides or streptogamin B. The macrolide efflux is encoded by two genes: *mef*(A) and *msr*(D). Two variants of *mef* genes are found in streptococci, *mef*(A) and *mef*(E), the first originally described in *Streptococcus pyogenes*[39] and the latter in *Streptococcus pneumoniae*[40]. These genes are grouped in the same *mef*(A) class of macrolide resistance genes, as they are highly homologous and share more than 90% nucleotide identity and 91% amino acid homology. The other gene of the efflux system, *msr*(D), is a homolog of the *Staphylococcus aureus* gene *msr*(A)[41] and was discovered later, as it was almost always found adjacent to the *mef*(A) gene. They are part of a single transcriptional unit and constitute a two-gene efflux transport system of the ABC superfamily, where *mef*(A) encodes the transmembrane channel and *msr*(D) encodes the two ATP-binding domains[42]. The respective contribution of the two gene products to macrolide resistance has been assessed and it was found that both genes are involved in macrolide resistance, but that only *msr*(D) is essential for the resistance phenotype[42,43].

3.3. Spread of macrolide resistance through mobile genetic elements in streptococci

The genes responsible for both types of macrolide resistance are widespread not only among streptococci, but also in other bacteria, both Gram-positive and Gram-negative, suggesting that they are easily exchanged by horizontal gene transfer through the association with mobile genetic elements. Many of the *erm* genes in streptococci have been found to be associated with conjugative and nonconjugative transposons, residing in the chromosomes, as well as on plasmids. The *erm*(B) gene, in particular, has been found on nonconjugative transposons such as Tn*917* and Tn*551*[34], and is often associated with the *tet*(M) gene, coding for tetracycline resistance, which is carried by transposons of the Tn*916* family, indicating that elements containing the *erm*(B) gene may be incorporated into transposons of this family[44]. Some examples are the Tn*6002*, resulting from the incorporation of an *erm*(B)-containing element into *orf20* of Tn*916*, or Tn*3872* that results from the incorporation of Tn*917* into *orf9* of Tn*916*[45]. Three mobile genetic elements have initially been identified in streptococci carrying the *mef*(A) and *msr*(D) gene pair: the transposon Tn*1207.1*, the 'mega' element and the prophage φ1207.3. The Tn*1207.1* was the first *mef*-carrying element to be described[46]. It is a nonconjugative transposon of 7,244 bp, which carries the *mef*(A) gene, considered to be typical of *S. pyogenes*. This transposon was found integrated into the *celB* gene, which encodes a ComEC homolog, a protein involved in DNA binding and transport during genetic transformation. The disruption of this coding sequence impairs the ability of the strains carrying the Tn*1207.1* of becoming competent for genetic transformation, resulting in the block of further genetic evolution of these strains. The second element discovered in *S. pneumoniae* was the 'mega' element (from macrolide efflux genetic assembly), which carries the *mef*(E) gene[47]. The element is 5,532bp long and its insertion in the pneumococcal chromosome was found to happen in at least five different sites, and also into a Tn*916*-like element[48]. Since Tn*1207.1* was found to carry *mef*(A), which is typically associated with *S. pyogenes*, but to be integrated into the chromosome of *S. pneumoniae*, clinical isolates of *S. pyogenes* that displayed the M phenotype of resistance were screened for the presence of genetic elements homologous to Tn*1207.1*. A genetic element carrying *mef*(A)-*msr*(D) genes was found in the clinical strain of *S. pyogenes* 2812A[49]. At the beginning,

this element, called Tn*1207.3*, was thought to be a conjugative transposon due to the fact that it could be transferred by conjugation to the chromosome of other streptococcal species, but was later identified as a prophage and was renamed φ1207.3[50]. The sequence analysis of this prophage revealed that is 52,491 bp long and that the 7,244 bp at the left end are identical to Tn*1207.1*.

Streptococci displaying dual macrolide resistance genotype, thus containing both *erm* and *mef*(A)/*msr*(D) genes, are also found worldwide[51]. This type of resistance is usually associated with the presence of the composite mobile genetic element Tn*2010*, which is a Tn*916*-like element with Mega element inserted into *orf6* and the *erm*(B) gene incorporated into *orf20* of Tn*916*[52,53].

4. Bioremediation

Bioremediation is a process by which organic wastes and environmental pollutants are biologically degraded or converted to less toxic or innocuous compounds by exploiting the metabolism of microorganisms, usually already residing in the environment[54]. Common microorganisms used in bioremediation processes include fungi, algae and bacteria, both gram-positives and gram-negatives[55]. The main advantage of this technique is that it is very low cost, has low energy consumption and is environmentally friendly, as it does not affect environmental properties. Bioremediation of several contaminated environments, including soils, sediments, and water, can be performed both through *in-situ* or *ex-situ* methods, depending on the site and pollutants characteristics[56]. The *in-situ* bioremediation takes place directly in the polluted environment, whereas the *ex-situ* method relies on the removal of the contaminated material from the environment and on the treatment to be performed elsewhere. Several toxic products are degraded through bioremediation processes, including heavy metals, nuclear waste, plastics and phthalates, and polycyclic aromatic compounds (PAHs). PAHs are a class of organic compounds consisting of two or more fused benzene rings arranged in linear, angular or cluster configurations. They are ubiquitous in the environment, present naturally in fossil fuels, and originate during the incomplete combustion of organic materials and as by-products of industrial processing[54,55,57]. These

compounds are characterized by high hydrophobicity and low water solubility, high lipophilicity and high persistence in the environment. Increase in the molecular weight and in the number of fused rings of PAHs results in the enhancement of the hydrophobicity and environmental persistence, along with the increase of the toxic, mutagenic and, in some cases, carcinogenic potential[54]. All these properties allow PAHs to be widely distributed and contaminate soils, water and air. The PAHs deriving from fossil combustion or oil refining are one of the main forms of anthropogenic pollution of both soils and waters.

4.1. Mobile genetic elements in bioaugmentation processes

The association of PAHs degradation genes with mobile genetic element is not new, and has been already observed in plasmids and transposons[58]. In fact, the use of mobile genetic elements harbouring these genes has already been proposed as a valid strategy to improve bioremediation of pollutants. The advantage of the use of MGEs in bioremediation processes is particularly evident in those situations in which laboratory strains are not able to thrive and degrade PAHs once introduced in the contaminated environments. This approach is named 'genetic bioaugmentation' and relies on the introduction of catabolic genes on self-transmissible mobile genetic elements in the environment, as opposed to introduce a high quantity of bacteria able to degrade PAHs. This allows for a higher concentration of the genes involved in bioremediation and the stimulation of horizontal gene transfer of these elements in microorganism already residing in the environment, allowing for an increased bioremediation efficiency[58,59].

5. Aims of this thesis

The aim of this thesis was to study mobile genetic elements involved in several processes, including stress responses, antibiotic resistance and catabolic metabolism.

In Chapter 2, the activation of an SOS-like response in *Streptococcus pneumoniae*, encoded by *Streptococcus pyogenes* φ1207.3 phage, was investigated. The activation of this response was

studied upon exposing to chemical and physical stresses two strain of *S. pneumoniae*, R6, carrying a Mismatch Repair System (*hex*+) and thus displaying low basal mutation rates, and Rx1, Mismatch repair-deficient (*hex*-), displaying higher mutation rates (hypermutable). In Chapter 3, the disbalancing of a different stress response system, the Envelope Stress Response (ESR) was evaluated as a therapeutic approach in *Escherichia coli*. Several pathways (σ^E, Cpx, Rcs, Bae, and Psp) of this system were investigated by testing the action of different antibiotics. The φ1207.3 genetic element, which carries both macrolide resistance genes and the SOS-like cassette, was first described as an Integrative and Conjugative Element (ICE) and later annotated as a prophage. To demonstrate that φ1207.3 encodes a functional phage, the element was transferred to the standard *S. pneumoniae* laboratory strain Rx1 (Chapter 4). To study the φ1207.3 transfer mechanism, which requires cell-to-cell contact, resembling conjugation, the cellular localization of φ1207.3 was investigated with immunological assays and Real-Time PCR, as reported in Chapter 5. A mating protocol for the transfer of large mobile genetic elements, including φ1207.3, was set up (described in Chapter 6). The complete genome sequence of the *S. pneumoniae* laboratory strain Rx1 is reported in Chapter 7. Deletion of *mef*(A) in the *mef*(A)-*msr*(D) efflux systems, carried by φ1207.3, only results in a two-fold decrease in the erythromycin minimal inhibitory concentration (MIC), while deletion of *msr*(D) abolished erythromycin resistance. In Chapter 8, it is reported the investigation of genes coding for Mef(A) homologous likely involved in *mef*(A) complementation in the *S. pneumoniae.* The characterization of the chromosomal integration site (*att*B) of the pneumococcal ICE Tn*5253,* carried out in *S. pneumoniae* with different backgrounds and other streptococcal and enterococcal species, is reported in Chapter 9. Finally, Chapter 10 describes the complete genome sequence of two *Mycobacterium chimaera* strains isolated from the hospital water reservoir of heater-cooling units. In one of these strains, it was reported the presence of an ICE carrying putative genes involved in the catabolic degradation of polycyclic aromatic hydrocarbons, important environmental pollutants.

6. References

1. Siefert JL. Defining the Mobilome. In: Gogarten MB, Gogarten JP, Olendzenski LC, eds. *Horizontal Gene Transfer: Genomes in Flux*. Humana Press; 2009:13-27. doi:10.1007/978-1-60327-853-9_2
2. Frost LS, Leplae R, Summers AO, Toussaint A. Mobile genetic elements: the agents of open source evolution. *Nat Rev Microbiol*. 2005;3(9):722-732. doi:10.1038/nrmicro1235
3. Naito M, Pawlowska TE. The role of mobile genetic elements in evolutionary longevity of heritable endobacteria. *Mob Genet Elem*. 2016;6(1):e1136375. doi:10.1080/2159256X.2015.1136375
4. Burrus V, Waldor MK. Shaping bacterial genomes with integrative and conjugative elements. *Res Microbiol*. 2004;155(5):376-386. doi:10.1016/j.resmic.2004.01.012
5. Johnson CM, Grossman AD. Integrative and Conjugative Elements (ICEs): What They Do and How They Work. *Annu Rev Genet*. 2015;49:577-601. doi:10.1146/annurev-genet-112414-055018
6. Botelho J, Schulenburg H. The Role of Integrative and Conjugative Elements in Antibiotic Resistance Evolution. *Trends Microbiol*. 2021;29(1):8-18. doi:10.1016/j.tim.2020.05.011
7. Brown-Jaque M, Calero-Cáceres W, Muniesa M. Transfer of antibiotic-resistance genes via phage-related mobile elements. *Plasmid*. 2015;79:1-7. doi:10.1016/j.plasmid.2015.01.001
8. Sullivan JT, Ronson CW. Evolution of rhizobia by acquisition of a 500-kb symbiosis island that integrates into a phe-tRNA gene. *Proc Natl Acad Sci*. 1998;95(9):5145. doi:10.1073/pnas.95.9.5145
9. Volkova VV, Lu Z, Besser T, Gröhn YT. Modeling the Infection Dynamics of Bacteriophages in Enteric Escherichia coli: Estimating the Contribution of Transduction to Antimicrobial Gene Spread. Schaffner DW, ed. *Appl Environ Microbiol*. 2014;80(14):4350-4362. doi:10.1128/AEM.00446-14
10. Brüssow H, Canchaya C, Hardt W-D. Phages and the Evolution of Bacterial Pathogens: from Genomic Rearrangements to Lysogenic Conversion. *Microbiol Mol Biol Rev*. 2004;68(3):560-602. doi:10.1128/MMBR.68.3.560-602.2004
11. Enault F, Briet A, Bouteille L, Roux S, Sullivan MB, Petit M-A. Phages rarely encode antibiotic resistance genes: a cautionary tale for virome analyses. *ISME J*. 2017;11(1):237-247. doi:10.1038/ismej.2016.90

12. Hews CL, Cho T, Rowley G, Raivio TL. Maintaining Integrity Under Stress: Envelope Stress Response Regulation of Pathogenesis in Gram-Negative Bacteria. *Front Cell Infect Microbiol*. 2019;9:313. doi:10.3389/fcimb.2019.00313
13. Foster PL. Stress-Induced Mutagenesis in Bacteria. *Crit Rev Biochem Mol Biol*. 2007;42(5):373-397. doi:10.1080/10409230701648494
14. Fang FC, Frawley ER, Tapscott T, Vázquez-Torres A. Bacterial Stress Responses during Host Infection. *Cell Host Microbe*. 2016;20(2):133-143. doi:10.1016/j.chom.2016.07.009
15. Witkin EM. RecA protein in the SOS response: milestones and mysteries. *Biochimie*. 1991;73(2-3):133-141. doi:10.1016/0300-9084(91)90196-8
16. Radman M. SOS Repair Hypothesis: Phenomenology of an Inducible DNA Repair Which is Accompanied by Mutagenesis. In: Hanawalt PC, Setlow RB, eds. *Molecular Mechanisms for Repair of DNA*. Springer US; 1975:355-367. doi:10.1007/978-1-4684-2895-7_48
17. Maslowska KH, Makiela-Dzbenska K, Fijalkowska IJ. The SOS system: A complex and tightly regulated response to DNA damage. *Environ Mol Mutagen*. 2019;60(4):368-384. doi:10.1002/em.22267
18. Butala M, Žgur-Bertok D, Busby SJW. The bacterial LexA transcriptional repressor. *Cell Mol Life Sci*. 2009;66(1):82-93. doi:10.1007/s00018-008-8378-6
19. Fornelos N, Browning DF, Butala M. The Use and Abuse of LexA by Mobile Genetic Elements. *Trends Microbiol*. 2016;24(5):391-401. doi:10.1016/j.tim.2016.02.009
20. Podlesek Z, Žgur Bertok D. The DNA Damage Inducible SOS Response Is a Key Player in the Generation of Bacterial Persister Cells and Population Wide Tolerance. *Front Microbiol*. 2020;11:1785. doi:10.3389/fmicb.2020.01785
21. Quinones M, Kimsey HH, Waldor MK. LexA Cleavage Is Required for CTX Prophage Induction. *Mol Cell*. 2005;17(2):291-300. doi:10.1016/j.molcel.2004.11.046
22. Nassar FJ, Rahal EA, Sabra A, Matar GM. Effects of Subinhibitory Concentrations of Antimicrobial Agents on *Escherichia coli* O157:H7 Shiga Toxin Release and Role of the SOS Response. *Foodborne Pathog Dis*. 2013;10(9):805-812. doi:10.1089/fpd.2013.1510
23. Úbeda C, Maiques E, Knecht E, Lasa Í, Novick RP, Penadés JR. Antibiotic-induced SOS response promotes horizontal dissemination of pathogenicity island-encoded virulence factors in staphylococci: Horizontal dissemination of virulence genes. *Mol Microbiol*. 2005;56(3):836-844. doi:10.1111/j.1365-2958.2005.04584.x
24. Beaber JW, Hochhut B, Waldor MK. SOS response promotes horizontal dissemination of antibiotic resistance genes. *Nature*. 2004;427(6969):72-74. doi:10.1038/nature02241

25. Erill I, Campoy S, Barbé J. Aeons of distress: an evolutionary perspective on the bacterial SOS response. *FEMS Microbiol Rev*. 2007;31(6):637-656. doi:10.1111/j.1574-6976.2007.00082.x
26. Au N, Kuester-Schoeck E, Mandava V, et al. Genetic Composition of the Bacillus subtilis SOS System. *J Bacteriol*. 2005;187(22):7655-7666. doi:10.1128/JB.187.22.7655-7666.2005
27. Prudhomme M, Attaiech L, Sanchez G, Martin B, Claverys J-P. Antibiotic Stress Induces Genetic Transformability in the Human Pathogen *Streptococcus pneumoniae*. *Science*. 2006;313(5783):89-92. doi:10.1126/science.1127912
28. Mitchell AM, Silhavy TJ. Envelope stress responses: balancing damage repair and toxicity. *Nat Rev Microbiol*. 2019;17(7):417-428. doi:10.1038/s41579-019-0199-0
29. Raivio TL. MicroReview: Envelope stress responses and Gram-negative bacterial pathogenesis: Envelope stress responses and virulence. *Mol Microbiol*. 2005;56(5):1119-1128. doi:10.1111/j.1365-2958.2005.04625.x
30. Grabowicz M, Silhavy TJ. Envelope Stress Responses: An Interconnected Safety Net. *Trends Biochem Sci*. 2017;42(3):232-242. doi:10.1016/j.tibs.2016.10.002
31. Wall E, Majdalani N, Gottesman S. The Complex Rcs Regulatory Cascade. *Annu Rev Microbiol*. 2018;72(1):111-139. doi:10.1146/annurev-micro-090817-062640
32. Guest RL, Raivio TL. Role of the Gram-Negative Envelope Stress Response in the Presence of Antimicrobial Agents. *Trends Microbiol*. 2016;24(5):377-390. doi:10.1016/j.tim.2016.03.001
33. Vázquez-Laslop N, Mankin AS. How Macrolide Antibiotics Work. *Trends Biochem Sci*. 2018;43(9):668-684. doi:10.1016/j.tibs.2018.06.011
34. Roberts MC. Update on macrolide-lincosamide-streptogramin, ketolide, and oxazolidinone resistance genes: MLSKO genes. *FEMS Microbiol Lett*. 2008;282(2):147-159. doi:10.1111/j.1574-6968.2008.01145.x
35. Schroeder MR, Stephens DS. Macrolide Resistance in Streptococcus pneumoniae. *Front Cell Infect Microbiol*. 2016;6. doi:10.3389/fcimb.2016.00098
36. Leclercq R, Courvalin P. Resistance to Macrolides and Related Antibiotics in Streptococcus pneumoniae. *Antimicrob Agents Chemother*. 2002;46(9):2727-2734. doi:10.1128/AAC.46.9.2727-2734.2002
37. Seppälä H, Skurnik M, Soini H, Roberts MC, Huovinen P. A Novel Erythromycin Resistance Methylase Gene (ermTR) in Streptococcus pyogenes. *Antimicrob Agents Chemother*. 1998;42(2):257-262. doi:10.1128/AAC.42.2.257
38. Camilli R, Del Grosso M, Iannelli F, Pantosti A. New Genetic Element Carrying the Erythromycin Resistance Determinant erm(TR) in Streptococcus pneumoniae. *Antimicrob Agents Chemother*. 2008;52(2):619-625. doi:10.1128/AAC.01081-07

39. Clancy J, Petitpas J, Dib-Hajj F, et al. Molecular cloning and functional analysis of a novel macrolide-resistance determinant, *mefA* , from *Streptococcus pyogenes* . *Mol Microbiol*. 1996;22(5):867-879. doi:10.1046/j.1365-2958.1996.01521.x
40. Tait-Kamradt A, Clancy J, Cronan M, et al. mefE is necessary for the erythromycin-resistant M phenotype in Streptococcus pneumoniae. *Antimicrob Agents Chemother*. 1997;41(10):2251-2255. doi:10.1128/AAC.41.10.2251
41. Roberts MC, Sutcliffe J, Courvalin P, Jensen LB, Rood J, Seppala H. Nomenclature for Macrolide and Macrolide-Lincosamide-Streptogramin B Resistance Determinants. *Antimicrob Agents Chemother*. 1999;43(12):2823-2830. doi:10.1128/AAC.43.12.2823
42. Iannelli F, Santoro F, Santagati M, et al. Type M Resistance to Macrolides Is Due to a Two-Gene Efflux Transport System of the ATP-Binding Cassette (ABC) Superfamily. *Front Microbiol*. 2018;9:1670. doi:10.3389/fmicb.2018.01670
43. Zhang Y, Tatsuno I, Okada R, et al. Predominant role of msr(D) over mef(A) in macrolide resistance in Streptococcus pyogenes. *Microbiology*. 2016;162(1):46-52. doi:10.1099/mic.0.000206
44. Chancey ST, Agrawal S, Schroeder MR, Farley MM, Tettelin H, Stephens DS. Composite mobile genetic elements disseminating macrolide resistance in Streptococcus pneumoniae. *Front Microbiol*. 2015;6. doi:10.3389/fmicb.2015.00026
45. Brenciani A, Bacciaglia A, Vecchi M, Vitali LA, Varaldo PE, Giovanetti E. Genetic Elements Carrying erm(B) in Streptococcus pyogenes and Association with tet(M) Tetracycline Resistance Gene. *Antimicrob Agents Chemother*. 2007;51(4):1209-1216. doi:10.1128/AAC.01484-06
46. Santagati M, Iannelli F, Oggioni MR, Stefani S, Pozzi G. Characterization of a Genetic Element Carrying the Macrolide Efflux Gene mef(A) in Streptococcus pneumoniae. *Antimicrob Agents Chemother*. 2000;44(9):2585-2587. doi:10.1128/AAC.44.9.2585-2587.2000
47. Gay K, Stephens DS. Structure and Dissemination of a Chromosomal Insertion Element Encoding Macrolide Efflux in *Streptococcus pneumoniae*. *J Infect Dis*. 2001;184(1):56-65. doi:10.1086/321001
48. Del Grosso M, Scotto d'Abusco A, Iannelli F, Pozzi G, Pantosti A. Tn2009, a Tn916-Like Element Containing mef(E) in Streptococcus pneumoniae. *Antimicrob Agents Chemother*. 2004;48(6):2037-2042. doi:10.1128/AAC.48.6.2037-2042.2004
49. Santagati M, Iannelli F, Cascone C, et al. The Novel Conjugative Transposon Tn1207.3 Carries the Macrolide Efflux Gene mef(A) in Streptococcus pyogenes. *Microb Drug Resist*. 2003;9(3):243-247. doi:10.1089/107662903322286445

50. Iannelli F, Santagati M, Santoro F, Oggioni MR, Stefani S, Pozzi G. Nucleotide sequence of conjugative prophage Φ1207.3 (formerly Tn1207.3) carrying the mef(A)/msr(D) genes for efflux resistance to macrolides in Streptococcus pyogenes. *Front Microbiol*. 2014;5:687-687. doi:10.3389/fmicb.2014.00687
51. Farrell DJ, Couturier C, Hryniewicz W. Distribution and antibacterial susceptibility of macrolide resistance genotypes in Streptococcus pneumoniae: PROTEKT Year 5 (2003–2004). *Int J Antimicrob Agents*. 2008;31(3):245-249. doi:10.1016/j.ijantimicag.2007.10.022
52. Del Grosso M, Camilli R, Iannelli F, Pozzi G, Pantosti A. The mef(E)-Carrying Genetic Element (mega) of Streptococcus pneumoniae: Insertion Sites and Association with Other Genetic Elements. *Antimicrob Agents Chemother*. 2006;50(10):3361-3366. doi:10.1128/AAC.00277-06
53. Del Grosso M, Northwood JGE, Farrell DJ, Pantosti A. The Macrolide Resistance Genes erm(B) and mef(E) Are Carried by Tn2010 in Dual-Gene Streptococcus pneumoniae Isolates Belonging to Clonal Complex CC271. *Antimicrob Agents Chemother*. 2007;51(11):4184-4186. doi:10.1128/AAC.00598-07
54. Cerniglia CE. Biodegradation of polycyclic aromatic hydrocarbons. *Biodegradation*. 1992;3(2):351-368. doi:10.1007/BF00129093
55. Bamforth SM, Singleton I. Bioremediation of polycyclic aromatic hydrocarbons: current knowledge and future directions. *J Chem Technol Biotechnol*. 2005;80(7):723-736. doi:10.1002/jctb.1276
56. Azubuike CC, Chikere CB, Okpokwasili GC. Bioremediation techniques-classification based on site of application: principles, advantages, limitations and prospects. *World J Microbiol Biotechnol*. 2016;32(11):180-180. doi:10.1007/s11274-016-2137-x
57. Peng R-H, Xiong A-S, Xue Y, et al. Microbial biodegradation of polyaromatic hydrocarbons. *FEMS Microbiol Rev*. 2008;32(6):927-955. doi:10.1111/j.1574-6976.2008.00127.x
58. Segura A, Molina L, Ramos JL. Plasmid-Mediated Tolerance Toward Environmental Pollutants. *Microbiol Spectr*. 2014;2(6). doi:10.1128/microbiolspec.PLAS-0013-2013
59. Top EM, Springael D, Boon N. Catabolic mobile genetic elements and their potential use in bioaugmentation of polluted soils and waters. *FEMS Microbiol Ecol*. 2002;42(2):199-208. doi:10.1111/j.1574-6941.2002.tb01009.x

CHAPTER 2

Prophage φ1207.3 is responsible for a temporary activation of a mutator phenotype in *Streptococcus pneumoniae*, resulting in increased survival and evolution during stress conditions

Valeria Fox[1], Francesco Santoro[1], Carmen Apicella[1], Sara Díaz-Díaz[2], José Manuel Rodríguez Martínez[3], Francesco Iannelli[1], Gianni Pozzi[1]

[1]*Laboratory of Molecular Microbiology and Biotechnology, Department of Medical Biotechnologies, University of Siena, 53100 Siena, Italy*

[2]*Unidad Clínica de Enfermedades Infecciosas, Microbiología y Medicina Preventiva, Hospital Universitario Virgen Macarena, Sevilla, Spain*

[3]*Departamento de Microbiología, Facultad de Medicina, Universidad de Sevilla, Sevilla, Spain*

Manuscript in preparation

1. Abstract

The SOS response is an inducible system activated by some bacteria in the presence of bacterial stress and extensive DNA damage, which allows for improved survival and continuous replication, but at the cost of elevated mutagenesis. All streptococcal species lack a canonical SOS response, but some display a similar SOS-like response, whereas in *Streptococcus pneumoniae* the mutagenic repair of UV-damaged DNA, related to an SOS-like response, has not been detected.

φ1207.3 is a prophage of *Streptococcus pyogenes* which carries the macrolide efflux resistance genes *mef*(A)/*msr*(D) and is able to move among streptococcal species. φ1207.3 DNA sequence analysis revealed also the presence of genes, from *orf6* to *orf11*, which show similarity to a gene cassette previously found in other streptococcal species and capable of mediating SOS-mutagenesis in *Streptococcus uberis*. In this work, φ1207.3 was transferred to *S. pneumoniae* to investigate whether its presence leads to the activation of an SOS-like response upon exposure to both physical and chemical stresses. Two groups of isogenic strains were constructed from *S. pneumoniae* strains R6 (*hex*+) and Rx1 (*hex*-) and used for evaluating survival and stress response after exposure to mitomycin C and UV-C light, by irradiating bacterial cells using an UV-C LED instrument. The pneumococcal strains carrying φ1207.3, containing the SOS-like cassette, showed a significant increase in UV-C light survival and in the mutation rate upon exposure to both mitomycin C and UV-C light, whereas no significant increase was observed in the control strains devoid of φ1207.3 and carrying a recombinant φ1207.3, with the SOS-like cassette deleted.

In conclusion, we demonstrated that φ1207.3 not only leads to drug resistance, but also carries a functional SOS-like cassette responsible for an SOS-like response in *S. pneumoniae*, which activates a transient hypermutable phenotype in response to stresses, resulting in an increased survival and increased probability of acquiring mutation, thus potentially representing a risk factor in clinical settings.

2. Introduction

Bacteria evolve by inheriting and accumulating genetic changes in their genomes. This genome evolution may occur through a variety of processes that include chromosomal rearrangements, horizontal gene transfer (HGT) and mutations. Mutations can be acquired spontaneously (spontaneous mutagenesis), when they occur without treatment of the organism with an exogenous agent and usually occur because of replication errors, as a consequence of lesions introduced into DNA during the normal growth of the cell, or due to the treatment by chemical or physical agents [1]. A way of measuring mutagenesis is by calculating the mutation rate, which, differently from the mutation frequency, which represents simply the proportion of mutant cells in a specific culture, is the probability of a mutation occurring per cell division and thus is also an estimation of the probability of a mutation occurring during the life of a bacterial cell[2–4]. Mutation rates differ between species and even between different regions of the genome of a single species and have a profound effect on the bacterial ability to survive, adapt and evolve in different conditions. Several factors can influence the mutation rate, including the fidelity of DNA replication (namely the presence of systems able to correct nucleotide misincorporations, like the Mismatch Repair System, or the DNA polymerases fidelity), DNA damage and the resultant repair pathways activity. In normal conditions, *Escherichia coli* replication is carried out by high fidelity polymerases which usually misinsert deoxynucleotides approximately 10^{-4}-10^{-6} per bp and possess a 3'-exo proofreading activity that may reduce this mutational load by about 100-fold, leading to a mutation rate of up to 10^{-8} per bp[5]. In the presence of bacterial stress and extensive DNA damage, *E. coli* has evolved an inducible system, termed the SOS response, which allows for improved survival and continuous replication, but at the cost of elevated mutagenesis[6,7]. The main proteins involved in this SOS response are LexA and RecA. In normal conditions, LexA is present as a homodimer which binds to the promoters of a group of genes, the SOS regulon, and acts as a transcriptional repressor. Upon DNA damage, RecA binds to ssDNA and becomes activated, resulting in the promotion of the autocleavage of LexA, which is no longer able to act as a repressor, leading to the

de-repression of the SOS genes[8]. In *E. coli*, the SOS response induces the increase of the expression of several genes with diverse functions, which are involved in DNA-damage tolerance and repair. One component of this response is the Translesion Synthesis (TLS)[9]. TLS is involved in the ability of cells to tolerate DNA damage, thus helping cells to avoid death as a consequence of unrepaired or unrepairable damage to their genomes. The TLS can act be both error-free, when the recombinational repair or copy choice DNA replication are involved, without resulting in the generation of mutations, or error-prone, when the polymerase V is recruited, which results in the generation of mutations[1]. Polymerase V is encoded by the *umuDC* operon, where *umuC* encodes a translesion DNA polymerase, belonging to an extended protein family called the Y family, while *umuD* encodes a protein that controls the biological roles of the UmuC protein. This polymerase has a relaxed fidelity for nucleotide incorporation, allowing for DNA synthesis in the presence of a DNA damage in the template, but also promoting the misincorporation of nucleotides at a higher frequency than the normal polymerases involved in replication (approximately 10^{-3}-10^{-4} per bp[10]). This polymerase also lacks an intrinsic proofreading activity, so that nucleotides wrongly inserted are not immediately excised, often resulting in mutagenesis[1].

All streptococcal species lack LexA and a canonical SOS response, but some contain a LexA-like repressor, which, like LexA, undergoes RecA-dependent self-cleavage in the presence of a DNA-damaging agent, and a SOS gene cassette[11]. *Streptococcus pneumoniae* lacks this LexA-like repressor and the mutagenic repair of UV-damaged DNA, related to a classical SOS response, has not be detected[12]. Nonetheless, the *com* regulon and genetic transformability were shown to be induced in *Streptococcus pneumoniae* upon induction with Mitomycin C and fluoroquinolones, suggesting that in this bacterium competence could play a role similar to that of the SOS response in *E.coli*[13]. UmuDC-like protein genes are not present in the pneumococcal genome; however, it was reported that ICE Tn*5253* encodes UmuC and UmuD homolog proteins[14]. The presence of Tn*5253* in the pneumococcal genome confers UV resistance to the cell, inducing a mutagenic SOS response[15]. An SOS-like gene cassette was found in several streptococcal species, , including *S.*

uberis, S. agalactiae, S. pyogenes, S. mitis, S. sanguinis and *S. thermophilus*, and was reported to be capable of mediating SOS mutagenesis in response to UV-light exposure in *S. uberis* [11]. This cassette includes genes coding for UmuC-like proteins, which are co-transcribed with a gene coding for a LexA-like repressor, the HdiR homolog (heat and inducible regulator, found in *Lactococcus lactis*[16]), and with other genes that may represent functional homologs of UmuD. This cassette is similar to the one present in the ICE Tn*5253* and other cassettes in other mobile genetic elements, such as the one of *S. pyogenes* φ1207.3. The genetic element Φ1207.3 (formerly Tn*1207.3*) is a prophage found in the clinical strain of *Streptococcus pyogenes* 2812A[17–19], which carries the *mef*(A)-*msr*(D) gene pair encoding an efflux transport system responsible for the type M resistance to macrolides [20]. Prophage DNA sequence analysis showed the presence of genes, from *orf6* to *orf11*, that show similarity to the gene cassette found by Varhimo and colleagues to mediate the SOS mutagenesis in streptococcal species. In particular, *orf11* is homologous to the HdiR LexA-like transcriptional repressor, *orf8* is homologous to the Tn5253 *umuC/orf70,* while *orf7* gene product is homologous to the YolD-like protein, which is predicted to be a functional equivalent of UmuD[21].

The aim of this study was to investigate the contribution of the Φ1207.3 genetic element to *S. pyogenes* and *S. pneumoniae* genome evolution and, in particular, to determine whether the presence of the SOS-like cassette of φ1207.3 leads to the activation of an SOS-like response in *S. pneumoniae*, known to lack the SOS response.

3. Materials and methods

3.1. Bacterial strains and growth conditions

All strains used in this work and their relevant properties are reported in Table 1.

Streptococcal strains were grown in Tryptic Soy Broth (TSB, BD) at 37°C without agitation. Culture starters were taken at an optical density at 590 nm (OD_{590}) ranging from 0.2 to 0.3 and were stored at -80°C in tubes containing glycerol at a final concentration of 10%. Solid media were

obtained by supplementing TSB with 1.5% agar (BD Difco) and 3% defibrinated horse blood (Liofilchem). When required, both liquid and solid media were supplemented with antibiotics at the following concentrations: 500μg/ml kanamycin, 0.5μg/ml erythromycin and 5μg/ml chloramphenicol.

3.2. Mating assays

Transfer of bacteriophage φ1207.3 was obtained through a plate mating experiment, as previously described [22]. Briefly, donor cells, carrying the phage, and recipient cells were grown separately in TSB in the presence of the appropriate antibiotics. Upon reaching the end of the exponential phase, cells were mixed at a donor-recipient 1:10 ratio, centrifuged, and the pellet was plated on TSA plates supplemented with 5% blood. Plates were incubated at 37°C in the presence of 5% CO_2 for 4h and cells were then recovered with a cotton swab and resuspended in TSB. To select for recombinants, cell suspension was plated following a multilayer plating procedure. For confirmation, genetic analysis and PCR were performed.

3.3. Mutagenic constructs by PCR SOEing

The *orf6-11* mutagenic construct containing the kanamycin resistance cassette (916 bp) flanked by the fragments upstream *orf6* (555 bp) and downstream of *orf11* (829 bp) was obtained by PCR SOEing method (Gene Splicing by Overlap Extension[23]), as previously described[24]. The primer pair IF149/IF210 was used to amplify the kanamycin resistance cassette [25], while IF242/IF239 and IF240/IF241 to amplify the flanking fragments. Assembly of the final construct (2260 bp) was obtained with the IF242/IF241 primer pair. PCR was carried out as previously described [26]. The PCR products were separated in a 0.8% agarose gel at 200 V for 30 minutes, stained for 15 minutes in a 0.1% Ethidium Bromide solution and visualized with UV light. Mutagenic constructs obtained directly from PCR reaction or after gel purification (NucleoSpin Gel and PCR Clean-up kit, Macherey-Nagel) were quantified using the Qubit 2.0 Fluorometer (Thermo Fisher Scientific) and used as donor DNA in transformation. All oligonucleotide primers used in this study for PCR mutagenesis and PCR confirmation are listed in Table 2.

3.4. Transformation

The obtained purified PCR construct was used as donor DNA in transformation experiments, with the *S. pneumoniae* R6 (*hex*+) [27] and *S. pneumoniae* Rx1 (naturally *hex*-) [28] strains as recipients. Competent cells for transformation were prepared as previously described [24]. Competence cells were then thawed, supplemented with 25 ng/ml Competence Stimulating Peptide (CSP), and 1 μg/ml of the purified DNA of the mutagenic construct, and incubated at 37°C for 45 minutes. The resulting mutant strain was selected for acquisition of kanamycin resistance by multilayer plating and genetic analysis [22].The deletion of the *orf6-11* cassette was finally confirmed by PCR.

3.5. UV fluence measurement

Ultraviolet light emitting diodes (LEDs) have different advantages compared to classical UV lamps: they are smaller and present a longer life span, do not use the toxic heavy metal mercury, and are monochromatic, meaning that they can produce UV light at a single wavelength. The latter characteristic allows the use of the optimum wavelength (about 265 nm) for germicidal effectiveness [29]. In this study, UV-C light experiments were carried out using a PearlLab Micro UV-C LED instrument (AquiSense Technologies, Erlanger, Kentucky, USA). The instrument is a compact system with interchangeable USB UV-C LEDs and dimming control, which can be used both for batch and static studies. The lower portion of the module was un-screwed, allowing us to use the lamp as a general light source. A system made of an instrument support and swappable and autoclavable mini-plates was 3D-designed and printed with Nylon-12 (Figure 1). The irradiance at 265nm of the ten instrument intensities were measured three times with a ILT1400 radiometer and SED240/W detector (International Light Technologies, Peabody, MA). Mean and standard deviation for each intensity is reported in Table 3. The UV fluence (measured in J/m^2) was obtained multiplying the irradiance (or more appropriately the fluence rate, which is the radiative flux through a three-dimensional external surface, i.e., a spherical microbe, measured in W/m^2) for the exposure time (in seconds). The UV fluence has sometimes been incorrectly called the UV dose, which refers to the total absorbed energy. However, in the case of microorganisms, only a few

percent of the incident ultraviolet light, which passes through the organism, is absorbed, thus UV fluence is more appropriate, since it relates to the incident UV energy, rather than absorbed UV energy [30].

3.6. UV-C light survival

UV-C survival was assessed by plating the cells after exposure to different UV fluences (0-6400 J/m^2) and by calculating the cell viability for each strain. Cells were grown at 37°C in TSB until reaching an OD_{590} of 0.6 (approximately corresponding to 1 x 10^8 CFU/ml), when they were centrifuged at 5,000 x *g* for 15 minutes, washed with sterile PBS 1X, and finally resuspended in PBS 1X. UV-C survival experiments were carried on by placing 1 ml of cells in the sterile mini plates and exposing them to different fluences, under continuous stirring. After UV-C irradiation, bacterial cells were plated immediately by multilayer plating [22] and plates were incubated overnight at 37°C. Bacterial cells that did not receive UV-C light were used as controls to measure the viable count. Cell viability was determined by counting the number of colonies, and survival was calculated based on the viable cell obtained in absence of UV-C light. Results are obtained from at least three independent experiments.

To choose the optimal parameters for the UV fluctuation tests, an additional survival experiment was performed by irradiating bacteria with the same UV fluence of 50 J/m^2 but varying irradiance and time.

3.7. Mutation rate estimation

Mutation rate was determined by fluctuation analysis in absence or presence of physical (UV-C light) and chemical (mitomycin C) stimuli. Strains were grown in TSB at 37°C until they reached an OD_{590} of approximately 0.6 and 1ml-aliquots, containing glycerol at a final concentration of 10%, were stored at -80°C to provide a stock for mutation rate experiments. Prior to freezing, both the viable count and the number of pre-existing rifampicin-resistant mutants was determined.

For mutation rate determination in absence of stimuli, a set of 10 independent cultures for each strain were inoculated with approximately 1 x 10^5 CFU from the same frozen starter culture. For

mutation rate determination following UV-C light induction, the starter cultures were irradiated at an UV fluence of 50 J/m^2 before inoculum. In order to determine the appropriate dilutions to obtain the same initial inoculum of 1 x 10^5 CFU, bacterial viability after irradiation was inferred by UV-C survival data. For determining the mutation rate in the presence of mitomycin C, a known prophage inducer and DNA damaging agent, a protocol similar to that of prophage induction was followed: the 10 independent cultures were inoculated with approximately 1 x 10^5 CFU from the same frozen starters and were grown at 37°C until they reached the early exponential phase (approximately OD_{590} = 0.1) when a final concentration of 100 ng/ml of mitomycin C was added. In all cases, cultures were then grown at 37°C until they reached mid-log phase (approximately at the 12^{th} generation) when the number of rifampicin-resistant mutants was determined by plating 0.1-ml aliquots following a multilayer plating procedure[22] in the presence of 20 μg/ml rifampicin. The viable count (N_t) was also determined by plating the appropriate dilutions from one representative culture in the absence of antibiotics. Plates were incubated at 37°C in presence of 5% CO_2 and colony counts were determined after 24h and 48h. The assay was repeated 3 times for each strain and the rifampicin-resistant mutant counts were pooled into single data sets representing 30 cultures per each condition of each strain[31]. The mutation rates (μ) determination and statistical analysis from the fluctuation assays were carried out using the R package rSalvador[32].

The expected number of mutations per culture (m) was first obtained with the use of the function *newton.LD.plating*, which computes the maximum likelihood estimates (MLE) of m, adjusting to the plating efficiency, i.e. when only a portion of the culture is plated. Once the estimate of m was obtained, the mutation rate (μ) was determined by dividing m by the number of cell divisions that had taken place. Since the final number of cells in a culture, N_t, arises from N_t-1 division, the mutation rate is:

$$\mu = \frac{m}{Nt - 1} \approx \frac{m}{Nt}$$

where N_t -1 is equal to the number of generations and can be approximated to N_t [4,32].

Differences in mutation rates were compared using the rSalvador R package[32]. rSalvador allows mutation rate comparison, taking into consideration both the plating efficiency and the final cell number N_t, which is a value that differs noticeably between different strains or particular experimental conditions. The recommended approaches comprise the likelihood ratio test (LRT)[32–34] or visually check the overlapping of the 84% C.I.s of two mutation rates: if the two C.I.s overlap, the test is not significant at the 5% level. Difference in the mutation rates obtained in this study were compared by likelihood ratio test (LRT) by applying the *compare.LD.plating* function pairwise among all conditions. The *p.adjust* R function was then used to correct the overall false positive rate of the obtained p values for multiple comparisons. Differences in the mutation rate were considered significant only when the adjusted p values were less than 0.05[31].

4. Results

4.1. Strain construction

We used two unencapsulated *Streptococcus pneumoniae* strains for constructing a group of three isogenic derivatives, (i) devoid of φ1207.3, (ii) carrying φ1207.3 and (iii)carrying a recombinant φ1207.3, devoid of the SOS-like gene cassette. The first group was constructed in *S. pneumoniae* R6 strain, which is a standard laboratory strain and displays a functional Mismatch Repair System (*hex*+)[27,28]. The second group, instead, was constructed in hypermutable *S. pneumoniae* Rx1 strain, naturally MMR-deficient (*hex*-)[28,35], thus exhibiting a naturally higher mutation rate baseline[36–38] , and engineered to lack natural competence for transformation[39].

4.2. UV fluence determination

Since the UV fluence is calculated by multiplying the irradiance for the exposure time, and since the instrument allowed for the use of ten different intensities, the same UV fluence could be obtained with the use of different parameters. To choose the optimal parameters for the UV fluctuation tests, an experiment was performed in which the bacterial survival was detected using the same UV fluence of 50 J/m^2 but varying the irradiance and the time (Figure 2). We observed

that the bacterial survival was in the same range (from 3 to 5%) for all the parameters tested, but that at higher irradiance intensities with lower exposure times, and at higher exposure times with lower intensities, the variability in the bacterial survival was higher. For this reason, the intermediate parameter, corresponding to intensity 6 of the instrument (irradiance of 2.057 W/m^2) and exposure time of 24s, was chosen for the UV fluctuation tests.

4.3. The SOS-like cassette of φ1207.3 confers UV-C resistance in *S. pneumoniae*

To assess whether the SOS-like cassette of φ1207.3 is involved in increased survival upon UV-C light treatment, the bacterial viability of the three isogenic strains of both groups was measured upon exposure to different UV-C fluences (0-6400 J/m^2).

For *S. pneumoniae* R6, comparison of the UV-C light survival of the three strains showed an increased resistance of FR173, carrying the φ1207.3 prophage, compared to the control strain FR172, not carrying φ1207.3, and the control strain FR174, carrying a recombinant φ1207.3, with the SOS-like cassette deleted, indicating an involvement of this cassette in the UV protection (Figure 3A). Only at high fluences (6400 J/m^2), the increase in the survival of the strain carrying the prophage is no more visible, possibly due to the fact that, at high UV fluences, the accumulation of damages induced by the UV-C light could be so high to cause the death of most of the bacterial cells, hindering the phage ability to exploit the bacterial cell machinery and fully activate the SOS-like response. Even for *S. pneumoniae* Rx1, naturally MMR-deficient, comparison of the UV-C light survival showed an increased resistance of FR169, carrying φ1207.3, compared to the other two control strains, FP11 (not carrying the phage) and FR171 (carrying the φ1207.3Δ*orf6-11*) (Figure 3B). Even in this case, the effect of the SOS-like cassette on UV-C resistance was visible at all UV fluences except for the 3200 and 6400 J/m^2 fluences, where the UV-C survival of the three strains was similar.

4.4. Mutation rate is increased in the presence of the φ1207.3 SOS-like cassette in *S. pneumoniae*, upon both mitomycin C and UV-C light exposure

The mutation rate of the three isogenic strains of the two groups was measured to determine whether the presence of the φ1207.3 phage, and in particular the SOS-like cassette, causes the activation of a SOS-like response in *S. pneumoniae*, defined as the increase of survival and mutagenesis, in response to chemical (mitomycin C) and physical (UV-C light) stresses. The mutation rate determination was obtained by measuring the arise of mutations causing rifampicin resistance. Rifampicin resistance occurs by mutation in the *rpoB* gene coding for the β subunit of RNA polymerase[40,41], allowing the polymerase to overcome the block caused by the antibiotic.

For the *S. pneumoniae* R6 group, exposure to UV-C light caused a significant increase of the mutation rate in the φ1207.3-carrying strain (10-fold increase, p-value <0.0001, Figure 4A), whereas no significant increase was observed in the other two control strains, FR172 devoid of the phage (0.8-fold increase, p-value=0.65) and FR174 carrying the recombinant φ1207.3 deleted of the *orf6-11* (0.8-fold increase, p-value=0.65). Upon exposure to mitomycin C, the φ 1207.3-carrying strain showed a significant increase in the mutation rate (2.9-fold increase, p-value=0.004, Figure 4A), while the control strains, FR172 and FR174, showed no significant increase in the mutation rate (1.8-fold increase, p-value=0.47, and 1.4-fold increase, p-value=0.57, respectively).

For the *S. pneumoniae* Rx1 group, induction with UV-C light showed a significant increase in mutagenesis in FR173, carrying the SOS-like cassette (1.3-fold increase, p-value = 0.004, Figure 4B) whereas no significant increase was observed in the other two control strains, FP11 devoid of the phage (1.0-fold increase, p-value=0.95) and FR171 carrying the recombinant φ1207.3 deleted of the *orf6-11* (1.1-fold increase, p-value=0.21). Mitomycin C induction showed a significant increase in the mutation rate of the φ1207.3-carrying strain FR169 (1.5-fold increase, p-value=0.004), while the increase in the FR171 strain, carrying the recombinant φ1207.3, was not significant (1.2-fold increase, p-value=0.18). The strain devoid of the phage, FP11, showed a significant decrease in the mutation rate (2.2-fold decrease, p-value=<0.0001) upon exposure to mitomycin C, in contrast to the other strains carrying the prophage.

5. Discussion

Despite the quite low mutation rates displayed by bacteria in stable environments, strains carrying higher mutation rates are normally found in both natural and clinical bacterial populations[42]. These strains, called mutators (or hypermutable strains), usually arise as a consequence of the loss of DNA proofreading ability during replication and have been found in populations of pathogenic bacteria[43], where are frequently exposed to variable and changing stressful conditions (antibiotic treatments, host defenses, etc.). These strains are frequently responsible for boosting the evolution, through acquisition and variation of virulence and resistance determinants[44]. The increase of the mutation rate represents a double-edged sword for bacteria. On one hand, a higher mutation rate increases the probability of acquiring beneficial mutations that allow these strains to better survive, adapt and evolve during stressful conditions. On the other hand, a higher mutation rate becomes detrimental in the long run, as it increases the probability of accumulating negative and lethal mutations, leading to decreased fitness of the mutators in the bacterial population. Bacteria have evolved a fine solution to balance the beneficial and harmful aspects of hypermutation. This solution consists of producing this hypermutable phenotype only when needed, by creating transient mutators able to increase the mutation rates in response to stresses and to revert back to normal mutation rates when the stress has ceased[45,46]. One way to achieve this temporary hypermutation is through the activation of an SOS repair system[6,7].

In the present work, we demonstrated that the *Streptococcus pyogenes* phage φ1207.3 not only is carries macrolide resistance but also codes for a gene cassette responsible for the activation of an SOS-like response in *Streptococcus pneumoniae*, known to lack it. The activation of this SOS-like cassette is only visible in the presence of stressful conditions, representing a transient activation of hypermutability, thus allowing for a reduced accumulation of detrimental mutations and simultaneously conferring an evolutionary advantage to bacterial cells. Mutators in bacterial and, particularly, pathogenic communities, represent a huge problem in clinical settings in many bacteria (even in *S. pneumoniae*[47–50]), since under stressful conditions, such as antibiotic treatments

(even at sub-inhibitory concentrations) and host defenses, they can lead to evolution of virulence and resistance traits, with consequent increase of therapeutic failures and occurrence of vaccine-escape mutants[31,51–55].

Tables

Table 1. **Bacterial strains used in this work and relative properties.**

Strain	Properties	References
S. pneumoniae R6		
FR172	*S. pneumoniae* R6 (*hex*+) unencapsulated derivative, Sm^R	This study
FR173	FR172 derivative carrying φ1207.3, Sm^R, Em^R	This study
FR174	FR172 derivative carrying φ1207.3Δ*orf6-11*, Sm^R, Em^R, Km^R	This study
S. pneumoniae Rx1		
FP11	*S. pneumoniae* Rx1 (*hex*-) unencapsulated competence deficient derivative, ΔcomC, Cm^R, Nov^R	[26,39]
FR169	FP11 derivative carrying φ1207.3, Cm^R, Nov^R, Em^R	This study
FR171	FP11 derivative carrying φ1207.3Δ*orf6-11*, Cm^R, Nov^R, Em^R, Km^R	This study

Notes: Sm, streptomycin; Em, erythromycin; Km, kanamycin; Cm^R, chloramphenicol; Nov^R, novobiocin

Table 2**. Oligonucleotides used in this study.**

Name	Sequence (5'-3')[a]	Target	Genbank ID: nucleotides
IF149	CAAGCTGGGGATCCGTTTGAT	Kanamycin resistance cassette, 5' end	AY334018.1: 5-25
IF210	CTAAAACAATTCATCCAGTAAAATAT	Kanamycin resistance cassette, 3' end	AY334019.1: 845-870
IF242	TTAAACCATGAAGAAGGAATTTC	Upstream fragment, 5' end	AY657002.1: 5634-5656
IF239	ATCAAACGGATCCCCAGCTTGGAGCAGTTCGATTTACTGTT	Upstream fragment, 3' end	AY657002.1: 6169-6188
IF240	ATATTTTACTGGATGAATTGTTTTAGGTTCCCCTCCTTTTTGTCTA	Downstream fragment, 5' end	AY657002.1: 9298-9317
IF241	CCCAAGCAGGTAAACGTCTA	Downstream fragment, 3' end	AY657002.1: 10095- 10114

[a]The underlined sequence is complementary to IF149 (for IF239) and IF210 (for IF240).

Table 3. **Irradiance at 265nm of the ten intensities of the PearlLab Micro instrument (Aquisense Technologies).** The irradiance (or fluence rate) at 265nm of the ten instrument intensities were measured three times with a ILT1400 radiometer and SED240/W detector (International Light Technologies, Peabody, MA). Mean and standard deviation for each intensity is reported.

Intensity	Mean irradiance ± SD (W/m^2)
1	$6.21 \times 10^{-2} \pm 8.08 \times 10^{-4}$
2	$1.74 \times 10^{-1} \pm 7.81 \times 10^{-3}$
3	$4.41 \times 10^{-1} \pm 1.11 \times 10^{-2}$
4	$8.79 \times 10^{-1} \pm 1.75 \times 10^{-2}$
5	$1.18 \times 10^{0} \pm 2.52 \times 10^{-2}$
6	$2.06 \times 10^{0} \pm 4.04 \times 10^{-2}$
7	$2.67 \times 10^{0} \pm 3.61 \times 10^{-2}$
8	$3.21 \times 10^{0} \pm 2.65 \times 10^{-2}$
9	$3.70 \times 10^{0} \pm 1.53 \times 10^{-2}$
10	$4.08 \times 10^{0} \pm 1.73 \times 10^{-2}$

FIGURE LEGEND

Figure 1. **UV-C LED instrument and 3D-printed holder, plates and lids.** A) An UV-C LED instrument (PearlLab Micro Aquisense Technologies) was used with a B) set of 3D-printed holder, autoclavable plates and lids.

Figure 2. **Detection of bacterial survival using the same UV fluence of 50 J/m^2 but varying the irradiance and the time.** On the x axis is reported the exposure time, on the left y axis the irradiance (W/m2) and on the right y axis the bacterial survival (%). The irradiance progression is indicated with an open circle, the survival with a filled square. Results are obtained from at least three independent experiments.

Figure 3. **Effect of different doses of UV-C light irradiation on *S. pneumoniae* cell survival.** A)UV-C light survival for the *S. pneumoniae* R6 isogenic group. The strain FR173 (filled square, in green), carrying the wild type φ1207.3, shows an increased cell survival at all UV fluences, except for UV fluence of 6400 J/m^2, compared to the other two strains, FR172 (open circle, in black) devoid of the phage, and FR174 (closed triangle, in red), which carries the phage deleted of the *orf*6-11. B) UV-C light survival for the *S. pneumoniae* Rx1 isogenic group. The strain FR169 (filled square, in green), carrying the wild type φ1207.3, shows an increased cell survival at all UV fluences, except for UV fluences of 3200 and 6400 J/m^2, compared to the other two strains, FP11 (open circle, in black) devoid of the phage, and FR171 (closed triangle, in red), which carries the phage deleted of the *orf*6-11. Results are reported as means of at least three independent experiments with standard deviations (error bars). In each experiment, 100% survival was based on the cell viability measured in plates not receiving UV irradiation (0 J/m^2).

Figure 4. **Mutation rates estimation in absence and presence of subinhibitory concentration of mitomycin C and UV-C light.** The mutation rates to rifampicin resistance are reported for A) the *S. pneumoniae* R6 isogenic group, and B) the *S. pneumoniae* Rx1 isogenic group. Not treated, absence of mitomycin C or UV-C light; Mitomycin C 100 ng/ml, mitomycin C added at the early

exponential phase at a final concentration of 100 ng/ml; 50 J/m^2, UV 50 J/m^2, cells receiving UV-C light irradiation at a UV fluence of 50 J/m^2. Results are reported as means of at least three independent experiments with 84% confidence intervals.

6. References

1. Friedberg EC, Friedberg EC, editors. DNA repair and mutagenesis. 2nd ed. Washington, D.C: ASM Press; 2006. 1118 p.
2. Pope CF, O'Sullivan DM, McHugh TD, Gillespie SH. A Practical Guide to Measuring Mutation Rates in Antibiotic Resistance. AAC. 2008 Apr;52(4):1209–14.
3. Rosche WA, Foster PL. Determining Mutation Rates in Bacterial Populations. Methods. 2000 Jan;20(1):4–17.
4. Foster PL. Methods for Determining Spontaneous Mutation Rates. In: Methods in Enzymology [Internet]. Elsevier; 2006 [cited 2021 Mar 6]. p. 195–213. Available from: https://linkinghub.elsevier.com/retrieve/pii/S0076687905090129
5. Goodman MF. Better living with hyper-mutation: Hypermutation. Environ Mol Mutagen. 2016 Jul;57(6):421–34.
6. Radman M. SOS Repair Hypothesis: Phenomenology of an Inducible DNA Repair Which is Accompanied by Mutagenesis. In: Hanawalt PC, Setlow RB, editors. Molecular Mechanisms for Repair of DNA [Internet]. Boston, MA: Springer US; 1975 [cited 2021 Mar 16]. p. 355–67. Available from: http://link.springer.com/10.1007/978-1-4684-2895-7_48
7. Maslowska KH, Makiela-Dzbenska K, Fijalkowska IJ. The SOS system: A complex and tightly regulated response to DNA damage. Environ Mol Mutagen. 2019 May;60(4):368–84.
8. Baharoglu Z, Mazel D. SOS, the formidable strategy of bacteria against aggressions. FEMS Microbiol Rev. 2014 Nov;38(6):1126–45.
9. Fijalkowska IJ, Schaaper RM, Jonczyk P. DNA replication fidelity in Escherichia coli: a multi-DNA polymerase affair. FEMS Microbiology Reviews. 2012 Nov 1;36(6):1105–21.
10. Tang M, Pham P, Shen X, Taylor J-S, O'Donnell M, Woodgate R, et al. Roles of E. coli DNA polymerases IV and V in lesion-targeted and untargeted SOS mutagenesis. Nature. 2000 Apr;404(6781):1014–8.
11. Varhimo E, Savijoki K, Jalava J, Kuipers OP, Varmanen P. Identification of a Novel Streptococcal Gene Cassette Mediating SOS Mutagenesis in Streptococcus uberis. JB. 2007 Jul 15;189(14):5210–22.
12. Gasc AM, Sicard N, Claverys JP, Sicard AM. Lack of SOS repair in Streptococcus pneumoniae. Mutation Research/Fundamental and Molecular Mechanisms of Mutagenesis. 1980 Apr;70(2):157–65.
13. Prudhomme M, Attaiech L, Sanchez G, Martin B, Claverys J-P. Antibiotic Stress Induces Genetic Transformability in the Human Pathogen *Streptococcus pneumoniae*. Science. 2006 Jul 7;313(5783):89–92.
14. Iannelli F, Santoro F, Oggioni MR, Pozzi G. Nucleotide sequence analysis of integrative conjugative element Tn5253 of Streptococcus pneumoniae. Antimicrob Agents Chemother. 2013/12/02 ed. 2014;58(2):1235–9.
15. Munoz-Najar U, Vijayakumar MN. An Operon That Confers UV Resistance by Evoking the SOS Mutagenic Response in Streptococcal Conjugative Transposon Tn5252. J Bacteriol. 1999 May 1;181(9):2782–8.
16. Savijoki K, Ingmer H, Frees D, Vogensen FK, Palva A, Varmanen P. Heat and DNA damage induction of the LexA-like regulator HdiR from Lactococcus lactis is mediated by RecA and ClpP: RecA and ClpP modulate the expression of HdiR. Molecular Microbiology. 2003 Sep 9;50(2):609–21.

17. Santagati M, Iannelli F, Cascone C, Campanile F, Oggioni MR, Stefani S, et al. The Novel Conjugative Transposon Tn1207.3 Carries the Macrolide Efflux Gene mef(A) in Streptococcus pyogenes. Microbial Drug Resistance. 2003 Aug;9(3):243–7.
18. Pozzi G, Iannelli F, Oggioni M, Santagati M, Stefani S. Genetic Elements Carrying Macrolide Efflux Genes in Streptococci. CDTID. 2004 Sep 1;4(3):203–6.
19. Iannelli F, Santagati M, Santoro F, Oggioni MR, Stefani S, Pozzi G. Nucleotide sequence of conjugative prophage Φ1207.3 (formerly Tn1207.3) carrying the mef(A)/msr(D) genes for efflux resistance to macrolides in Streptococcus pyogenes. Front Microbiol. 2014 Dec 9;5:687–687.
20. Iannelli F, Santoro F, Santagati M, Docquier J-D, Lazzeri E, Pastore G, et al. Type M Resistance to Macrolides Is Due to a Two-Gene Efflux Transport System of the ATP-Binding Cassette (ABC) Superfamily. Front Microbiol. 2018 Jul 31;9:1670.
21. Permina EA, Mironov AA, Gelfand MS. Damage-repair error-prone polymerases of eubacteria: association with mobile genome elements. Gene. 2002 Jun;293(1–2):133–40.
22. Iannelli F, Santoro F, Fox V, Pozzi G. A Mating Procedure for Genetic Transfer of Integrative and Conjugative Elements (ICEs) of Streptococci and Enterococci. MPs. 2021 Aug 28;4(3):59.
23. Horton RM, Cai Z, Ho SN, Pease LR. Gene Splicing by Overlap Extension: Tailor-Made Genes Using the Polymerase Chain Reaction. BioTechniques [Internet]. 2013 Mar 1 [cited 2021 Mar 6];54(3). Available from: https://www.future-science.com/doi/10.2144/000114017
24. Iannelli F, Pozzi G. Method for Introducing Specific and Unmarked Mutations Into the Chromosome of Streptococcus pneumoniae. MB. 2004;26(1):81–6.
25. Pearce BJ, Iannelli F, Pozzi G. Construction of new unencapsulated (rough) strains of Streptococcus pneumoniae. Research in Microbiology. 2002;5.
26. Santoro F, Oggioni MR, Pozzi G, Iannelli F. Nucleotide sequence and functional analysis of the tet (M)-carrying conjugative transposon Tn5251 of Streptococcus pneumoniae: Tn5251 of Streptococcus pneumoniae. FEMS Microbiology Letters. 2010 Apr 28;no-no.
27. Hoskins J, Alborn WE, Arnold J, Blaszczak LC, Burgett S, DeHoff BS, et al. Genome of the Bacterium *Streptococcus pneumoniae* Strain R6. J Bacteriol. 2001 Oct;183(19):5709–17.
28. Shoemaker NB, Guild WR. Destruction of low efficiency markers is a slow process occurring at a heteroduplex stage of transformation. Molec Gen Genet. 1974 Dec;128(4):283–90.
29. Kowalski W. Ultraviolet Germicidal Irradiation Handbook: UVGI for Air and Surface Disinfection [Internet]. Berlin, Heidelberg: Springer Berlin Heidelberg; 2009 [cited 2021 Mar 6]. Available from: http://link.springer.com/10.1007/978-3-642-01999-9
30. Bolton JR, Linden KG. Standardization of Methods for Fluence (UV Dose) Determination in Bench-Scale UV Experiments. J Environ Eng. 2003 Mar;129(3):209–15.
31. Silayeva O, Engelstädter J, Barnes AC. Evolutionary epidemiology of Streptococcus iniae: Linking mutation rate dynamics with adaptation to novel immunological landscapes. Infect Genet Evol. 2020 Nov;85:104435.
32. Zheng Q. rSalvador: An R Package for the Fluctuation Experiment. G3 (Bethesda). 2017 Dec 4;7(12):3849–56.
33. Zheng Q. Methods for comparing mutation rates using fluctuation assay data. Mutation Research/Fundamental and Molecular Mechanisms of Mutagenesis. 2015 Jul;777:20–2.
34. Zheng Q. Comparing mutation rates under the Luria–Delbrück protocol. Genetica. 2016 Jun;144(3):351–9.

35. Guild WR, Shoemaker NB. Mismatch correction in pneumococcal transformation: donor length and hex-dependent marker efficiency. J Bacteriol. 1976 Jan;125(1):125–35.
36. Tiraby J-G, Fox MS. Marker Discrimination in Transformation and Mutation of Pneumococcus. Proceedings of the National Academy of Sciences. 1973 Dec 1;70(12):3541–5.
37. Tiraby J-G, Fox Ms. Marker Discrimination And Mutagen-Induced Alterations In Pneumococcal Transformation. Genetics. 1974 Jul 1;77(3):449–58.
38. Claverys JP, Lacks SA. Heteroduplex deoxyribonucleic acid base mismatch repair in bacteria. Microbiol Rev. 1986 Jun;50(2):133–65.
39. Iannelli F, Pozzi G. Protocol for conjugal transfer of genetic elements in Streptococcus pneumoniae. In 2007.
40. Wehrli W. Rifampin: Mechanisms of Action and Resistance. Clinical Infectious Diseases. 1983 Jul 1;5(Supplement_3):S407–11.
41. Goldstein BP. Resistance to rifampicin: a review. J Antibiot. 2014 Sep;67(9):625–30.
42. Tanaka MM, Bergstrom CT, Levin BR. The Evolution of Mutator Genes in Bacterial Populations: The Roles of Environmental Change and Timing. Genetics. 2003 Jul 1;164(3):843–54.
43. Sundin GW, Weigand MR. The microbiology of mutability. FEMS Microbiology Letters. 2007 Dec;277(1):11–20.
44. Denamur E, Matic I. Evolution of mutation rates in bacteria. Mol Microbiol. 2006 May;60(4):820–7.
45. Eliopoulos GM, Blazquez J. Hypermutation as a Factor Contributing to the Acquisition of Antimicrobial Resistance. Clinical Infectious Diseases. 2003 Nov 1;37(9):1201–9.
46. Chopra I, O'Neill AJ, Miller K. The role of mutators in the emergence of antibiotic-resistant bacteria. Drug Resistance Updates. 2003 Jun;6(3):137–45.
47. Negri M-C, Morosini M-I, Baquero M-R, Campo R del, Blázquez J, Baquero F. Very Low Cefotaxime Concentrations Select for Hypermutable Streptococcus pneumoniae Populations. AAC. 2002 Feb;46(2):528–30.
48. Gould CV, Sniegowski PD, Shchepetov M, Metlay JP, Weiser JN. Identifying Mutator Phenotypes among Fluoroquinolone-Resistant Strains of Streptococcus pneumoniae Using Fluctuation Analysis. AAC. 2007 Sep;51(9):3225–9.
49. Cortes PR, Piñas GE, Albarracin Orio AG, Echenique JR. Subinhibitory concentrations of penicillin increase the mutation rate to optochin resistance in Streptococcus pneumoniae. Journal of Antimicrobial Chemotherapy. 2008 Nov;62(5):973–7.
50. Henriques-Normark B, Blomberg C, Dagerhamn J, Bättig P, Normark S. The rise and fall of bacterial clones: Streptococcus pneumoniae. Nat Rev Microbiol. 2008 Nov;6(11):827–37.
51. Giraud A, Matic I, Radman M, Fons M, Taddei F. Mutator Bacteria as a Risk Factor in Treatment of Infectious Diseases. Antimicrob Agents Chemother. 2002 Mar;46(3):863–5.
52. Labat F, Pradillon O, Garry L, Peuchmaur M, Fantin B, Denamur E. Mutator phenotype confers advantage in *Escherichia coli* chronic urinary tract infection pathogenesis. FEMS Immunology & Medical Microbiology. 2005 Jun;44(3):317–21.
53. Oliver A, Mena A. Bacterial hypermutation in cystic fibrosis, not only for antibiotic resistance. Clinical Microbiology and Infection. 2010 Jul;16(7):798–808.

54. Jolivet-Gougeon A, Kovacs B, Le Gall-David S, Le Bars H, Bousarghin L, Bonnaure-Mallet M, et al. Bacterial hypermutation: clinical implications. Journal of Medical Microbiology. 2011 May 1;60(5):563–73.
55. Gifford DR, Berríos-Caro E, Joerres C, Galla T, Knight CG. Mutators drive evolution of multi-resistance to antibiotics. bioRxiv. 2019 Jan 1;643585.

Figure 1

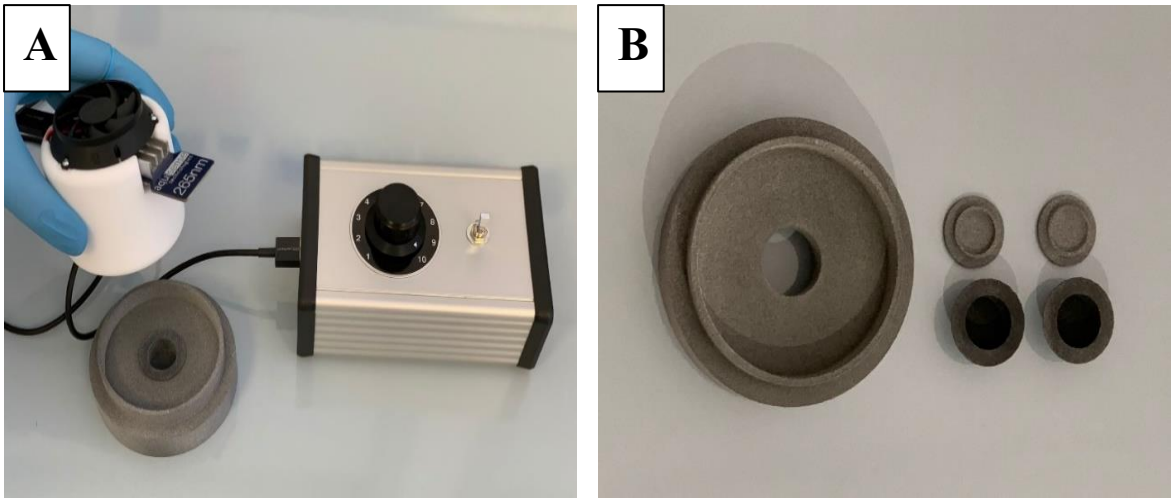

Figure 2

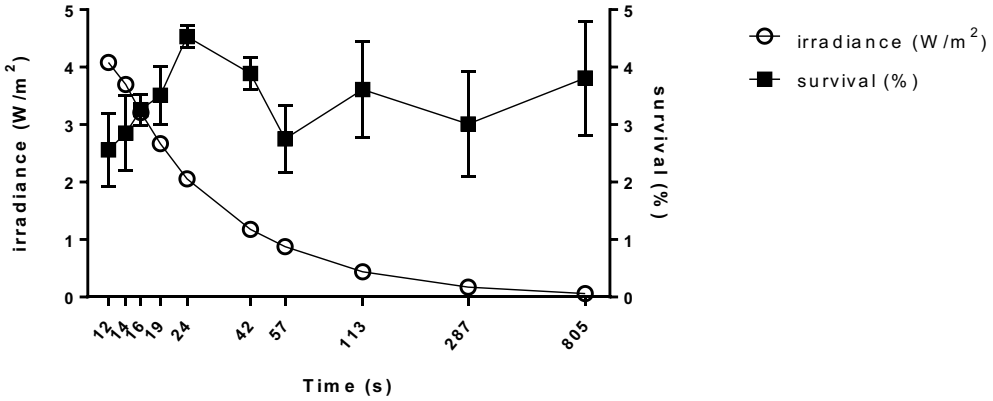

Figure 3

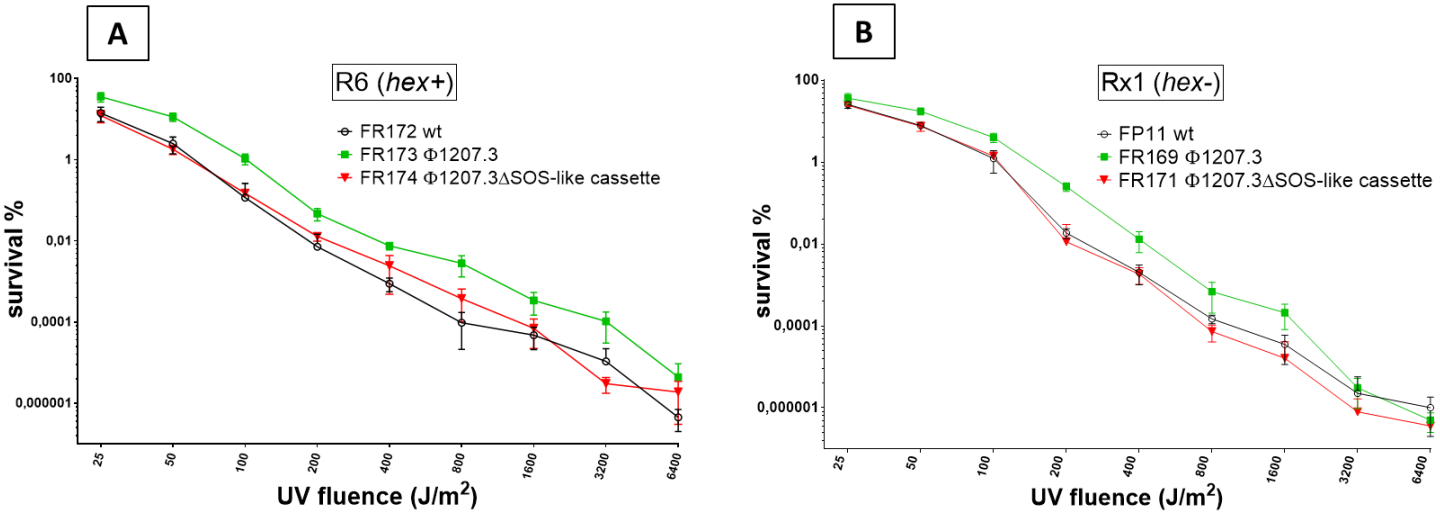

Figure 4

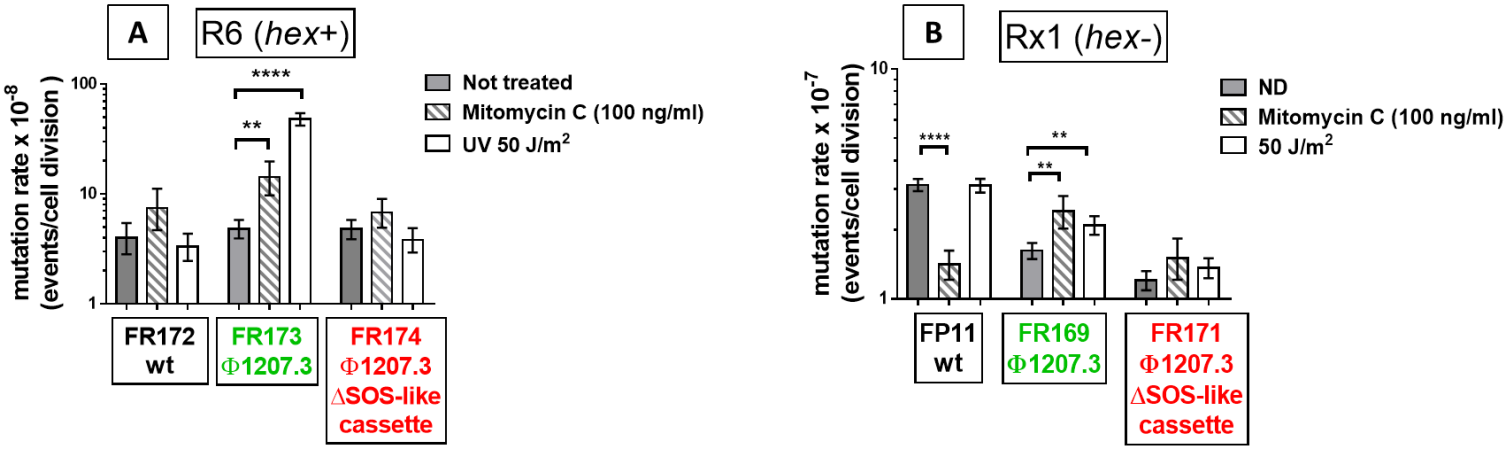

CHAPTER 3

Disbalancing Envelope Stress Responses as a Strategy for Sensitization of Escherichia coli to Antimicrobial Agents

Esther Recacha[1,2,3], Valeria Fox[4], Sara Díaz-Díaz[2,3,5], Ana García-Duque[1], Fernando Docobo-Pérez[2,3,5], Álvaro Pascual[1,2,3,5] and José Manuel Rodríguez-Martínez[2,3,5]

[1]*Unidad Clínica de Enfermedades Infecciosas, Microbiología y Medicina Preventiva, Hospital Universitario Virgen Macarena, Seville, Spain*

[2]*Red Española de Investigación en Patología Infecciosa (REIPI), Instituto de Salud Carlos III, Madrid, Spain*

[3]*Instituto de Biomedicina de Sevilla (IBiS), Hospital Universitario Virgen del Rocío/CSIC/Universidad de Sevilla, Seville, Spain*

[4]*Laboratory of Molecular Microbiology and Biotechnology, Department of Medical Biotechnologies, University of Siena, Siena, Italy*

[5]*Departamento de Microbiología, Universidad de Sevilla, Seville, Spain*

Frontiers in Microbiology 2021

frontiers in Microbiology

ORIGINAL RESEARCH
published: 07 April 2021
doi: 10.3389/fmicb.2021.653479

Disbalancing Envelope Stress Responses as a Strategy for Sensitization of *Escherichia coli* to Antimicrobial Agents

Esther Recacha[1,2,3], Valeria Fox[4], Sara Díaz-Díaz[2,3,5], Ana García-Duque[1], Fernando Docobo-Pérez[2,3,5], Álvaro Pascual[1,2,3,5] and José Manuel Rodríguez-Martínez[2,3,5]*

[1] Unidad Clínica de Enfermedades Infecciosas, Microbiología y Medicina Preventiva, Hospital Universitario Virgen Macarena, Seville, Spain, [2] Red Española de Investigación en Patología Infecciosa (REIPI), Instituto de Salud Carlos III, Madrid, Spain, [3] Instituto de Biomedicina de Sevilla (IBiS), Hospital Universitario Virgen del Rocío/CSIC/Universidad de Sevilla, Seville, Spain, [4] Laboratory of Molecular Microbiology and Biotechnology, Department of Medical Biotechnologies, University of Siena, Siena, Italy, [5] Departamento de Microbiología, Universidad de Sevilla, Seville, Spain

OPEN ACCESS

Edited by:
Weihui Wu, Nankai University, China

Reviewed by:
Krisztina M. Papp-Wallace, Louis Stokes Cleveland VA Medical Center, United States
Marisa Winkler, Brigham and Women's Hospital and Harvard Medical School, United States

***Correspondence:**
Esther Recacha
erecachavillamor@gmail.com

Specialty section:
This article was submitted to Antimicrobials, Resistance and Chemotherapy, a section of the journal Frontiers in Microbiology

Received: *14 January 2021*
Accepted: *15 March 2021*
Published: *07 April 2021*

Citation:
Recacha E, Fox V, Díaz-Díaz S, García-Duque A, Docobo-Pérez F, Pascual Á and Rodríguez-Martínez JM (2021) Disbalancing Envelope Stress Responses as a Strategy for Sensitization of Escherichia coli to Antimicrobial Agents. Front. Microbiol. 12:653479. doi: 10.3389/fmicb.2021.653479

Disbalancing envelope stress responses was investigated as a strategy for sensitization of *Escherichia coli* to antimicrobial agents. Seventeen isogenic strains were selected from the KEIO collection with deletions in genes corresponding to the σ^E, Cpx, Rcs, Bae, and Psp responses. Antimicrobial activity against 20 drugs with different targets was evaluated by disk diffusion and gradient strip tests. Growth curves and time-kill curves were also determined for selected mutant-antimicrobial combinations. An increase in susceptibility to ampicillin, ceftazidime, cefepime, aztreonam, ertapenem, and fosfomycin was detected. Growth curves for Psp response mutants showed a decrease in optical density (OD) using sub-MIC concentrations of ceftazidime and aztreonam (Δ*pspA* and Δ*pspB* mutants), cefepime (Δ*pspB* and Δ*pspC* mutants) and ertapenem (Δ*pspB* mutant). Time-kill curves were also performed using 1xMIC concentrations of these antimicrobials. For ceftazidime, 2.9 $\log_{10}$ (Δ*pspA* mutant) and 0.9 $\log_{10}$ (Δ*pspB* mutant) decreases were observed at 24 and 8 h, respectively. For aztreonam, a decrease of 3.1 $\log_{10}$ (Δ*pspA* mutant) and 4 $\log10_{10}$ (Δ*pspB* mutant) was shown after 4–6 h. For cefepime, 4.2 $\log_{10}$ (Δ*pspB* mutant) and 2.6 $\log_{10}$ (Δ*pspC* mutant) decreases were observed at 8 and 4 h, respectively. For ertapenem, a decrease of up to 6 $\log_{10}$ (Δ*pspB* mutant) was observed at 24 h. A deficient Psp envelope stress response increased *E. coli* susceptibility to beta-lactam agents such as cefepime, ceftazidime, aztreonam and ertapenem. Its role in repairing extensive inner membrane disruptions makes this pathway essential to bacterial survival, so that disbalancing the Psp response could be an appropriate target for sensitization strategies.

Keywords: envelope stress responses, bacterial sensitization, beta-lactams, antimicrobial resistance, Gram-negative bacteria

INTRODUCTION

Since antimicrobial resistance is increasing worldwide, new targets (Dickey et al., 2017; Recacha et al., 2017; Cattoir and Felden, 2019) need to be sought, either to find new antimicrobial families or to increase the susceptibility of bacterial populations (Laxminarayan et al., 2013). Envelope stress responses are important pathways for bacterial survival in the presence of stressors, including antimicrobials (Guest and Raivio, 2016; Hersch et al., 2020), and their alteration could be proposed as a strategy for weakening bacteria. The Gram-negative envelope is composed of inner membrane (IM), periplasm, containing a thin peptidoglycan (PG) layer, and outer membrane (OM). This envelope provides Gram-negative bacteria with protection against external environmental agents, including antibiotics (Silhavy et al., 2010). The σ^E, Cpx, Rcs, Bae and Psp systems are the main envelope stress response pathways in Gram-negative bacteria for restoring homeostasis to cells with induced envelope damage and are activated in different ways (Guest and Raivio, 2016; Mitchell and Silhavy, 2019). The σ^E response detects perturbations in outer membrane (OM) or lipopolysaccharide (LPS) biogenesis through interactions between either the exposed C-terminus of misfolded outer membrane proteins (OMPs) and the DegS periplasmic protease, or between the anti-anti-s factor RseB and periplasmic LPS molecules, respectively. These both initiate a regulated intramembrane proteolysis cascade ultimately leading to the liberation of σ^E from a membrane-bound anti-sigma factor and the upregulation of adaptive factors, including chaperones, proteases, membrane biogenesis proteins, and a set of small RNAs that downregulate OMP production (Ades, 2004; Ruiz and Silhavy, 2005; Valentin-Hansen et al., 2007; Lima et al., 2013; Flores-Kim and Darwin, 2014; Kim, 2015). The Cpx response is regulated by the CpxA sensor kinase and response regulator CpxR. Envelope stresses causing protein misfolding, and adhesion, inactivate the inhibitor CpxP, trigger CpxA-mediated phosphorylation of CpxR, and altered expression of protein foldases and proteases, respiratory complexes, transporters, and cell wall biogenesis enzymes that impact resistance to a number of antibiotics, particularly aminoglycosides (Raivio, 2014). The Rcs response is regulated by a two-component phosphorelay consisting of two inner membrane (IM)-associated sensor kinase molecules, RcsC and RcsD, together with a cytoplasmic response regulator, RcsB. Multiple environmental parameters and conditions leading to a weakened envelope activate RcsC and/or RcsD, which together catalyze the phosphorylation of RcsB, leading to changes in the expression of genes associated with capsule production, motility, virulence, biofilm formation, and other envelope proteins (Majdalani and Gottesman, 2005; Huang et al., 2006). The Rcs pathway has been linked to resistance to a number of microbially and host produced antimicrobials including beta-lactam antibiotics, cationic antimicrobial peptides and bile (Hirakawa et al., 2003; Erickson and Detweiler, 2006; Laubacher and Ades, 2008; Farris et al., 2010; Farizano et al., 2014). The Psp response is activated by changes linked to the aberrant localization of OM secretin complexes and other conditions that disrupt the IM, including the dissipation of the proton motive force. These signals are transduced through changes in interactions between a set of Psp proteins that ultimately lead to the liberation of the PspF transcription factor from the inhibitor PspA and the upregulated production of a limited set of adaptive factors capable of fostering endurance and survival (Flores-Kim and Darwin, 2014, 2016). Finally, Bae response is controlled by the two-component system made up of the sensor kinase BaeS and its cognate partner BaeR. This pathway is activated by antimicrobial compounds made by plants, animals, and microbes, as well as metals, and can stimulate resistance to broad classes of these substances, primarily, it appears, through the regulation of the multidrug RND efflux pumps AcrD and MdtABC, together with the common OM component TolC (Baranova and Nikaido, 2002; Raffa and Raivio, 2002; Cordeiro et al., 2014; Lin et al., 2014).

The aim of this study was to investigate the effect of alteration of the envelope stress response pathways of the σ^E, Cpx, Rcs, Bae, and Psp systems on sensitization to antimicrobial agents targeting the bacterial cell wall, protein, RNA, DNA or folic acid synthesis.

MATERIALS AND METHODS

Bacterial Strains

A set of 17 *E. coli* strains derived from *E. coli* BW25113 belonging to the KEIO collection were used (Baba et al., 2006). Strains were selected with defective envelope stress responses, with deletions in genes for the σ^E (*rseA* and *rseB* genes), Cpx (*cpxA*, *cpxR*, *cpxP,* and *nlpE* genes), Rcs (*rcsF*, *rcsA*, *rcsC*, *rcsD,* and *rcsB* genes), Bae (*baeR* and *baeS* genes) and Psp responses (*pspA*, *pspB*, *pspC,* and *pspF* genes) (**Supplementary Table 1**). Each deletion was verified by PCR (**Supplementary Table 2**).

Antimicrobial Susceptibility Testing

Antimicrobial susceptibility was determined by disk diffusion (Oxoid®, United Kingdom) and gradient strip tests (Liofilchem®, Italy), using CLSI reference methods (Clinical and Laboratory Standards Institute, 2016.). Any mutant-antimicrobial combination with a halo size that differed by more than 3 mm by disk diffusion from the wild-type (*E. coli* BW25113) was selected for the gradient strip test.

The antimicrobials used were: penicillin G, ampicillin, amoxicillin/clavulanic acid, cefoxitin, ceftazidime, cefepime, ertapenem, imipenem, aztreonam, gentamicin, amikacin, tetracycline, chloramphenicol, colistin, rifampicin, nalidixic acid, ciprofloxacin, sulfonamides compound, sulfamethoxazole/trimethoprim, and fosfomycin.

Growth Curve Assays

Growth curves were performed for mutant-antimicrobial combinations with a decrease of MIC determined by gradient strip tests. Psp mutants (except Δ*pspF*) were tested to betalactams agents listed in **Table 1** despite not showing decreases in MIC value. After overnight culture in Mueller-Hinton broth (MHB) at 37°C, bacterial suspensions were diluted to achieve an OD_{625nm} of 0.1 (*ca.* 10^8 CFU/mL), then diluted 10^{-4}-fold in MHB medium containing sublethal concentrations (0.5xMIC and

TABLE 1 | Susceptibility test determined by gradient strip tests.

	Strain	MIC[a] AMP	Fold change[b]	MIC CAZ	Fold change	MIC FEP	Fold change	MIC ETP	Fold change	MIC ATM	Fold change	MIC FOS	Fold change	MIC IPM	Fold change	MIC AK	Fold change	MIC C	Fold change
	BW[c]	6		0.19		0.032		0.012		0.047		0.5		0.19		0.5		8	
σ^E response	Δ*rseA*	–		–		–		–		–		0.5	1	–		–		–	
Cpx response	Δ*cpxA*	–		–		–		0.016	0.75	–		–		–		–		8	1
	Δ*cpxR*	8	0.75	0.19	1	0.032	1	0.012	1	0.047	1	0.5	1	–		2	0.25	–	
	Δ*cpxP*	–		–		–		–		0.047	1	0.5	1	–		–		–	
Rcs response	Δ*rcsF*	–		–		–		0.016	0.75	–		–		0.19	1	–		–	
	Δ*rcsC*	–		–		0.064	0.5	0.016	0.75	–		0.5	1	0.25	0.76	–		–	
	Δ*rcsD*	–		0.19	1	0.032	1	0.012	1	0.032	1.5	0.38	1.3	–		–		–	
	Δ*rcsB*	–		0.19	1	0.032	1	0.012	1	0.047	1	0.5	1	0.19	1	–		–	
Bae response	Δ*baeR*	–		0.125	1	0.032	1	0.012	1	0.032	1.5	0.5	1	–		–		8	1
	Δ*baeS*			–		–		–		–		0.5	1	–		–		–	
Psp response	Δ*pspA*	–		0.094	2	0.023	1.4	0.008	1.5	0.047	1	–		–		–		–	
	Δ*pspB*	–		0.094	2	0.023	1.4	0.012	1	–		–		–		–		–	
	Δ*pspC*	4	1.5	0.125	1.5	–		0.012	1	0.032	1.5	0.5	1	–		–		8	1
	Δ*pspF*	–		0.19	1	0.032	1	0.016	0.75	–		0.5	1	–		–		8	1

AMP, ampicillin; CAZ, ceftazidime; FEP, cefepime; ETP, ertapenem; ATM, aztreonam; FOS, fosfomycin; IPM, imipenem; AK, amikacin; C, chloramphenicol.

[a] *MIC (mg/L) of antimicrobial agent by gradient strip test.*

[b] *Fold reduction of MIC compared to the MIC of strains (wild-type SOS response).*

[c] *Wild-type (E. coli BW25113).*

Cells with no data correspond to mutant-antimicrobial combinations that were not determined.

Green cells- susceptibility increased to antimicrobials; Yellow cells- No changes in susceptibility; Red cells- Resistance increased (relative to wild-type).

0.25xMIC relative to wild-type) of each antimicrobial agent. One hundred and fifty microliters of the diluted bacterial culture were then distributed among 96-well transparent flat bottom plates (Greiner Bio-One, Germany). Cultures were incubated at 37°C on an orbital shaker and agitated (2-mm orbital shaking, 450 rpm, 10 s) for 24 h, and measured with an Infinite 200 PRO plate reader (Tecan). Optical density (OD_{595}) measurements were obtained every 20 min. At least 4 biological replicates were measured for each condition in at least two independent assays.

Time-Kill Curve Assays

To show the effect of alteration of the stress response pathways on bacterial viability, time-kill curve assays were performed with the Δ*pspA,* Δ*pspB* Δ*pspC* mutants. MHB with 1xMIC concentrations of ceftazidime (CAZ), cefepime (FEP), ertapenem (ETP), ampicillin (AMP), and aztreonam (ATM) were used. Antimicrobial concentrations were relative to the MICs for strains harboring unmodified stress responses (wild-type). Growth in drug-free broth was evaluated in parallel as a control. Cultures were incubated at 37°C with shaking at 250 rpm. An initial inoculum of 10^5 CFU/mL was used in all experiments; bacterial concentrations were determined at 0, 2, 4, 6, 8, and 24 h by colony counting.

Statistical Analysis

All statistical analyses were performed using Graphpad Prism 6 software[1]. The Student's *t*-test was used for statistical evaluation when two groups were compared. Differences were considered significant when $P < 0.05$.

RESULTS

Sensitization of *E. coli* to Antimicrobials Agents Determined by Disk Diffusion and Gradient Strip Test

Twenty antimicrobials were tested by disk diffusion (**Supplementary Table 3**) in the initial screening (340 mutant-drug combinations were tested). Psp response was the most sensitized stress pathway with 22.5% of drug-gene deletion combinations affected, followed in descending order, by the Rcs (18%), Bae (17.5%), Cpx (13.7%), and σ^E responses (2.5%). To confirm these data, the gradient strip test (**Table 1**) was used to evaluate the activity of 9 antimicrobials (ampicillin, ceftazidime, cefepime, ertapenem, imipenem, aztreonam, amikacin, chloramphenicol, and fosfomycin) in 14 mutants (Δ*rseA,* Δ*cpxA,* Δ*cpxR,* Δ*cpxP,* Δ*rcsF,* Δ*rcsC,* Δ*rcsD,* Δ*rcsB,* Δ*baeR,* Δ*baeS,* Δ*pspA,* Δ*pspB,* Δ*pspC, and* Δ*pspF*). The mutants that showed antimicrobial sensitization were the following: Δ*rcsD* showed a consistent 1.5- and 1.3-fold decrease in MIC values of aztreonam and fosfomycin, respectively; Δ*baeR,* showed a 1.5-fold decline in the MIC of aztreonam; Δ*pspA* showed 2-, 1. 4-, and 1.5-fold decreases in the MICs of ceftazidime (**Supplementary Figure 1**), cefepime and ertapenem, respectively; Δ*pspB* showed a 2- and 1.4-fold decrease in the MIC of ceftazidime (**Supplementary Figure 1**) and cefepime, respectively, and finally, Δ*pspC* showed a 1.5-fold decrease in the MICs of ampicillin, ceftazidime and aztreonam.

Each mutant-antimicrobial combination that showed sensitization by gradient strips was tested with growth curves to analyze bacterial growth after short and long incubation periods in the presence of the antimicrobials cited above to confirm the previous results. The generalized sensitization of Psp mutants to beta-lactam agents (**Table 1**) led to growth curves even although no changes in MIC values were observed. The Δ*pspB* mutant showed clear sensitization with differences for aztreonam, ceftazidime, cefepime and ertapenem relative to wild-type. After 24 h, no growth was observed in the presence of aztreonam at 0.5xMIC (optical density, OD value 0.32) ($p < 0.01$, compared to wild-type, OD value 0.08) (**Figures 1D–F**), a decrease in OD was observed in the presence of ceftazidime at 0.25xMIC (OD value 0.33) ($p < 0.0001$, compared to wild-type BW25113, OD value 0.5) and at 0.5xMIC (OD value 0.16) ($p < 0.05$, relative to wild-type, OD value 0.3) (**Figures 1M–O**), and also in cefepime at 0.5xMIC (OD value 0.11) ($p < 0.05$, relative to wild-type, OD value 0.21) (**Figures 1D–F**). After 8 h of incubation, a decrease in OD was also observed at 0.25xMIC of cefepime (OD value 0.13) ($p < 0.0001$, compared to wild-type, OD value 0.25) (**Figures 1G–I**) and at 0.5xMIC of ertapenem (OD value 0.14) ($p < 0.0001$, relative to wild-type, OD value 0.29) (**Figures 1P–R**). The Δ*pspA* and Δ*pspC* mutants showed no growth at 0.5xMIC of aztreonam (OD value 0.10) ($p < 0.01$, compared to wild-type, OD value 0.27) (**Figures 1A–C**) until 12 h and no growth was observed at 0.5xMIC of cefepime (OD value 0.08) ($p < 0.0001$, relative to wild-type, OD value 0.30) (**Figures 1J–L**) at 24 h, respectively. No significant decrease in growth was observed for other mutant-antimicrobial combinations, and a paradoxical effect was observed with aztreonam (**Supplementary Figures 2–4**).

The Impact of Psp Response Alteration on Bactericidal Activity of Beta-Lactam Antimicrobials

Psp mutants (Δ*pspA*, Δ*pspB,* and Δ*pspC*) were the selected mutants due to its significant sensitizing effect to antimicrobials compared to the wild-type and was therefore used for time-kill assays to study cell viability in the presence of 1xMIC concentrations of beta-lactam agents selected. A bactericidal effect was observed for Δ*pspA* and Δ*pspC* mutants in the presence of AMP with drops up to 1 $\log_{10}$ ($p < 0.01$) at 8 h (**Figures 2A,B**). To note, a bacteriostatic effect was observed with the rest of the antimicrobials evaluated. At 1xMIC CAZ and ATM for Δ*pspA*, Δ*pspB,* and Δ*pspC* mutants, reductions of 2.2 $\log_{10}$ ($p < 0.0001$), 0.9 $\log_{10}$ ($p = 0.117$, ns) and 2.5 $\log_{10}$ ($p < 0.0001$), respectively, were observed at 6–8 h for the first agent (**Figures 2C–E**), maintaining growth delay at 24 h and drops of 3.1 $\log_{10}$ ($p < 0.01$), 4 $\log_{10}$ ($p < 0.01$) and 3.9 $\log_{10}$ ($p < 0.01$), respectively, were observed at 4–6 h for the second drug (**Figures 2J–L**). At 1xMIC ETP, reductions of 6 $\log_{10}$ ($p < 0.01$) for Δ*pspB* mutant and 1.7 $\log_{10}$

[1]https://www.graphpad.com

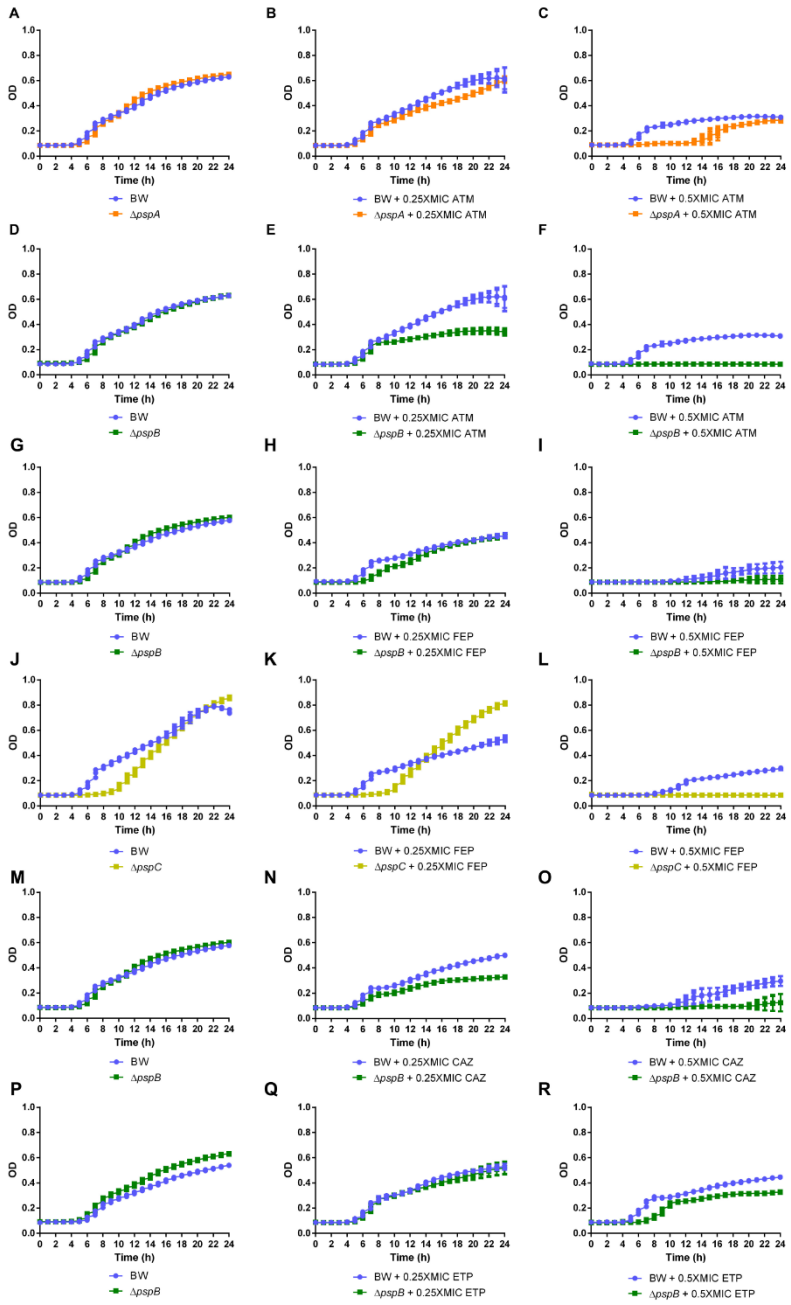

FIGURE 1 | Growth curves in the presence of aztreonam (ATM) for Δ*pspA* **(B,C)** and Δ*pspB* **(E,F)** mutants, cefepime (FEP) for Δ*pspB* **(H,I)** and Δ*pspC* **(K,L)** mutants, ceftazidime (CAZ) for Δ*pspB* **(N,O)** mutant and ertapenem (ETP) for Δ*pspB* **(Q,R)** mutant at concentrations of 0.25xMIC and 0.5xMIC relative to wild-type (BW25113) and their respective controls without antimicrobials **(A,D,G,J,M,P)**.

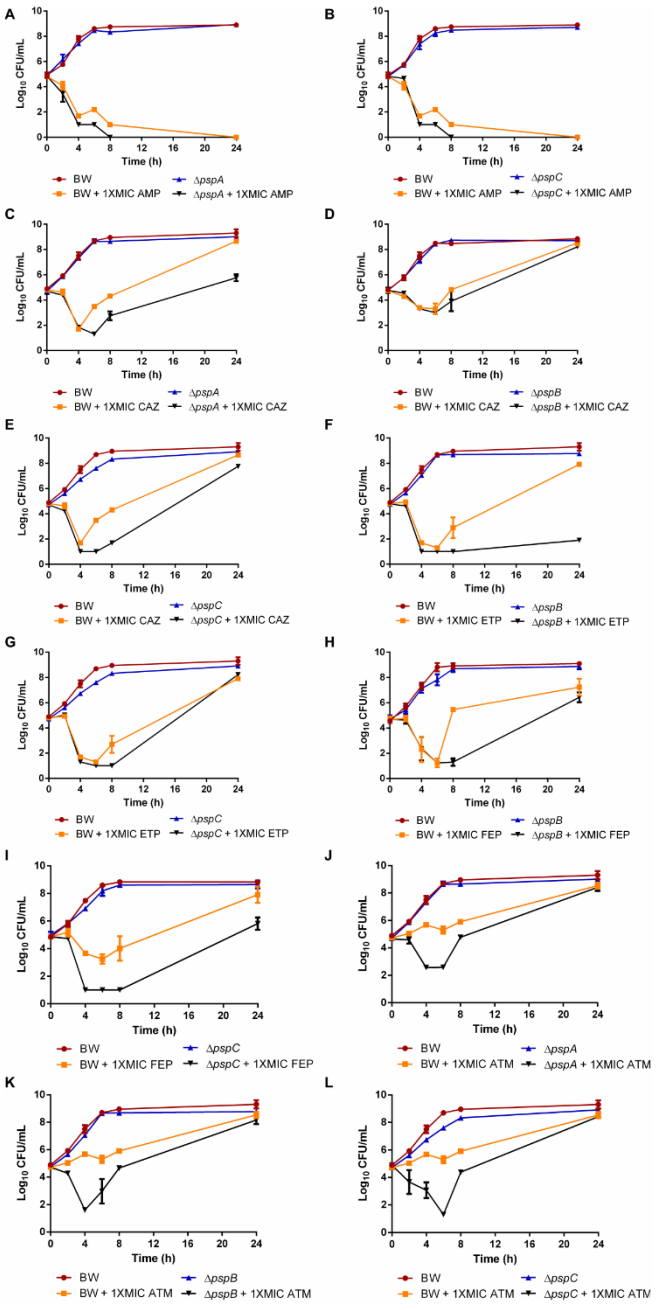

FIGURE 2 | Time-kill curves in the presence of ampicillin (AMP) for Δ*pspA* and Δ*pspC* mutants **(A,B)**, ceftazidime (CAZ) for Δ*pspA*, Δ*pspB*, and Δ*pspC* mutants **(C–E)**, ertapenem (ETP) for Δ*pspB* and Δ*pspC* mutants **(F,G)**, cefepime (FEP) for Δ*pspB* and Δ*pspC* mutants **(H,I)**, aztreonam (ATM) for Δ*pspA*, Δ*pspB*, and Δ*pspC* mutants **(J–L)** at 1xMIC relative to wild-type (BW25113) using low initial inoculum.

($p < 0.05$) for Δ*pspC* mutant were observed at 24 and 8 h, respectively (**Figures 2F,G**) and drops of 4.2 $\log_{10}$ ($p < 0.0001$) for Δ*pspB* mutant and 3 $\log_{10}$ ($p < 0.01$) for Δ*pspC* mutant were found after treatment with FEP at 8 h (**Figures 2H,I**). No differences in cell viability loss were observed for Δ*pspB* mutant in the presence of ampicillin or for Δ*pspA* mutant in the presence of ertapenem and cefepime (**Supplementary Figures 5A–C**).

DISCUSSION

Apart from the search for new drugs, new strategies are also necessary to prevent the emergence of resistance and extend the life of antimicrobial agents. Envelope stress responses are a set of coordinated physiological mechanisms that sense envelope damage or defects and trigger transcriptome alterations to mitigate this stress. In general terms, these pathways are focused on outer membrane stress (σ^E response), inner membrane stress (Cpx, and Psp responses), damage through exposure to toxic molecules (Bae response) and alterations in outer membrane permeability, changes in peptidoglycan biosynthesis and defects in lipoprotein trafficking (Rcs response) (Mitchell and Silhavy, 2019). Psp-activated IM disruptions tend to be more severe than those required to activate Cpx, being the first extensive disruptions that result in the loss of proton motive force (van der Laan et al., 2003; Maxson and Darwin, 2004; Becker et al., 2005), which could explain the greater effect on sensitization in strains deficient in this response.

Previous studies have evaluated the effect of mutations on the envelope stress response through deletion of certain genes (Nicoloff et al., 2017) or overactivation responses (McEwen and Silverman, 1980; Cosma et al., 1995; Danese et al., 1995), with sensitization to antimicrobials infrequently used in clinics (rifampicin or bacitracin) (Nicoloff et al., 2017) when RseA was deleted. In the present study, we evaluated a putative strategy consisting of disbalancing of envelope stress responses in the presence of antimicrobials from different families, including cell wall-disturbing agents (penicillins, cephalosporins, carbapenems, aztreonam, colistin, and fosfomycin), protein synthesis inhibitors (aminoglycosides, tetracyclines, and chloramphenicol), RNA synthesis inhibitors (rifampin), DNA synthesis inhibitors (fluoroquinolones) and folic acid synthesis inhibitors (sulfonamides and trimethoprim). It is important to highlight the clinical relevance of our set of selected antimicrobials for the treatment of infections caused by Gram-negative bacteria and the wide spectrum of targets covered, listed above. Gene deletions that affected sensitization to antimicrobials involved the Rcs response (*rcsD*, aztreonam and fosfomycin), the Bae response (*baeR*, aztreonam) and the Psp response (*pspA*, ceftazidime, cefepime and ertapenem; *pspB*, ceftazidime and ertapenem; *pspC*, ampicillin, ceftazidime, aztreonam). Beta-lactams constituted 83% of the antimicrobials to which strains were sensitized by gradient strip test, and the cell wall was the target in 100% of them.

Alteration of the Psp response was the envelope stress pathway with the greatest effect on sensitization in the presence of antimicrobials, as demonstrated by growth curves and time-kill curve assays. Various components are involved in the Psp response, notably PspB (inner membrane protein). Under activating conditions, PspB and PspC interact with PspA (PspF inhibitor), which releases PspF (response regulator) (Yamaguchi et al., 2013), which interacts with RNA polymerase to increase *psp* gene transcription (Jovanovic et al., 1996; Lloyd et al., 2004). Specifically, deletion of the *pspA, pspB and pspC* genes had the greatest impact on cell viability and bacterial growth in the presence of beta-lactams antimicrobials, mainly ampicillin, aztreonam, cefepime, ceftazidime and ertapenem, enhancing the bactericidal effect of this family of agents.

Another important aspect is that the target of these antimicrobials in the cell wall of *E. coli* is primarily PBP3 (ampicillin, cefepime, ceftazdime, aztreonam) and PBP2 (ertapenem) which are involved in cell division whose inhibition lead to filamentation and the formation of spherical cells, respectively (Hayes and Orr, 1983; Bush and Bradford, 2016; Rodvold et al., 2018). Nevertheless, the underlying interaction between these agents and the Psp response proteins is unknown. We could hypothesize that the double damage of the bacterial envelope: inner membrane damage due to *psp* deletion and the beta-lactam antimicrobials effect acting on the PBPs proteins, trigger a sensitization effect reducing bacterial growth a increasing antimicrobial lethality.

In general terms, the effect on antimicrobial sensitization in the tested mutants was moderate but consistent; however, it could be interesting to test other essential genes (*rpoE, degS, rseP, cpxQ, igaA*) involved in envelope stress responses, although these were not available in the KEIO collection.

The emergence of innovative therapeutic strategies, in combination with more conventional approaches, is advancing our understanding of interactions between microbiota, host and pathogenic bacteria. Questions that remain to be answered include how disruption of the envelope stress response could impact not only harmful bacteria, but also healthy ones, causing microbiota impairment and associated disorders, such as *C. difficile* infection (Bäumler and Sperandio, 2016).

In conclusion, a defective Psp envelope stress response increases *E. coli* susceptibility to beta-lactams antimicrobials, and is particularly remarkable with aztreonam, cefepime, ceftazidime and ertapenem. The role of this system in repairing extensive disruptions to the inner membrane makes this pathway essential to bacterial survival. Its use as a potential target for bacterial sensitization deserves in-depth evaluation.

DATA AVAILABILITY STATEMENT

The raw data supporting the conclusions of this article will be made available by the authors, without undue reservation.

AUTHOR CONTRIBUTIONS

VF, SD-D, and AG-D performed the lab assays. ER interpreted the data and wrote the manuscript with input from all co-authors. JR-M and ER designed and guided the execution

of all experiments. FD-P, ÁP, and JR-M supervised the project and contributed to the interpretation of the results and valuable discussion. All authors contributed to the article and approved the submitted version.

FUNDING

This study was supported by the Instituto de Salud Carlos III, Ministerio de Economía y Competitividad—co-financed by European Development Regional Fund "A way to achieve Europe" ERDF, Spanish Network for Research in Infectious Diseases [REIPI RD12/0015 and RD16/0016]. Supported by the Plan Nacional de I+D+i 2013–2016 and Instituto de Salud Carlos III, Subdirección General de Redes y Centros de Investigación Cooperativa, Ministerio de Economía, Industria y Competitividad, Spanish Network for Research in Infectious Diseases (PI14/00940, PI17/01501, PI20/00239, RD16/0016/0001, and REIPI RD16/0016/0009)—co-financed by European Development Regional Fund "A way to achieve Europe," Operative Programme Intelligent Growth 2014–2020.

SUPPLEMENTARY MATERIAL

The Supplementary Material for this article can be found online at: https://www.frontiersin.org/articles/10.3389/fmicb.2021.653479/full#supplementary-material

REFERENCES

Ades, S. E. (2004). Control of the alternative sigma factor σE in *Escherichia coli*. *Curr. Opin. Microbiol.* 7, 157–162. doi: 10.1016/j.mib.2004.02.010

Baba, T., Ara, T., Hasegawa, M., Takai, Y., Okumura, Y., Baba, M., et al. (2006). Construction of *Escherichia coli* K-12 in-frame, single-gene knockout mutants: the Keio collection. *Mol. Syst. Biol.* 2:msb4100050. doi: 10.1038/msb4100050

Baranova, N., and Nikaido, H. (2002). The BaeSR two-component regulatory system activates transcription of the yegMNOB (mdtABCD) transporter gene cluster in *Escherichia coli* and increases its resistance to novobiocin and deoxycholate. *J. Bacteriol.* 184, 4168–4176. doi: 10.1128/JB.184.15.4168-4176.2002

Bäumler, A. J., and Sperandio, V. (2016). Interactions between the microbiota and pathogenic bacteria in the gut. *Nature* 535, 85–93. doi: 10.1038/nature18849

Becker, L. A., Bang, I.-S., Crouch, M.-L., and Fang, F. C. (2005). Compensatory role of PspA, a member of the phage shock protein operon, in rpoE mutant *Salmonella enterica* serovar Typhimurium. *Mol. Microbiol.* 56, 1004–1016. doi: 10.1111/j.1365-2958.2005.04604.x

Bush, K., and Bradford, P. A. (2016). β-Lactams and β-Lactamase inhibitors: an overview. *Cold Spring Harb. Perspect. Med.* 6:a025247. doi: 10.1101/cshperspect.a025247

Cattoir, V., and Felden, B. (2019). Future antibacterial strategies: from basic concepts to clinical challenges. *J. Infect. Dis.* 220, 350–360. doi: 10.1093/infdis/jiz134

Clinical and Laboratory Standards Institute (2016). *Performance Standards for Antimicrobial Susceptibility Testing: Twenty-Sixth Informational Supplement M100-S26*. Wayne, PA: CLSI.

Cordeiro, R. P., Krause, D. O., Doria, J. H., and Holley, R. A. (2014). Role of the BaeSR two-component regulatory system in resistance of *Escherichia coli* O157:H7 to allyl isothiocyanate. *Food Microbiol.* 42, 136–141. doi: 10.1016/j.fm.2014.03.011

Cosma, C. L., Danese, P. N., Carlson, J. H., Silhavy, T. J., and Snyder, W. B. (1995). Mutational activation of the Cpx signal transduction pathway of *Escherichia coli* suppresses the toxicity conferred by certain envelope-associated stresses. *Mol. Microbiol.* 18, 491–505. doi: 10.1111/j.1365-2958.1995.mmi_18030491.x

Danese, P. N., Snyder, W. B., Cosma, C. L., Davis, L. J., and Silhavy, T. J. (1995). The Cpx two-component signal transduction pathway of Escherichia coli regulates transcription of the gene specifying the stress-inducible periplasmic protease, DegP. *Genes Dev.* 9, 387–398. doi: 10.1101/gad.9.4.387

DIckey, S. W., Cheung, G. Y. C., and Otto, M. (2017). Different drugs for bad bugs: antivirulence strategies in the age of antibiotic resistance. *Nat. Rev. Drug Discov.* 16, 457–471. doi: 10.1038/nrd.2017.23

Erickson, K. D., and Detweiler, C. S. (2006). The Rcs phosphorelay system is specific to enteric pathogens/commensals and activates ydeI, a gene important for persistent *Salmonella* infection of mice. *Mol. Microbiol.* 62, 883–894. doi: 10.1111/j.1365-2958.2006.05420.x

Farizano, J. V., Torres, M. A., Pescaretti, M. L. M., and Delgado, M. A. (2014). The RcsCDB regulatory system plays a crucial role in the protection of *Salmonella enterica* serovar Typhimurium against oxidative stress. *Microbiology* 160, 2190–2199. doi: 10.1099/mic.0.081133-0

Farris, C., Sanowar, S., Bader, M. W., Pfuetzner, R., and Miller, S. I. (2010). Antimicrobial peptides activate the rcs regulon through the outer membrane lipoprotein RcsF. *J. Bacteriol.* 192, 4894–4903. doi: 10.1128/JB.00505-10

Flores-Kim, J., and Darwin, A. J. (2014). Regulation of bacterial virulence gene expression by cell envelope stress responses. *Virulence* 5, 835–851. doi: 10.4161/21505594.2014.965580

Flores-Kim, J., and Darwin, A. J. (2016). The phage shock protein response. *Annu. Rev. Microbiol.* 70, 83–101. doi: 10.1146/annurev-micro-102215-095359

Guest, R. L., and Raivio, T. L. (2016). Role of the gram-negative envelope stress response in the presence of antimicrobial agents. *Trends Microbiol.* 24, 377–390. doi: 10.1016/j.tim.2016.03.001

Hayes, M. V., and Orr, D. C. (1983). Mode of action of ceftazidime: affinity for the penicillin-binding proteins of *Escherichia coli* K12, *Pseudomonas aeruginosa* and *Staphylococcus aureus*. *J. Antimicrob. Chemother.* 12, 119–126. doi: 10.1093/jac/12.2.119

Hersch, S. J., Watanabe, N., Stietz, M. S., Manera, K., Kamal, F., Burkinshaw, B., et al. (2020). Envelope stress responses defend against type six secretion system attacks independently of immunity proteins. *Nat. Microbiol.* 5, 706–714. doi: 10.1038/s41564-020-0672-6

Hirakawa, H., Nishino, K., Hirata, T., and Yamaguchi, A. (2003). Comprehensive studies of drug resistance mediated by overexpression of response regulators of two-component signal transduction systems in *Escherichia coli*. *J. Bacteriol.* 185, 1851–1856. doi: 10.1128/JB.185.6.1851-1856.2003

Huang, Y.-H., Ferrières, L., and Clarke, D. J. (2006). The role of the Rcs phosphorelay in *Enterobacteriaceae*. *Res. Microbiol.* 157, 206–212. doi: 10.1016/j.resmic.2005.11.005

Jovanovic, G., Weiner, L., and Model, P. (1996). Identification, nucleotide sequence, and characterization of PspF, the transcriptional activator of the *Escherichia coli* stress-induced psp operon. *J. Bacteriol.* 178, 1936–1945. doi: 10.1128/JB.178.7.1936-1945.1996

Kim, D. Y. (2015). Two stress sensor proteins for the expression of sigmaE regulon: DegS and RseB. *J. Microbiol.* 53, 306–310. doi: 10.1007/s12275-015-5112-6

Laubacher, M. E., and Ades, S. E. (2008). The Rcs phosphorelay is a cell envelope stress response activated by peptidoglycan stress and contributes to intrinsic antibiotic resistance. *J. Bacteriol.* 190, 2065–2074. doi: 10.1128/JB.01740-07

Laxminarayan, R., Duse, A., Wattal, C., Zaidi, A. K. M., Wertheim, H. F. L., Sumpradit, N., et al. (2013). Antibiotic resistance—the need for global solutions. *Lancet Infect. Dis.* 13, 1057–1098. doi: 10.1016/S1473-3099(13)70318-9

Lima, S., Guo, M. S., Chaba, R., Gross, C. A., and Sauer, R. T. (2013). Dual Molecular Signals mediate the bacterial response to outer-membrane stress. *Science* 340, 837–841. doi: 10.1126/science.1235358

Lin, M.-F., Lin, Y.-Y., Yeh, H.-W., and Lan, C.-Y. (2014). Role of the BaeSR two-component system in the regulation of *Acinetobacter baumannii adeAB* genes and its correlation with tigecycline susceptibility. *BMC Microbiol.* 14:119. doi: 10.1186/1471-2180-14-119

Lloyd, L. J., Jones, S. E., Jovanovic, G., Gyaneshwar, P., Rolfe, M. D., Thompson, A., et al. (2004). Identification of a new member of the phage shock protein response in *Escherichia coli*, the phage shock protein G (PspG). *J. Biol. Chem.* 279, 55707–55714. doi: 10.1074/jbc.M408994200

Majdalani, N., and Gottesman, S. (2005). The Rcs phosphorelay: a complex signal transduction system. *Annu. Rev. Microbiol.* 59, 379–405. doi: 10.1146/annurev.micro.59.050405.101230

Maxson, M. E., and Darwin, A. J. (2004). Identification of inducers of the *Yersinia enterocolitica* phage shock protein system and comparison to the regulation of the RpoE and Cpx extracytoplasmic stress responses. *J. Bacteriol.* 186, 4199–4208. doi: 10.1128/JB.186.13.4199-4208.2004

McEwen, J., and Silverman, P. (1980). Chromosomal mutations of *Escherichia coli* that alter expression of conjugative plasmid functions. *Proc. Natl. Acad. Sci.U.S.A.* 77, 513–517. doi: 10.1073/pnas.77.1.513

Mitchell, A. M., and Silhavy, T. J. (2019). Envelope stress responses: balancing damage repair and toxicity. *Nat. Rev. Microbiol.* 17, 417–428. doi: 10.1038/s41579-019-0199-0

Nicoloff, H., Gopalkrishnan, S., and Ades, S. E. (2017). Appropriate regulation of the σE-dependent envelope stress response is necessary to maintain cell envelope integrity and stationary-phase survival in *Escherichia coli*. *J. Bacteriol.* 199:e00089–17. doi: 10.1128/JB.00089-17

Raffa, R. G., and Raivio, T. L. (2002). A third envelope stress signal transduction pathway in *Escherichia coli*. *Mol. Microbiol.* 45, 1599–1611. doi: 10.1046/j.1365-2958.2002.03112.x

Raivio, T. L. (2014). Everything old is new again: an update on current research on the Cpx envelope stress response. *Biochim. Biophys. Acta Mol. Cell Res.* 1843, 1529–1541. doi: 10.1016/j.bbamcr.2013.10.018

Recacha, E., Machuca, J., Díaz de Alba, P., Ramos-Güelfo, M., Docobo-Pérez, F., Rodriguez-Beltrán, J., et al. (2017). Quinolone resistance reversion by targeting the SOS response. *MBio* 8:e00971–17. doi: 10.1128/mBio.00971-17

Rodvold, K. A., Gotfried, M. H., Chugh, R., Gupta, M., Patel, A., Chavan, R., et al. (2018). Plasma and intrapulmonary concentrations of cefepime and zidebactam following intravenous administration of WCK 5222 to healthy adult subjects. *Antimicrob. Agents Chemother.* 62:e00682–18. doi: 10.1128/AAC.00682-18

Ruiz, N., and Silhavy, T. J. (2005). Sensing external stress: watchdogs of the *Escherichia coli* cell envelope. *Curr. Opin. Microbiol.* 8, 122–126. doi: 10.1016/j.mib.2005.02.013

Silhavy, T. J., Kahne, D., and Walker, S. (2010). The bacterial cell envelope. *Cold Spring Harb. Perspect. Biol.* 2:a000414. doi: 10.1101/cshperspect.a000414

Valentin-Hansen, P., Johansen, J., and Rasmussen, A. A. (2007). Small RNAs controlling outer membrane porins. *Curr. Opin. Microbiol.* 10, 152–155. doi: 10.1016/j.mib.2007.03.001

van der Laan, M., Urbanus, M. L., ten Hagen-Jongman, C. M., Nouwen, N., Oudega, B., Harms, N., et al. (2003). A conserved function of YidC in the biogenesis of respiratory chain complexes. *Proc. Natl. Acad. Sci. U.S.A.* 100, 5801–5806. doi: 10.1073/pnas.0636761100

Yamaguchi, S., Reid, D. A., Rothenberg, E., and Darwin, A. J. (2013). Changes in Psp protein binding partners, localization and behaviour upon activation of the *Yersinia enterocolitica* phage shock protein response. *Mol. Microbiol.* 87, 656–671. doi: 10.1111/mmi.12122

Conflict of Interest: The authors declare that the research was conducted in the absence of any commercial or financial relationships that could be construed as a potential conflict of interest.

CHAPTER 4

Streptococcus pyogenes φ1207.3 is a functional bacteriophage carrying macrolide efflux genes *mef*(A) and *msr*(D) and capable of conjugative lysogenic transfer among Streptococci

Francesco Santoro, Gabiria Pastore, Valeria Fox, Francesco Iannelli, Gianni Pozzi

Laboratory of Molecular Microbiology and Biotechnology,

Department of Medical Biotechnologies,

University of Siena, 53100 Siena, Italy

Manuscript in preparation

1.1. Abstract

Streptococcus pyogenes prophage φ1207.3 carries the *mef*(A)-*msr*(D) efflux resistance genes, responsible for the type M macrolide resistance. φ1207.3 was discovered in the clinical strain of *Streptococcus pyogenes* 2812A and was initially thought to be a conjugative transposon, called Tn*1207.3*, due to its transfer mechanism, which resembled conjugation. Later, sequence analysis revealed that is a prophage and for this reason it was renamed φ1207.3. Since *Streptococcus pyogenes* genomes are often characterized by the presence of several prophages and ICEs integrated in their genome, the study of a single prophage is not easy. For this reason, the aim of this study was to functionally characterize φ1207.3 in the *S. pneumoniae* host. We transferred φ1207.3 to a pneumococcal laboratory strain, devoid of other prophages or Integrative Conjugative Elements (ICEs). We obtained phage preparations by inducing the φ1207.3 lytic cycle with mitomycin C and observed them at the Transmission Electron Microscopy (TEM). We demonstrated that φ1207.3 is a functional bacteriophage, able to produce mature phage particles, with a morphology consistent with that of *Siphoviridae* family. φ1207.3 does not seem to undergo a lytic cycle with evident cell lysis, even though induction with mitomycin C produces a limited phage burst, as suggested by the impairment in cell growth and the early entrance in the stationary phase. φ1207.3 transfer to pneumococcal recipients could be obtained only when a plate mating protocol was used, indicating that φ1207.3 particles are able to transfer their own genome, but that they require cell-to-cell contact.

1.2. Introduction

Macrolide resistance in streptococci occurs through two main mechanisms, target site modification, leading to the MLS_B phenotype, conferring resistance to macrolides, lincosamides and streptogramin B, and drug efflux, leading to the M phenotype, conferring resistance only to 14- and 15- membered macrolides[1,2]. The second mechanism is due to the presence of the *mef*(A)-*msr*(D) gene pair, which encodes an efflux transport system of the ABC superfamily, where *mef*(A) codes for the transmembrane channel and *msr*(D) for the ATP-binding domains[3]. Macrolide resistance genes in streptococci are carried by mobile genetic elements and spread among different types of bacteria, both Gram-positive and Gram-negative. The *mef*(A)-*msr*(D) gene pair is carried by several mobile genetic elements, such as the prophage φ1207.3[4]. Prophage φ1207.3 was discovered in the clinical strain of *Streptococcus pyogenes* 2812A and was initially thought to be a conjugative transposon, called Tn*1207.3*, due to its transfer mechanism, which resembled conjugation[5]. Sequence analysis revealed that is a prophage, thus it was renamed φ1207.3[6]. This element contains a complete copy of Tn*1207.1* at its left end and integrates in the *S. pyogenes* chromosome at a specific GA dinucleotide target site within the *comEC* gene, which codes for a protein involved in DNA binding and transport during genetic transformation, causing a GA site duplication. Prophage φ1207.3 could be transferred to *Streptococcus pneumoniae* and *Streptococcus gordonii*, only by a mechanism fitting the operational definition of conjugation, whereas transfer could not be obtained using culture supernatant[5]. The integration in the *S. pneumoniae* chromosome occurred in the pneumococcal homolog of *comEC*, *celB* [6].

Bacteriophages are the most abundant entities on the biosphere, with an estimated total number of virus-like particles on Earth close to 10^{31}[7–10]. Nonetheless, phages are rarely found to directly encode antibiotic resistance genes[11] and their transfer rarely occurs between different bacterial species. *Streptococcus pyogenes* genomes are often characterized by the presence of several prophages and ICEs integrated in their genome[12–14]. For this reason, it is usually not easy to study the biology of a single prophage in the original *S. pyogenes* host. The aim of this study was to

transfer prophage φ1207.3 to a pneumococcal laboratory strain, devoid of other prophages or Integrative Conjugative Elements (ICEs), and to functionally characterize it in the pneumococcal host.

1.3. Materials and methods

1.3.1. Bacterial strains and culture conditions

All strains used in this work and their relevant properties are reported in Table 1. Streptococcal strains were grown in Tryptic Soy Broth (TSB, BD), or, when needed, Tryptic Soy Broth without dextrose (TSB/wo, BD), at 37°C. Starter cultures were taken at an optical density at 590 nm (OD_{590}) ranging from 0.2 to 0.3 and were stored at -80°C in tubes containing glycerol at a final concentration of 10%. Solid media were obtained by supplementing TSB with 1.5% agar (BD Difco) and 3% defibrinated horse blood (Liofilchem). When required, both liquid and solid media were supplemented with antibiotics at the following concentrations: 0.5 µg/ml erythromycin, 10 µg/ml novobiocin, 500 µg/ml streptomycin, 3 µg/ml chloramphenicol, 500 µg/ml kanamycin.

1.3.2. Bioinformatic analysis

The VIRFAM webserver (http://biodev.cea.fr/virfam/) for remote homology detection of viral family proteins [15] was used to analyze the structural proteins of φ1207.3 and assess the family of the head-tail-neck module.

1.1.1. φ1207.3 lysogenic transfer to *Streptococcus pneumoniae* laboratory strain

Lysogenic transfer of bacteriophage φ1207.3 from the *Streptococcus pyogenes* 2812A to a laboratory *Streptococcus pneumoniae* strain was obtained through plate mating experiments [16]. Briefly, donor cells (2812A), carrying the phage, and recipient cells (FP10, a derivative of laboratory *S. pneumoniae* strain Rx1[17] were grown separately at 37°C in TSB in the presence of the appropriate antibiotics. Upon reaching the end of the exponential phase (OD_{590}= 0.8), cells were mixed at a donor-recipient 1:10 ratio, centrifuged at 3,000 x *g* for 15 minutes, and the pellet was plated on TSA plates supplemented with 5% blood. Plates were incubated at 37°C in the presence

of 5% CO_2 up to 4 h, cells were then recovered with a cotton swab and resuspended in TSB with final concentration of glycerol of 10%. To select for recombinants, the cell suspension was then plated following a multilayer plating procedure, as previously described [16,18]. For confirmation, genetic analysis was performed as previously described [19]. Transfer frequency and identification of spontaneous mutations were obtained by plating each parent strain alone. Recombinants were carefully screened by genetic analysis and the transfer of φ1207.3 was confirmed by PCR analysis.

1.1.2. Lytic cycle induction with Mitomycin C and phage preparations

Induction of the bacteriophage φ1207.3 lytic cycle was performed with mitomycin C, a known prophage inducer[20]. Strains were inoculated in 600 ml of TSB and grown at 37°C until reaching the early exponential phase (OD_{590} = 0.05-0.1), when the culture was split in two halves, one receiving mitomycin C (Sigma Aldrich) at a sub-MIC concentration (100 ng/ml), and one untreated. After 2 hours of growth at 37°C, cultures were taken and, after the addition of EDTA at a final concentration of 10 mM, 6 tubes of 44 ml each were centrifuged two times at 5,000 x *g* for 40 minutes at 4°C, in order to eliminate bacterial cells and debris. The supernatant was then supplemented with a protease inhibitor mix (Sigma Aldrich) and 6 tubes of 37 ml were ultracentrifuged at 20,000 x *g* for 2 hours at 10°C with a SW32Ti rotor (Optima L-90K Ultracentrifuge; Beckman Coulter). Supernatant was then removed and the pellet containing the phages was resuspended with 100 µl of TM buffer (50 mM Tris-HCl, 10 mM $MgSO_4$) for each ultracentrifuge tube[21]. Phage preparations obtained were then used for TEM imaging and lysogenic transfer experiments.

1.1.3. Transmission electron microscopy (TEM) imaging

Transmission electron microscopy (TEM) of phage preparations of mitomycin C induced samples was performed at University of Siena, Department of Life Sciences. Three µl of phage suspension were placed onto a glow-discharged Formvar-coated 300 mesh copper grid and allowed to adsorb for 2 min. Excess liquid was removed with filter paper and a drop of 2% uranyl acetate was added, given time to wet fully and then blotted dry. Samples were observed in a TECNAI G^2 transmission

electron microscope operated at 100 kV with magnification of 60,000 ×. Measurements of head diameter, tail length were tested for homogeneity. About 10 representative meshes were observed for each preparation, and 200 fields were observed in each mesh.

1.1.4. Double Agar Overlay Plaque Assay

Fifty µl of the phage suspension were added to 100 µl of a bacterial suspension of the indicator pneumococcal strain FP10. This solution was added to 3 ml of the top agar (TSB with 0.4% agarose), mixed gently, and poured into a 90-mm petri dish containing 25 ml of TSA with 10 mM $CaCl_2$. The plates were dried for 10 min at room temperature then inverted and incubated overnight at 37°C with 5% CO_2 [22].

1.1.5. Lysogenic transfer experiments

Phage preparations were used in lysogenic transfer experiments to assess their ability to transfer the phage genome to non-competent pneumococcal strains, following a protocol already described [16]. Cells to be used as recipients were grown in TSB broth at 37°C to an OD_{590} of 0.8, where 900 µl (about 10^9 CFUs) were centrifuged at 3,000 x *g* for 15 min. The supernatants were removed, and the cells were resuspended in 100 µl of phage preparation. A recipient-only control containing bacteria and phage buffer was included in each experiment. Suspensions were incubated for 15 min at 37°C and then plated on TSA plates with 5% blood and incubated up to 4 hours. After incubation, the cells were harvested with a sterile swab and suspended in 1 ml of TSB containing 10% glycerol. Scoring of lysogens was performed by multilayer plating with appropriate antibiotics as described above. Lysogenic transfer frequency was expressed as the number of recombinants per recipient. Experiments were performed in triplicate and putative lysogens were analyzed by PCR.

1.1.6. Quantitative PCR

qPCR assay was performed with the KAPA SYBR FAST qPCR Master Mix (2X) Kit (Kapa Biosystems) in a LightCycler 1.5 (Roche) instrument, following the procedure of Santoro et al.,2018 [23]. The reaction mix was prepared in a final volume of 20 µl and contained 1X KAPA SYBR FAST qPCR reactive, 200 µM of each primer and 1 µl of starting template. The thermal

cycling program comprised 3 minutes of initial denaturation at 95°C, then 40 cycles of: denaturation for 0 seconds at 95°C, annealing for 20 seconds at 50°C, extension for 10 seconds at 72°C. The temperature transition rate was 20°C/s in the denaturation and annealing steps and 5°C/s in the polymerisation step. Melting curve was integrated at the end of the run by increasing temperature from 40°C to 95°C with a ramping of 0.05°C/s and acquiring fluorescence continuously. The primer pairs used are: (i) IF264 (5'- CTTGCTCTCACTTATTATATT-3') and IF162 (5'-TGATGATTATATAAATTGTGAGTT-3'), a pair of divergent primers, directed at the ends of the phage genome, amplifying a fragment of 227 bp and used to quantify the phage circular forms; (ii) IF138 (5'-CAGATCAAGAAATCAAACTCCAA-3') and IF139 (5'-CAGCATCATCTACAGAAACTC-3'), which amplified a 171 bp fragment of chromosomal *gyrB* gene, used for standardization of the results. Serial dilutions of chromosomal DNA with known concentration were used to build a standard curve for the *gyrB* gene, as already described [23].

1.2. Results

1.2.1. Bioinformatic analysis predicts that φ1207.3 belongs to the *Siphoviridae* family

Predicted protein sequences of φ1207.3 were subjected to Virfam analysis for the identification of Head-Neck-Tail module proteins [15]. Eight proteins were assigned to a functional protein superfamily based on both sequence homology and respective position on the prophage sequence (Table 2). Overall, the phage was assigned to Siphoviridae with type 1 (cluster 2) Neck, a family of viruses that includes other phages infecting *Firmicutes* bacteria. Virfam assigned the 228 amino acid-long Orf41 to the Major capsid protein family, based on an HHsearch homology of 28% with the CDT-1 phage major capsid protein (GenBank accession number NC_009514.1)[24]. The analysis of this latter protein reveals a large (652 aa) multidomain protein containing both a clp protease domain at the N-terminal and a major capsid protein domain at the C-terminal, resembling the tripartite capsid protein of *Salmonella* phage Gifsy-2[25]. Based on domain prediction by Pfam [6], we believe that the actual Major Capsid protein of φ1207.3 is Orf42, while Orf41 is probably a

protease involved in the process of capsid maturation and in the cleavage of the capsid protein. Virfam predicted that the proteins from Orf43 to Orf47 constitute the neck-tail module of φ 1207.3, in particular, Orf43 is the adaptor protein, Orf44 is the Head-closure protein, Orf45 is the Neck protein, Orf46 is the Tail completion protein, while Orf47 is the major tail protein. Virfam did not identify a sheath protein, which is typical of Myophages only. The bioinformatic prediction was able to identify all the structural proteins needed for the assembly of a complete phage particle.

1.2.2. Transfer to *Streptococcus pneumoniae* laboratory strain

The genome of *S. pyogenes* is shaped by the presence of prophages [26], in fact most complete genome sequences of *S. pyogenes* show the presence of at least 2 prophages with a maximum of 8 in the genome of MGAS10394 [27] (GenBank accession number CP000003.1.). The assembled genome of 2812A, the clinical strain in which φ1207.3 was found, showed the presence of another 2 prophages integrated (data not shown), one homologous to φ315.3 [28] and another homologous to φ5005.3 [29]. It is therefore difficult to study the biology of a single prophage in the original *S. pyogenes* host. We constructed the *S. pneumoniae* strain FR1 (*comC*$^-$, *cps*$^-$, φ1207.3) by mating *S. pyogenes* 2812A with the recipient model strain FP10 (*comC*$^-$, *cps*$^-$), a derivative of laboratory strain Rx1 [30] which is devoid of prophage sequences and integrative conjugative elements.

Transfer of φ1207.3 to the laboratory model of *Streptococcus pneumoniae* was achieved through mating at a frequency of 3×10^{-5} recombinants/donor. Upon transfer, φ1207.3 integrated in the *celB* coding sequence.

1.2.3. φ1207.3 induction by mitomycin C

Growth of FR1, carrying φ1207.3, was monitored after the addition of 100 ng/ml mitomycin C, a DNA damaging agent classically used to induce the lytic cycle of prophages and that in *S. pneumoniae* also triggers the competence pathway [31]. Even upon induction with mitomycin C, FR1 produced a limited phage burst, without evidence of cell lysis (Figure 1). The generation time (G) and the time occurring between the addition of the mitomycin C and the entry of the stationary phase (t) were calculated for FR1 and compared to the growth without mitomycin C induction.

The generation time of FR1 was 50 minutes in absence and 75 minutes in the presence of the mitomycin C stimulus. In the untreated culture, the stationary phase was reached after 205 minutes, thus after 4.1 generations (n = t/G), whereas in the treated culture it was reached after 121 minutes, corresponding to 1.6 generations. Hence, albeit bacteriophage φ1207.3 does not seem to possess a lytic cycle, with evident phage burst, mitomycin C causes a significant, phage-specific growth impairment, as the treated culture reached the stationary phase 2.5 generations before the untreated culture. The growth impairment is specifically conferred by the presence of φ1207.3, because FR1 is competence deficient and the growth of the control strain FP10 was not affected by mitomycin C.

1.2.4. φ1207.3 belongs to the *Siphoviridae* family

Observation of the ultracentrifuged phage preparations at the TEM showed the presence of phage particles with an icosahedral, electron dense capsid and a long, non-contractile tail, with tail fibers visible in some images. The head was found to be 62 nm in diameter, while the tail was 175 nm (± 1 nm) in length and 8 nm in diameter. The morphology observed is consistent with a member of the *Siphoviridae* family, in accordance with the bioinformatic prediction (Figure 2).

1.2.5. Lysogenic transfer of φ1207.3

We used phage preparations to assess their ability to transfer the phage genome to a non-competent pneumococcal recipient. Lysogenic transfer was obtained at an average frequency of 7.5×10^{-6} lysogens/recipient, indicating that φ1207.3 particles are able to transfer their own genome. Phage particles were also diluted to assess the minimum number of phages required to obtain a detectable transfer: we could not detect lysogens when using less than 10^3 phages, as quantified by qPCR (< 2.8×10^{-8} lysogens/recipient, Figure 3). Since we did not include a filtering step, our phage preparations also contained a residual number of bacteria (about 5×10^4 CFU/ml), to rule out the contribution of whole bacterial cells to phage transfer we performed mating experiments using serial dilutions of bacteria and we could not detect phage transfer when using less than 6×10^6 donor bacteria (< 8.3×10^{-9} lysogens/recipient). Finally, we assessed the kinetics of phage transfer in a time course experiment varying the incubation time of the phage preparation with bacteria from

30 minutes to 4 hours. The number of recombinant lysogens was stable over time, indicating that phage transfer efficiently occurs within 30 minutes from the contact with the recipient cell (Figure 4).

1.3. Discussion

Bacteriophages play an important role in shaping the physiology and pathogenesis of *S. pyogenes*: they carry several virulence genes - such as superantigens, DNases, and phospholipases - mediate the horizontal transfer of host genes, and, as in the case of φ1207.3, the spread of antibiotic resistance[14]. The mechanism of transfer of *S. pyogenes* phages has not been completely elucidated. Some phages undergo a lytic cycle upon induction by specific stimuli, such as the DNA damaging agent Mitomycin C, while others tend to remain in a lysogenic state. It is difficult to study the biology of single phages in the *S. pyogenes* original host, as most strains are polylysogenic, harboring up to 8 different prophages [27], even if strains not carrying phages were reported [32], and Euler and colleagues developed a method for knocking out phages from the *S. pyogenes* genome [33].

In this work, we transferred φ1207.3 to a pneumococcal laboratory strain to study its functionality. We demonstrated that φ1207.3 is able to produce mature phage particles, with a morphology consistent with that of *Siphoviridae* family. φ1207.3 does not seem to undergo a lytic cycle with evident cell lysis, even though induction with mitomycin C produces a limited phage burst, as suggested by the impairment in cell growth and the early entrance in the stationary phase (2.5 generations before the control). φ1207.3 transfer to pneumococcal recipients could be obtained at an average frequency of 7.5×10^{-6} lysogens/recipient only when a plate mating protocol was used, indicating that φ1207.3 particles are able to transfer their own genome, but that they require cell-to-cell contact.

In conclusion, we demonstrated that φ1207.3, carrying the *mef*(A)-*msr*(D) macrolide efflux resistance genes, is a functional bacteriophage belonging to the *Siphoviridae* family, able to transfer

to different bacterial species through a mechanism which resembles conjugation and is dependent on cell-to-cell contact.

Tables

Table 1. **Bacterial strains used in this work and relative properties.**

Strain	Properties	References
2812A	Italian clinical strain of Streptococcus pyogenes carrying φ1207.3, Em^R	Santagati et al., 2003[5]
FP10	Streptococcus pneumoniae Rx1 unencapsulated, competence deficient derivative, ΔcomC, Cm^R, Sm^R	Iannelli and Pozzi, 2007[34]
FR1	FP10 derivative carrying φ1207.3 integrated in celB, ΔcomC, Cm^R, Sm^R, Em^R	This study

Em, erythromycin; Cm, chloramphenicol; Sm, streptomycin

Table 2. **φ1207.3 structural proteins identified by Virfam webserver**

ORF	Protein superfamily	Detection method	Identities with proteins in Aclame Phages	Sequence identity (%)
39	TermL	Blast (e-value=$6x10^{-77}$)	D3	33
			HK022	33
			HK97	33
40	Portal	HHsearch (prob=100%)	phi644-2	39
			phiKO2	39
			phiE125	39
41	MCP	HHsearch (prob=100%)	cdtI	28
43	Ad1	HHsearch (prob=98.46%)	Bcep176	24
			phi1026b	24
			P27	21
44	Hc1	HHsearch (prob=99.96%)	phi-105	25
			Geobacillus virus E2	23
			phi3626	22
45	Ne1	HHsearch (prob=100%)	bacteriophage bv1	36
			GBSV1	36
			bIL285	35
46	Tc1	HHsearch (prob=100%)	bacteriophage bv1	41
			GBSV1	41
			Geobacillus virus E2	38
47	MTP	Blast (e-value=$2x10^{-48}$)	bIL285	50
			GBSV1	42
			bacteriophage bv1	41

FIGURE LEGEND

Figure 1. **Growth curve in absence and presence of mitomycin C induction.**

Induction with mitomycin C was studied in strain FR1 carrying φ1207.3 (A) and its parental strain FP10, not carrying φ1207.3 (B) by adding a sub-MIC concentration of mitomycin C (100 ng/ml) at the beginning of the exponential phase (OD_{590} = 0.05-0.1) and comparing the growth with the uninduced cultures. The growths of the induced (black square) and not induced (white square) cultures were followed by measuring the optical density every 30 minutes. The time of addition of the mitomycin C stimulus is indicated by a black arrow. No evident cell lysis, with the drop in the optical density, was detected for both strains, but FR1 strain, carrying the prophage, entered the stationary phase 2.5 generations before FP10, devoid of the phage. Results are reported as means and standard deviations resulting from at least three independent experiments.

Figure 2. **Morphology of φ1207.3 at the TEM.** Transmission electron microscopy (TEM) performed after negative staining showed a morphology consistent with a Siphovirus. The head showed an icosahedral symmetry and had a diameter of 62 nm while the tail was non-contractile and 175 nm (± 1 nm) long. Putative tail fibers are indicated by an arrow. Scale is reported.

Figure 3. **Lysogenic transfer mediated by different amounts of phage particles.** The minimum number of phages required to obtain detectable transfer was assessed by testing different dilutions of phage particles. No lysogens were detected when using less than 10^3 phages. The lysogenic transfer frequency was calculated as number of lysogens per recipient cell.

***Figure 4*. Time-course of the lysogenic transfer of φ1207.3.** The kinetics of phage transfer was investigated in a time course experiment, by varying the incubation time of phage preparation with bacteria from 30 minutes to 4 hours. Number of recombinant lysogens (black square) was stable over time, while the lysogenic transfer frequency (red diamond, calculated as number of lysogens per recipient cell) decreased with time, suggesting that phage transfer efficiently occurs in the first 30 minutes after contact with the recipient cells.

1.4. References

1. Roberts MC. Update on macrolide-lincosamide-streptogramin, ketolide, and oxazolidinone resistance genes: MLSKO genes. FEMS Microbiology Letters. 2008 Apr 9;282(2):147–59.
2. Leclercq R, Courvalin P. Resistance to Macrolides and Related Antibiotics in Streptococcus pneumoniae. AAC. 2002 Sep;46(9):2727–34.
3. Iannelli F, Santoro F, Santagati M, Docquier J-D, Lazzeri E, Pastore G, et al. Type M Resistance to Macrolides Is Due to a Two-Gene Efflux Transport System of the ATP-Binding Cassette (ABC) Superfamily. Front Microbiol. 2018 Jul 31;9:1670.
4. Pozzi G, Iannelli F, Oggioni M, Santagati M, Stefani S. Genetic Elements Carrying Macrolide Efflux Genes in Streptococci. CDTID. 2004 Sep 1;4(3):203–6.
5. Santagati M, Iannelli F, Cascone C, Campanile F, Oggioni MR, Stefani S, et al. The Novel Conjugative Transposon Tn1207.3 Carries the Macrolide Efflux Gene mef(A) in Streptococcus pyogenes. Microbial Drug Resistance. 2003 Aug;9(3):243–7.
6. Iannelli F, Santagati M, Santoro F, Oggioni MR, Stefani S, Pozzi G. Nucleotide sequence of conjugative prophage Φ1207.3 (formerly Tn1207.3) carrying the mef(A)/msr(D) genes for efflux resistance to macrolides in Streptococcus pyogenes. Front Microbiol. 2014 Dec 9;5:687–687.
7. Hendrix RW, Smith MCM, Burns RN, Ford ME, Hatfull GF. Evolutionary relationships among diverse bacteriophages and prophages: All the world's a phage. Proceedings of the National Academy of Sciences. 1999 Mar 2;96(5):2192–7.
8. Clokie MR, Millard AD, Letarov AV, Heaphy S. Phages in nature. Bacteriophage. 2011 Jan;1(1):31–45.
9. Bar-On YM, Phillips R, Milo R. The biomass distribution on Earth. Proc Natl Acad Sci USA. 2018 Jun 19;115(25):6506–11.
10. Mushegian AR. Are There 10 ^{31} Virus Particles on Earth, or More, or Fewer? Margolin W, editor. J Bacteriol [Internet]. 2020 Apr 9 [cited 2021 Aug 13];202(9). Available from: https://journals.asm.org/doi/10.1128/JB.00052-20
11. Enault F, Briet A, Bouteille L, Roux S, Sullivan MB, Petit M-A. Phages rarely encode antibiotic resistance genes: a cautionary tale for virome analyses. ISME J. 2017 Jan;11(1):237–47.
12. Beres SB, Musser JM. Contribution of Exogenous Genetic Elements to the Group A Streptococcus Metagenome. Ahmed N, editor. PLoS ONE. 2007 Aug 29;2(8):e800.

13. Bessen DE, McShan WM, Nguyen SV, Shetty A, Agrawal S, Tettelin H. Molecular epidemiology and genomics of group A Streptococcus. Infection, Genetics and Evolution. 2015 Jul;33:393–418.
14. McShan WM, Nguyen SV. The Bacteriophages of Streptococcus pyogenes. :30.
15. Lopes A, Tavares P, Petit M-A, Guérois R, Zinn-Justin S. Automated classification of tailed bacteriophages according to their neck organization. BMC Genomics. 2014;15(1):1027.
16. Iannelli F, Santoro F, Fox V, Pozzi G. A Mating Procedure for Genetic Transfer of Integrative and Conjugative Elements (ICEs) of Streptococci and Enterococci. MPs. 2021 Aug 28;4(3):59.
17. Smith MD, Guild WR. A Plasmid in Streptococcus pneumoniae. 1979;137:5.
18. Iannelli F, Pozzi G. Method for Introducing Specific and Unmarked Mutations Into the Chromosome of Streptococcus pneumoniae. MB. 2004;26(1):81–6.
19. Santoro F, Oggioni MR, Pozzi G, Iannelli F. Nucleotide sequence and functional analysis of the tet (M)-carrying conjugative transposon Tn5251 of Streptococcus pneumoniae: Tn5251 of Streptococcus pneumoniae. FEMS Microbiology Letters. 2010 Apr 28;no-no.
20. OTSUJI N, SEKIGUCHI M, IIJIMA T, TAKAGI Y. Induction of Phage Formation in the Lysogenic Escherichia coli K-12 by Mitomycin C. Nature. 1959 Oct 1;184(4692):1079–80.
21. Bernheimer HP. Lysogenic pneumococci and their bacteriophages. Journal of Bacteriology. 1979;138(2):618–24.
22. Kropinski AM, Mazzocco A, Waddell TE, Lingohr E, Johnson RP. Enumeration of Bacteriophages by Double Agar Overlay Plaque Assay. In: Clokie MRJ, Kropinski AM, editors. Bacteriophages: Methods and Protocols, Volume 1: Isolation, Characterization, and Interactions [Internet]. Totowa, NJ: Humana Press; 2009. p. 69–76. Available from: https://doi.org/10.1007/978-1-60327-164-6_7
23. Santoro F, Romeo A, Pozzi G, Iannelli F. Excision and Circularization of Integrative Conjugative Element Tn5253 of Streptococcus pneumoniae. Front Microbiol. 2018 Jul 31;9:1779.
24. Asakura M, Hinenoya A, Alam MS, Shima K, Zahid SH, Shi L, et al. An inducible lambdoid prophage encoding cytolethal distending toxin (Cdt-I) and a type III effector protein in enteropathogenic Escherichia coli. Proc Natl Acad Sci U S A. 2007 Sep 4;104(36):14483–8.
25. Effantin G, Maurizi MR, Steven AC. Binding of the ClpA unfoldase opens the axial gate of ClpP peptidase. J Biol Chem. 2010/03/16 ed. 2010 May 7;285(19):14834–40.
26. Banks DJ, Beres SB, Musser JM. The fundamental contribution of phages to GAS evolution, genome diversification and strain emergence. Trends in Microbiology. 2002 Nov;10(11):515–21.

27. Banks DJ, Porcella SF, Barbian KD, Beres SB, Philips LE, Voyich JM, et al. Progress toward Characterization of the Group A *Streptococcus* Metagenome: Complete Genome Sequence of a Macrolide-Resistant Serotype M6 Strain. J INFECT DIS. 2004 Aug 15;190(4):727–38.
28. Beres SB, Sylva GL, Barbian KD, Lei B, Hoff JS, Mammarella ND, et al. Genome sequence of a serotype M3 strain of group A Streptococcus: phage-encoded toxins, the high-virulence phenotype, and clone emergence. Proc Natl Acad Sci U S A. 2002 Jul 23;99(15):10078–83.
29. Sumby P, Porcella SF, Madrigal AG, Barbian KD, Virtaneva K, Ricklefs SM, et al. Evolutionary Origin and Emergence of a Highly Successful Clone of Serotype M1 Group A *Streptococcus* Involved Multiple Horizontal Gene Transfer Events. J INFECT DIS. 2005 Sep;192(5):771–82.
30. Shoemaker NB, Guild WR. Destruction of low efficiency markers is a slow process occurring at a heteroduplex stage of transformation. Molec Gen Genet. 1974 Dec;128(4):283–90.
31. Prudhomme M, Attaiech L, Sanchez G, Martin B, Claverys J-P. Antibiotic Stress Induces Genetic Transformability in the Human Pathogen *Streptococcus pneumoniae*. Science. 2006 Jul 7;313(5783):89–92.
32. Beres SB, Kachroo P, Nasser W, Olsen RJ, Zhu L, Flores AR, et al. Transcriptome Remodeling Contributes to Epidemic Disease Caused by the Human Pathogen *Streptococcus pyogenes*. mBio. 2016 Jul 6;7(3):e00403-16, /mbio/7/3/e00403-16.atom.
33. Euler CW, Juncosa B, Ryan PA, Deutsch DR, McShan WM, Fischetti VA. Targeted Curing of All Lysogenic Bacteriophage from Streptococcus pyogenes Using a Novel Counter-selection Technique. Beall B, editor. PLoS ONE. 2016 Jan 12;11(1):e0146408.
34. Iannelli F, Pozzi G. Protocol for conjugal transfer of genetic elements in Streptococcus pneumoniae. In 2007.

Figure 1

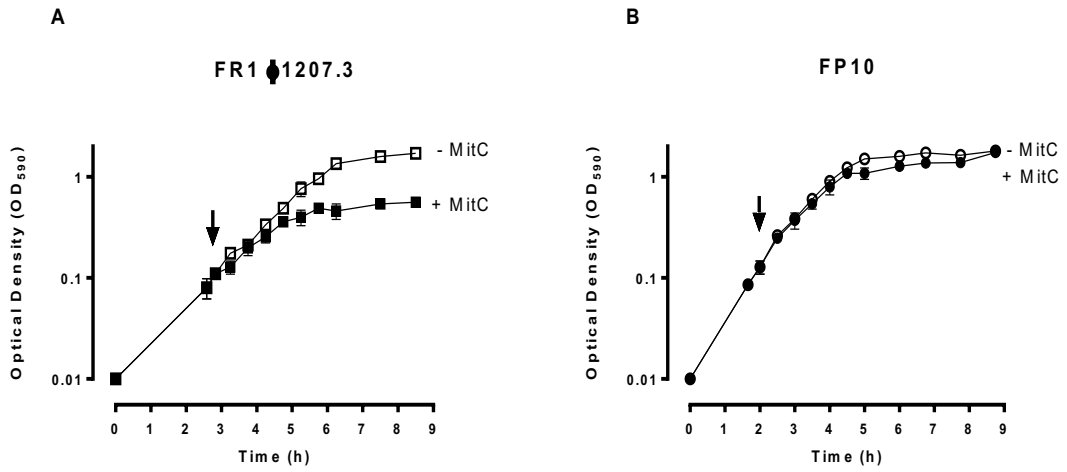

Figure 2

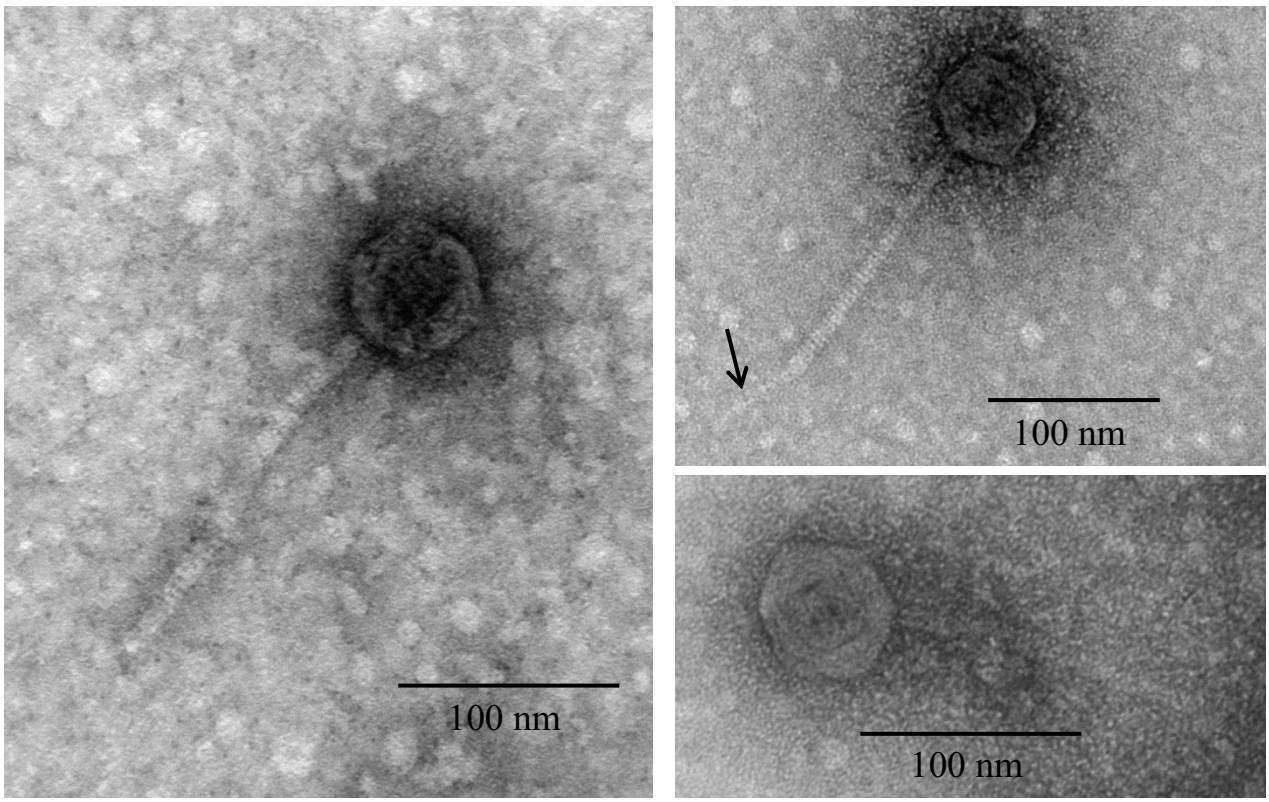

Figure 3

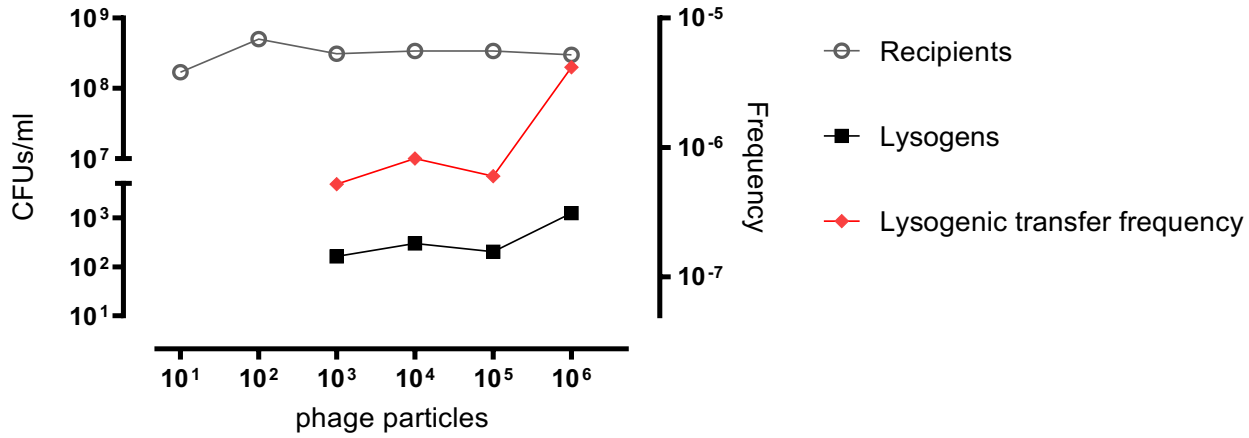

Figure 4

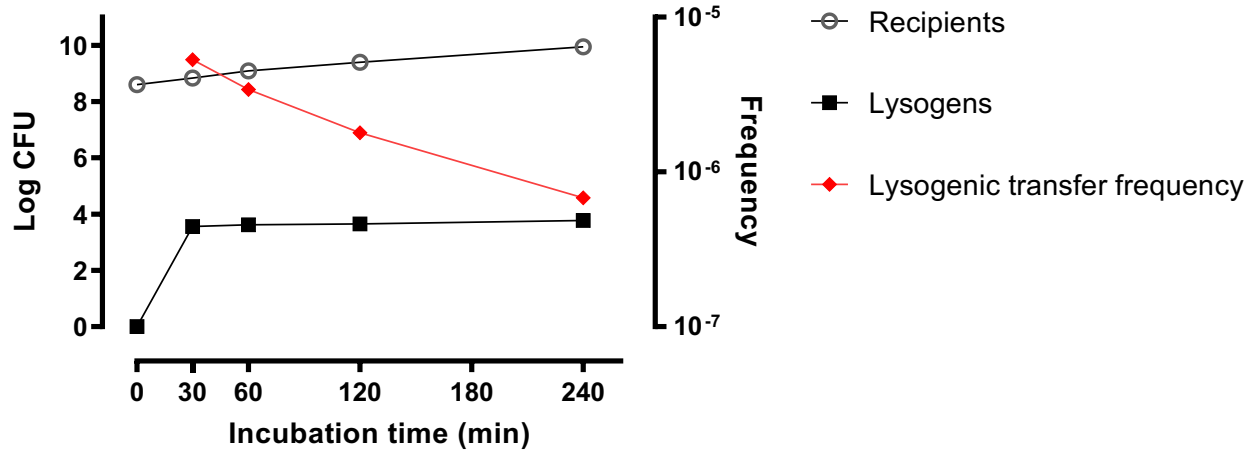

CHAPTER 5

Quantification of bacteriophage φ1207.3 presence in culture supernatant and on the bacterial surface

Francesco Santoro, Valeria Fox, Gabiria Pastore, Francesco Iannelli, Gianni Pozzi

Laboratory of Molecular Microbiology and Biotechnology,

Department of Medical Biotechnologies,

University of Siena, 53100 Siena, Italy

Manuscript in preparation

1. Abstract

The *Streptococcus pyogenes* φ1207.3 is a bacteriophage that carries the *mef*(A)/*msr*(D) gene pair, responsible for macrolide efflux. In previous studies, we demonstrated that this phage does not seem to undergo a lytic cycle with evident cell lysis. Furthermore, φ1207.3 could be transferred to *Streptococcus pneumoniae* and *Streptococcus gordonii* only by a mechanism fitting the operational definition of conjugation, whereas transfer could not be obtained using culture supernatant. For these reasons, in this study we investigated the cellular localization of φ1207.3. Following induction with mitomycin C, φ1207.3 presence in the culture supernatant and on the bacterial surface was investigated through Real-Time PCR and immunological assays. We demonstrated that the number of phage particles attached to bacterial cells exceeds the number of phages that we find in cultures supernatants by 3 orders of magnitude, suggesting that its lysogenic transfer is likely to be dependent on the cell-to-cell contact rather than on the interaction of a free-floating phage particle with a bacterial cell. We also studied the involvement of the Major Capsid (MCP) and Major Tail (MTP) Proteins and suggested that these structural proteins are involved in φ1207.3 transfer, MCP being crucial for the correct assembly of viral particles, while MTP by acting as an attachment site for the Tail Fibers, which are likely involved in the host cell recognition and receptor binding.

2. Introduction

Bacteriophages are the most abundant entities on the biosphere, with an estimated total number of virus-like particles on Earth close to 10^{31}[1–4]. They are typically grouped in two categories, based on their life cycle: lytic and lysogenic (temperate) phages. Lytic phages are defined by their ability, at the end of the viral replicative cycle, to lyse cells, usually causing their destruction, and release newly formed bacteriophage particles. Lysogenic phages, instead, are defined by their ability to integrate their DNA into the host bacterium's chromosome, becoming a stable genetic element that can be passed to daughter cells during cell division. Once integrated in the host genome, they are referred to as prophages, and play a fundamental role in shaping the biology of many bacteria. This lysogenic state is usually extremely stable, allowing the prophages to remain integrated through many cell divisions, but sometime this state may be reversed to the lytic cycle, in a process called prophage induction. Different stimuli can cause the induction of different prophages[5], but usually they include treatments that damage the cellular DNA or inhibit DNA replication, like chemicals (e.g. Mitomycin C[6] and antibiotics [7]) and physical stresses (e.g. UV light,[8,9]). Induction of prophages usually results in the release of a great amount of phage particles, mostly in the range of 10^{8}-10^{11} phage particles/ml[10,11]. The mechanism of transfer of *Streptococcus pyogenes* phages has not been completely elucidated. Some phages undergo a lytic cycle upon induction by specific stimuli, such as the DNA damaging agent Mitomycin C, while others tend to remain in a lysogenic state.

φ1207.3 is a bacteriophage found integrated in *Streptococcus pyogenes* genome that carries the *mef*(A)/*msr*(D) gene pair, responsible for macrolide efflux[12–14]. Prophage φ1207.3 could be transferred to *Streptococcus pneumoniae* and *Streptococcus gordonii* only by a mechanism fitting the operational definition of conjugation, whereas transfer could not be obtained using culture supernatant[12]. Due to its transfer mechanism, it was initially thought to be a conjugative transposon, called Tn*1207.3*, but sequence analysis revealed that is a prophage and thus it was renamed φ1207.3[13]. Previous studies (unpublished) demonstrated that this phage does not seem

to undergo a lytic cycle with evident cell lysis and that even induction with mitomycin C only produces a limited phage burst. The absence of an evident prophage induction and its transfer mechanism which resembles conjugation, likely being dependent on cell-to-cell contact among bacterial cells, prompted us to investigate the cellular localization of φ1207.3. The aim of this study was thus to quantify the φ1207.3 presence in the culture supernatant and to investigate the amount of phage particles present on the bacterial surface through immunological assays.

3. Materials and methods

3.1. Bacterial strains and culture conditions

All strains used in this work and their relevant properties are reported in Table 1.

Streptococcal strains were grown in Tryptic Soy Broth (TSB, BD), or, when needed, Tryptic Soy Broth without dextrose (TSB/wo, BD), at 37°C. Starter cultures were taken at an optical density at 590 nm (OD_{590}) ranging from 0.2 to 0.3 and were stored at -80°C in tubes containing glycerol at a final concentration of 10%. Solid media were obtained by supplementing TSB with 1.5% agar (BD Difco) and 3% defibrinated horse blood (Liofilchem). When required, both liquid and solid media were supplemented with antibiotics at the following concentrations: 0.5 μg/ml erythromycin, 10 μg/ml novobiocin, 500 μg/ml streptomycin, 3 μg/ml chloramphenicol, 500 μg/ml kanamycin.

3.2. Lytic cycle induction with Mitomycin C and phage preparations

Induction of the bacteriophage φ1207.3 lytic cycle was performed with mitomycin C, a known prophage inducer[6]. Strains were inoculated in 600 ml of TSB and grown at 37°C until reaching the early exponential phase (OD_{590} = 0.05-0.1), when the culture was split in two halves, one receiving mitomycin C (Sigma Aldrich) at a sub-MIC concentration (100 ng/ml), and one untreated. After 2 hours of growth at 37°C, with measuring of the optical density every 30 minutes, cultures were taken and, after the addition of 10 mM EDTA, 6 tubes of 44 ml each were centrifuged two times at 5,000 x *g* for 40 minutes at 4°C, in order to eliminate bacterial cells and debris. The supernatant was then supplemented with a protease inhibitor mix (Sigma Aldrich) and 6 tubes of 37

ml were ultracentrifuged at 20,000 x *g* for 2 hours at 10°C with a SW 32 Ti rotor (Optima L-90K Ultracentrifuge; Beckman Coulter). Supernatant was then removed and the pellet containing the phages was resuspended with 100 µl of TM buffer (50 mM Tris-HCl, 10 mM $MgSO_4$) for each ultracentrifuge tube[15]. Phage preparations obtained were then used for transduction experiments, TEM imaging and quantitative PCR (qPCR). The extent of the concentration of phages by ultracentrifuge protocol was calculated. Six tubes of 37 ml were used to concentrate the bacterial cultures, resulting in a total of 222 ml of bacterial supernatant. These 222 ml were then concentrated into 700 µl (100 µl used to resuspend the pellet of each of the 6 tubes, plus 100 µl in excess, accounting for remaining surnatant), thus leading to a concentration of 317.14 times.

3.3. Transmission electron microscopy (TEM) imaging

Transmission electron microscopy (TEM) of phage preparation of mitomycin C induced samples was performed at University of Siena, Department of Life Sciences. Three µl of phage suspension were placed onto a glow-discharged Formvar-coated 300 mesh copper grid and allowed to adsorb for 2 min. Excess liquid was removed with filter paper and a drop of 2% uranyl acetate was added, given time to wet fully and then blotted dry. Samples were observed in a TECNAI G^2 transmission electron microscope operated at 100 kV with magnification of 60,000 ×. Measurements of head diameter, tail length were tested for homogeneity. About 10 representative meshes were observed for each preparation, and 200 fields were observed in each mesh. The number of phage particles for each grid was calculated multiplying the number of phages in a mesh for the number of meshes in a grid (300). The number of phage particles/ml of phage preparation was then calculated and used to quantify the theoretical number of phage particles/ml of bacterial culture supernatant.

3.4. Quantitative PCR

qPCR assay was performed with the KAPA SYBR FAST qPCR Master Mix (2X) Kit (Kapa Biosystems) in a LightCycler 1.5 (Roche) instrument, following the procedure of Santoro et al.,2018[16]. The reaction mix was prepared in a final volume of 20 µl and contained 1X KAPA SYBR FAST qPCR reactive, 200 µM of each primer and 1 µl of starting template. Phage

preparations were preheated for 5 minutes at 90°C before being subjected to PCR. The thermal cycling program comprised 3 minutes of initial denaturation at 95°C, then 40 cycles of: denaturation for 0 seconds at 95°C, annealing for 20 seconds at 50°C, extension for 10 seconds at 72°C. The temperature transition rate was 20°C/s in the denaturation and annealing steps and 5°C/s in the polymerisation step. Melting curve was integrated at the end of the run by increasing temperature from 40°C to 95°C with a ramping of 0.05°C/s and acquiring fluorescence continuously. The primer pairs used are: (i) IF264/IF162, a primer of divergent primers, directed at the ends of the phage genome, amplifying a fragment of 227 bp and used to quantify the phage circular forms; (ii) IF285/IF286, amplifying a 260 bp fragment, used for quantifying prophage *mef(*A) gene; (iii) IF138/IF139, which amplified a 171 bp fragment of chromosomal *gyrB* gene, used for standardization of the results. All primer pairs sequences are listed in Table 2. Serial dilutions of chromosomal DNA with known concentration were used to build a standard curve for the *gyrB* gene, by plotting the threshold cycle against the number of chromosome copies. This standard curve was then used for all the experiments and was recalled in the instrument software to quantify, for each sample tested, the number of *mef*(A) gene copies and circular intermediates. Analysis of the melting curves was performed to discern amplified products from the formation of primer dimers. As for the semi-quantification by TEM imaging, the number of circular genomes copies/ml of phage preparations was converted to number of circular genomes copies/ml of bacterial supernatant.

3.5. Antibody design and synthesis

Antibody orf42-1 (anti-capsid) was produced by Genscript. Rabbit polyclonal antibodies were generated using peptide antigens designed and optimized using the Optimum Antigen™ Design Tool (Genscript). The peptide antigen sequence was cISDRQGRSFKRLNE, corresponding to amino acids 349-362 of the predicted protein sequence of *orf42*. A cysteine was automatically applied to the N terminus of the peptide and conjugated to Keyhole limpet hemocyanin (KLH).

Rabbits were immunized subcutaneously at day 0 with 0.2 mg of peptide-KLH conjugate and boosted at days 14, 35 and 56. Antibodies had an ELISA titer ≥ 1:64,000.

3.6. Western Blot Assay for the detection of capsid protein

Protein lysates were obtained by growing the strains in TSB at 37°C until early exponential phase (OD_{590} = 0.1), when 1 ml-aliquots were centrifuged at 13,000 x *g* for 5 minutes. Bacterial pellets were resuspended in 1 ml of 10 mM Tris HCl (pH = 8), 1 mg/ml of lysozyme (Sigma Aldrich) was added, and samples were incubated at 37°C for 20 minutes. Following centrifugation at 13,000 x *g,* pellets were resuspended in 20 µl of 10 mM Tris HCl, 1 mM EDTA, 2% SDS. The quantification of protein lysates was performed with the Bradford assay, building a standard curve with Bovine Serum Albumin (BSA, Sigma Aldrich). SDS-page electrophoresis was performed using precast polyacrylamide gels (NUPAGE Bis-Tris 4-12%, Invitrogen). Serial dilutions of the protein samples were mixed with 2 µl of Reducing Agent (Invitrogen), 5 µl of Loading Buffer (NUPAGE LDS Sample Buffer, Invitrogen) and Tris, to reach a final volume of 20 µl. Before loading on the gels, samples were denatured at 70°C for 10 minutes. Together with the samples, a molecular weight protein marker (Novex Sharp Pre-Stained Protein Standard, ThermoFisher Scientific) was loaded. The gel was run for 40 minutes at 180 V. Protein samples were transferred to Polyvinylidene difluoride membranes (iBlot® Transfer Stack, PVDF, ThermoFisher Scientific) and blocked with TBS containing 0.1% Tween20 and 3% milk and incubated with shaking for 3 hours at RT. The primary antibody (orf42-1, rabbit IgG) was then added at a dilution of 1:4,000 and incubated for 2 hours and 30 minutes at RT with shaking. The membrane was washed 3 times with TBS containing 0.1% Tween20 and 3% milk with shaking at RT for 3 minutes. The secondary antibody (goat anti-rabbit IgG alkaline phosphatase AP conjugate, Southern Biotech) was added at a dilution of 1:10,000 and incubation occurred for 1 hour at RT with shaking. Washing was performed again three times for 3 minutes and one time for 15 minutes. Immunodetection was performed by placing the membrane in a working solution, containing 100 mM Tris, 100 mM NaCl, 5 mM MgCl at pH = 9.5, supplemented with 5-bromo-4-chloro-3-indolyl phosphate (BCIP, Thermo Fisher Scientific)

and nitro blue tetrazolium (NBT, Thermo Fisher Scientific), by incubating at RT for 10 minutes. The reaction was stopped by adding water and a washing step was performed for 3 times. A calibration curve was obtained by loading on the same gel serial dilutions of Ovalbumin (OVA, Sigma) at known concentrations (4 µg to 125 ng). The density of the bands was quantified using the ImageJ software (National Institutes of Health, USA).

3.7. Immunofluorescence

Cells were grown to an OD_{590} of 0.1 in TSB/wo, harvested by centrifugation, washed with PBS, and resuspended in 1:20 of the original volume in cold TSB. 2 µl of the bacterial suspension (roughly corresponding to 2×10^6 cells) were applied to a well of a ten-well glass side (ThermoFisher Scientific), air dried, and fixed with ethanol. Next, 4 µl of anti-capsid Ab (16 µg/ml) were added to the well and incubated for 30 min at 37°C in a moist chamber. After washing with PBS and PBS with 0.05% Tween, 4 µl of goat anti-rabbit IgG antiserum (1:100 dilution) conjugated with FITC (Sigma Aldrich) were added to each well. The slide was then washed and observed under a fluorescence microscope (Leica DM1000, Leica Microsystems), using a 100 × oil objective.

3.8. Flow cytometry analysis

The presence of phage capsid protein on the bacterial cell surface was evaluated by flow cytometry. Bacterial cells were grown in TSB/wo at 37°C until reaching the early exponential phase (OD_{590} = 0.1), were centrifuged at 7500 x *g* for 10 minutes at 4°C, and the pellet was resuspended in 1 ml of PBS with 1% BSA. After washing with PBS-BSA 1 %, a blocking step was performed with PBS-BSA 1% by incubating at 37°C for 30 minutes. The primary antibody (orf 42-1, rabbit IgG) was then added at a dilution of 1:250 and incubation occurred at 4°C for 1 hour with shaking. Samples were washed repeatedly with PBS-BSA 1% and the secondary antibody (anti-rabbit IgG FITC, Sigma Aldrich) was added at a dilution of 1:100. After incubating 30 minutes at 4°C with shaking, samples were fixed with 4% formaldehyde in PBS before undergoing flow cytometry analysis. Cells were then centrifuged, resuspended in 300 µl of PBS and analyzed using a BD Accuri C6 Plus Flow Cytometer (BD). The instrument lasers were aligned using the BD Accuri Spherotech 8-Peak

(FL1-FL3) and 6-Peak (FL4) Validation Beads (BD). For each sample, 100,000 events were acquired. Data were analyzed with the FlowJo software (TreeStar, OR, USA).

3.9. Immunogold TEM

The presence of phage capsid protein on the bacterial cell surface was evaluated by immunological detection in electron microscopy. Cells were grown until early exponential phase (OD_{590} = 0.1), when 1 ml-aliquots were taken and centrifuged at 5000 x *g* for 10 minutes. Cells were washed and blocked with PBS-BSA 1% for 30 minutes at 37°C in agitation. After centrifugation at 5000 x *g* for 10 minutes, the primary antibody (orf42-1) was added 1:250 in 100 µl of PBS-BSA 1% and samples were incubated at 4°C for 1h in agitation. Samples were again centrifuged and washed 2 times with 0.5 ml of PBS-BSA 1% and the secondary antibody (Alexa Fluor 488-10 nm colloidal gold, Life Technologies), was added, at serial dilutions from 1:40 to 1:320, in 100 µl of PBS-BSA 1%. Incubation was performed for 30 minutes at 37°C in agitation, then samples were centrifuged and washed. Finally, the cells were carefully washed and fixed with 4% formaldehyde in PBS. A drop of suspension was placed onto a glow-discharged Formvar-coated 300 mesh copper grid and allowed to adsorb for 2 minutes. Excess liquid was removed with filter paper and a drop of 2% ammonium molybdate was added, given time to wet fully and then was blotted dry. Samples were observed in a TECNAI G^2 transmission electron microscope operated at 100kV with magnification of 60,000 ×.

3.10. Capsid and tail mutant construction by SOEing PCR

The *orf42* (Major Capsid Protein, MCP) mutagenic construct containing the kanamycin resistance cassette (1033 bp), flanked by the fragments upstream (650 bp) and downstream (481 bp) of *orf42* was obtained by Gene Splicing by Overlap Extension[17], as previously described[18]. The primer pair IF149/IF210 was used to amplify the kanamycin resistance cassette[19], while IF1001/IF233 and IF915/IF1002 to amplify the flanking fragments. Assembly of the final construct was obtained with the IF1001/IF1002 primer pair. The *orf47* (Major Tail Protein, MTP) mutagenic construct containing the kanamycin resistance cassette (876 bp), flanked by the fragments upstream (535 bp)

and downstream (566 bp) of *orf47* was obtained. The primer pair IF149/IF190 was used to amplify the kanamycin resistance cassette), IF1003/IF918 and IF919/IF1004 were used to amplify the flanking fragments. All oligonucleotide primers used are listed in Table 2. PCR was performed with a KAPA HiFi PCR Kit (Kapa Biosystems) in a reaction mix of 25 µl, containing the High-Fidelity Buffer 1X, a tracer solution (Tartrazine 0.24 mg/mL and 1.25% Ficoll), 300 µM of a dNTPs mix, 200 µM of each primer, and 0.4 U of the KAPA HiFi DNA Polymerase. The PCR thermal profile, following manufacturer instructions, was: 1 cycle at 95°C for 3 minutes, followed by 30 cycles at 50°C-55°C for 15 sec (depending on the melting temperature of primers), 72°C for 30 sec-2 min (depending on the length of fragment), 98°C for 10 sec, and finally 1 cycle at 50°C-55°C for 1 min and 72°C for 5 min. PCR products were separated in a 0.8% agarose gel at 200 V for 30 minutes, stained for 15 minutes in a 0.1% Ethidium Bromide solution and visualized with UV light. Mutagenic constructs, obtained directly from PCR reaction or gel purification (NucleoSpin Gel and PCR Clean-up kit, Macherey-Nagel) were quantified using the Qubit 2.0 Fluorometer (Thermo Fisher Scientific) and used as donor DNA in transformation.

3.11. Competent cells preparation and transformation

The obtained purified PCR constructs were used as donor DNA in transformation experiments. FP84 (*S. pneumoniae* strain *comC*-, *cps*-, φ1207.3 integrated in the alternative site *relX*) was used as recipient in transformation experiments. Competent cells for transformation were prepared by inoculating bacteria in 10 ml of warm TSB/GP (TSB supplemented with 20% glucose, 0.5M K_2HPO_4) and by growing them at 37°C until the beginning of the exponential phase (OD_{590} of 0.05-0.1). Cells were then diluted 1:100 in 40 ml of warm CTM (TSB supplemented with 20% glucose, 0.5M K_2HPO_4, 4% BSA, 1% $CaCl_2$) and, after 30 minutes, culture starters were taken every 15 minutes for 2 hours, placed in tubes containing 10% glycerol, previously left on ice and alcohol, and frozen at -70°C. For genetic transformation, competent cells were thawed, supplemented with Competence Stimulating Peptide-1 (CSP-1), at a final concentration of 25 ng/ml, and purified DNA of the mutagenic constructs, at a final concentration of 1 µg/ml, and incubated at 37°C for 45

minutes. The resulting mutant strains were selected for acquisition of kanamycin resistance by multilayer plating and genetic analysis. The deletion of the *orf*42 and *orf*47 was finally confirmed by PCR and sequencing.

4. Results

4.1. Phage preparations are enriched for φ1207.3

Quantification of φ1207.3 was performed by qPCR and with a semi-quantitative approach based on the TEM imaging, for both mitomycin C treated and untreated phage preparations.

We used qPCR to quantify the copy number of (i) the joints between the ends of φ1207.3 sequence, i.e. the circular or concatemeric forms of phage DNA, (ii) the *mef*(A) gene of φ1207.3, and (iii) the chromosomal gene *gyrB*, in both bacterial culture and phage preparations (Table 3). We estimated about 1.87 x 10^7 phage particles/ml in the mitomycin C phage preparation and 1.03 x 10^7 phage particles/ml in the untreated phage preparation. These values corresponded, respectively, to 4.13 x 10^4 and 2.28 x 10^4 phage particles/ml of the original bacterial supernatant. Phage preparations, both treated with mitomycin C and untreated, showed an enrichment in concatemeric phage genomes and *mef*(A) gene copy number when compared to the bacterial culture from which they were obtained. The enrichment in concatemeric phage genomes was 38-fold in the untreated cultures and 70-fold in the mitomycin C treated cultures, while the enrichment for the resistance gene was 7.8- and 38-fold, respectively. The number of copies of the *gyrB* gene was 5-10 times lower in the phage preparations than in the bacterial culture.

A semi-quantitative approach based on the TEM was also implemented to quantify the number of φ1207.3 particles in the culture supernatant. We estimated about 2.37 x 10^6 phage particles/ml in the mitomycin C phage preparation and 9.33 x 10^5 phage particles/ml in the untreated phage preparation. These values corresponded, respectively, to 5.22 x 10^3 and 2.06 x 10^3 phage particles/ml of the original bacterial supernatant and are concordant with the qPCR estimates (Table 4).

4.2. Φ1207.3 Major Capsid Protein is localized on the bacterial surface

Since (i) the number of phage particles recovered from concentration of culture supernatants was low, (ii) the induction of the phage with mitomycin C did not cause cell lysis, and (iii) the phage transfer seemed to be dependent on cell-to-cell contact (dati prima parte), we asked whether phages were preferentially localized within the bacterial cell or on its surface rather than being released in culture supernatants. To test this hypothesis, we performed Western blot analysis on lysates of bacterial strains FP10 and FR1 using a rabbit polyclonal antibody directed against a 15 aa-long peptide on the C terminal portion of the predicted protein sequence of Orf42, φ1207.3 major capsid protein. The analysis showed a band of approximately 28 kDa present in FR1 (carrying the bacteriophage) and not present in FP10 (not carrying the bacteriophage) (Figure 1). This length is coherent with a proteolytic cleavage by the Clp-protease, encoded by *orf41*, on the native major capsid protein, which was calculated to have a molecular weight of 44.4 kDa. The cleavage site predicted by the Merops software (https://merops.sanger.ac.uk/cgi-bin/pepsum?id=S14.001;type=P), is located after amino acid 126 of the major capsid protein, leaving a processed protein of 270 amino acids in length with a predicted molecular weight of 29.5 kDa. Whole bacterial cells from liquid culture of FR1 were then assayed by flow cytometry to investigate the cellular localization of the major capsid protein, using the same antibody. Strain FP10 was used as negative control, as it does not carry the bacteriophage. A further negative control was obtained by treating the cells only with the secondary antibody. Figure 2 shows the overlapped fluorescence histograms of FP10 (in blue) and FR1 (in red). A subpopulation of FR1 cells has a fluorescence peak which is absent in FP10, demonstrating that the major capsid protein is present on the surface of cells harboring φ1207.3. The major capsid protein positive population includes 11.9 % of the total cells in the population, suggesting that each of these cells has at least one pro-head or assembled head on the bacterial surface. To further confirm these results, we used the antibody directed against the major capsid protein in an immune TEM experiment. Small clusters of

reacting antibodies, ranging from 1 to 15, could be observed on the cell surface of many FR1 cells (Figure 3), suggesting the presence of phage particles associated with the bacterial surface.

4.3. MCP and MTP are likely to play a role in φ1207.3 transfer

Major Capsid and Major Tail protein mutants were constructed to determine whether these two structural proteins are involved in the φ1207.3 transfer. qPCR analysis showed that MTP mutant can produce phage circular genomes (Figure 4), suggesting that MTP absence does not prevent circular and concatemeric genomes packaging. When observed at the TEM, MTP mutant also showed the presence of phage particles with an icosahedral capsid (Figure 5) demonstrating that the absence of the Major Tail Protein does not affect phage capsid assembly. For MCP, instead, qPCR analysis revealed that circular genomes are produced at a lower extent compared to the wt (FP84) (Figure 4), showing that the Major Capsid Protein deletion impairs genome packaging, and no phage particles could be observed at the TEM, suggesting an essential role of the Major Capsid Protein on correct phage assembly. φ1207.3 lysogenic transfer was not obtained for both mutants (Table 5). For the MCP mutant, the absence of transfer was likely due to the absence of assembled phage particles, as none could be observed at the transmission electron microscopy, whereas for MTP mutant, it is possible that the protein is essential for a successful phage transfer, for the cell-to-cell interaction.

5. Discussion

Bacteriophages play an important role in shaping the physiology and pathogenesis of *S. pyogenes*, they carry several virulence genes – such as superantigens, DNases, and phospholipases-, mediate the horizontal transfer of host genes and, as in the case of φ1207.3, the spread of antibiotic resistance[20]. We previously demonstrated that φ1207.3 is able to produce mature phage particles, with a morphology consistent with that of *Siphoviridae* family (unpublished results). φ1207.3 does not seem to undergo a lytic cycle with evident cell lysis, even though induction with mitomycin C produces a limited phage burst, as suggested by the impairment in cell growth and the early

entrance in the stationary phase. Furthermore, we demonstrated that ultracentrifuged phage preparations obtained in the presence of mitomycin C are enriched in both φ1207.3 circular forms and resistance genes compared to the uninduced ones. Nonetheless, even upon mitomycin induction, the estimated quantity of φ1207.3 in the culture supernatant (about 10^4 particles/ml of culture supernatant) is relatively scarce when compared to other bacteriophages[10,11].

Here, we demonstrated that the major capsid protein is present on the surface of bacterial cells carrying φ1207.3 integrated into the genome. In an exponentially growing bacterial culture (roughly containing 10^8 CFU/ml), the proportion of cells positive for the presence of the major capsid protein is higher than 10%. If we assume that each positive cell has a complete phage particle attached to the surface, the number of phage particles attached to cells exceeds the number of phages that we find in cultures supernatants by 3 orders of magnitude. The lysogenic transfer of φ1207.3 is therefore likely to be dependent on the cell-to-cell contact rather than on the interaction of a free-floating phage particle with a bacterial cell. Study on the Major Capsid and Major Tail Protein suggests that these structural proteins are involved in φ1207.3 transfer, MCP being crucial for the correct assembly of viral particles, while MTP by acting as an attachment site for the Tail Fibers, which are likely involved in the host cell recognition and receptor binding.

In conclusion, we demonstrated that φ1207.3, carrying the *mef*(A)-*msr*(D) macrolide efflux resistance genes, is able to transfer to different bacterial species through a mechanism which resembles conjugation and is dependent on cell-to-cell contact. We propose that this mechanism of transfer may be explained by the presence of the phage particles on the bacterial surface, rather than in the culture supernatant, and hypothesized that the major structural proteins, MCP and MTP, may play a role in this mechanism. To our knowledge, this is the first evidence of a bacteriophage lysogenic transfer mechanism relying on cell-to-cell contact.

Tables

Table 1. **Bacterial strains used in this work and relative properties.**

Strain	Properties	References
2812A	Italian clinical strain of Streptococcus pyogenes carrying φ1207.3, Em^R	Santagati et al., 2003[12]
FP10	Streptococcus pneumoniae Rx1 unencapsulated, competence deficient derivative, ΔcomC, Cm^R, Sm^R	Iannelli and Pozzi, 2007[21]
FR1	FP10 derivative carrying φ1207.3 integrated in celB, ΔcomC, Cm^R, Sm^R, Em^R	Santoro et al. (unpublished)
FP84	FP10 derivative carrying φ1207.3 integrated in relX, ΔcomC, Cm^R, Sm^R, Em^R	This study
FR164	FP84 derivative carrying φ1207.3Δorf42, ΔcomC, Cm^R, Sm^R, Em^R, Km^R	This study
FR165	FP84 derivative carrying φ1207.3Δorf47, ΔcomC, Cm^R, Sm^R, Em^R, Km^R	This study

Em, erythromycin; Cm, chloramphenicol; Sm, streptomycin; Km, kanamycin

Table 2. **Oligonucleotides used in this work.**

Primer	5'-3' sequence
IF138	CAGATCAAGAAATCAAACTCCAA
IF139	CAGCATCATCTACAGAAACTC
IF140	GCTACTCCTCCTAAGAACAA
IF162	TGATGATTATATAAATTGTGAGTT
IF210	CTAAAACAATTCATCCAGTAAAATAT
IF233	ATCAAACGGATCCCCAGCTTG-TTTGTCCATAGTATAAATGTCCT
IF264	CTTGCTCTCACTTATTATATT
IF276	TGTGAGTTAGTGGGTACG
IF283	ATACTAGAATCTCCCCTACA
IF285	GGTCTTGTCTATGGCTTC
IF286	CTAAAAGTGGCGTAACCG
IF915	ATATTTTACTGGATGAATTGTTTTAG-CTATCTACGAGTTGATACTTCTG
IF918	ATCAAACGGATCCCCAGCTTG-TATGTTCTCCTTCTTAAAATG
IF919	ATATTTTACTGGATGAATTGTTTTAG-TCGCAAGTGGAGGTAGTCGT
IF1001	TTGGGGATGAGGTAACTCCT
IF1002	CAAGTGAGGCGACTTCTGAATC
IF1003	GGAAACGAGTAGCACGTCCA
IF1004	CCAGTGCCATCCCAATAGAGATG

[a] The sequences underlined are sequences complementary to the kanamycin resistance cassette primers IF149 (for primers IF233 and IF918) and IF210 (for the primers IF915 and IF919).

Table 3. **Quantification of φ1207.3 phage genomes by qPCR.** The results of the qPCR analysis are reported as copies/ml of ultracentrifuged phage preparations, both induced and not induced with mitomycin C, and of bacterial cultures in exponential phase not ultracentrifuged. Fold enrichment is reported as the ratio between ultracentrifuged phage preparations, both in the presence (MitC) and

absence (no MitC) of mitomycin C, and not centrifuged bacterial cultures. Both phage preparations resulted in an increase in circular forms and resistance gene, although in both cases the increase was higher in the mitomycin C treated phage preparations. The amount of chromosomal gene *gyrB* measured in both preparations, instead, was lower. Results are reported as means and standard deviations, resulting from at least three independent experiments.

	Concatemeric genomes - copies/ml (± SD)	**Resistance gene – *mef*(A) - copies/ml (± SD)**	**Chromosomal gene – *gyrB* - copies/ml (± SD)**
Phage preparations (MitC)[a]	1.9×10^7 ($\pm 1.8 \times 10^7$)	1.9×10^8 ($\pm 2.1 \times 10^8$)	9.2×10^5 ($\pm 3.9 \times 10^5$)
Phage preparations (no MitC)[b]	1.0×10^7 ($\pm 1.3 \times 10^7$)	3.8×10^7 ($\pm 4.0 \times 10^7$)	3.9×10^5 ($\pm 2.3 \times 10^5$)
Bacterial cultures[c]	2.7×10^5 ($\pm 4.6 \times 10^4$)	4.9×10^6 ($\pm 3.3 \times 10^6$)	5.5×10^6 ($\pm 4.0 \times 10^6$)
Fold enrichment (MitC)	*70*	*38*	*0.2*
Fold enrichment (no MitC)	*38*	*7.8*	*0.1*

[a]Concentrated supernatant of cultures induced with Mitomycin C
[b]Concentrated supernatant of cultures not induced with Mitomycin C
[c]Bacteria in their growth medium, in exponential phase

***Table 4*. Quantification of φ1207.3 phage particles by a TEM semi-quantitative approach.** Quantification of φ1207.3 was performed by counting the phage particles of both mitomycin C induced (MitC) and not induced (no MitC) phage preparations in the TEM grid. The number of phage particles was converted first to phage particles/ml of phage preparations and was then transformed to the number of phage particles/ml of culture supernatant. Results are reported as means and standard deviations, resulting from three independent experiments.

	Phage particles/ml of phage preparations (± SD)	Phage particles/ml of culture supernatant (± SD)
Phage preparations (MitC)[a]	2.37×10^6 ($\pm 9.96 \times 10^5$)	5.22×10^3 ($\pm 2.20 \times 10^3$)
Phage preparations (no MitC)[b]	9.33×10^5 ($\pm 2.31 \times 10^5$)	2.06×10^3 ($\pm 5.10 \times 10^2$)

[a]Concentrated supernatant of cultures induced with Mitomycin C
[b]Concentrated supernatant of cultures not induced with Mitomycin C

Table 5. **Frequencies of lysogenic transfer of MCP and MTP mutants.** Mean of three replicates with standard deviation is reported.

	Frequency of lysogenic transfer
wild type φ1207.3 (FP84)	$3.69 \times 10^{-7} \pm 2.15 \times 10^{-7}$
MCP mutant (FR164)	$<9.02 \times 10^{-8} \pm 1.18 \times 10^{-8}$
MTP mutant (FR165)	$<8.05 \times 10^{-8} \pm 2.88 \times 10^{-8}$

FIGURE LEGENDS

Figure 1. **Western blot detection of φ1207.3 Major Capsid Protein using the or42-1 antibody.** Lanes 1 and 2: FP10, parental strain, not carrying φ1207.3, 10 and 15 μg of bacterial lysate loaded, respectively; lanes 3 and 4: FR1, strain carrying φ1207.3, 10 and 15 μg of bacterial lysate loaded, respectively.

Figure 2. **Flow cytometry analysis of FP10 and FR1 strains using the orf42-1 antibody, directed against the φ1207.3 Major Capsid Protein.** Overlap of the fluorescence of the parental strain FP10, not carrying φ1207.3 (blue) and FR1, carrying φ1207.3 (red). A subpopulation of FR1 cells (11.9 %) has a fluorescence peak which is absent in FP10.

Figure 3. **Immunogold TEM detection of φ1207.3 Major Capsid Protein on the surface of FR1 cells, with the use of antibody orf42-1.** Small clusters of reacting antibodies (1-15) are found on the cell surface of cells harbouring φ1207.3. Scale is reported.

Figure 4. **qPCR analysis of circular forms of wild type φ1207.3 and MCP and MTP mutants.** MTP mutant can produce phage circular genomes, while MCP mutant is able to produce circular genomes with a lower value (about 10-fold) compared to the wild type (wt). Culture, not centrifuged bacterial cultures; no MitC, ultracentrifuged phage preparations not induced with mitomycin C; MitC, mitomycin C induced ultracentrifuged phage preparations.

Figure 5. **Major Tail Protein mutant observed at the TEM.** Transmission electron microscopy of FR165 performed after negative staining showed structures consistent with viral capsids. Scale is reported.

6. References

1. Hendrix RW, Smith MCM, Burns RN, Ford ME, Hatfull GF. Evolutionary relationships among diverse bacteriophages and prophages: All the world's a phage. Proceedings of the National Academy of Sciences. 1999 Mar 2;96(5):2192–7.
2. Clokie MR, Millard AD, Letarov AV, Heaphy S. Phages in nature. Bacteriophage. 2011 Jan;1(1):31–45.
3. Bar-On YM, Phillips R, Milo R. The biomass distribution on Earth. Proc Natl Acad Sci USA. 2018 Jun 19;115(25):6506–11.
4. Mushegian AR. Are There 10^{31} Virus Particles on Earth, or More, or Fewer? Margolin W, editor. J Bacteriol [Internet]. 2020 Apr 9 [cited 2021 Aug 13];202(9). Available from: https://journals.asm.org/doi/10.1128/JB.00052-20
5. Little JW. Lysogeny, Prophage Induction, and Lysogenic Conversion. In: Waldor MK, Friedman DI, Adhya SL, editors. Phages [Internet]. Washington, DC, USA: ASM Press; 2014 [cited 2021 Aug 16]. p. 37–54. Available from: http://doi.wiley.com/10.1128/9781555816506.ch3
6. OTSUJI N, SEKIGUCHI M, IIJIMA T, TAKAGI Y. Induction of Phage Formation in the Lysogenic Escherichia coli K-12 by Mitomycin C. Nature. 1959 Oct 1;184(4692):1079–80.
7. López E, Domenech A, Ferrándiz M-J, Frias MJ, Ardanuy C, Ramirez M, et al. Induction of Prophages by Fluoroquinolones in Streptococcus pneumoniae: Implications for Emergence of Resistance in Genetically-Related Clones. Beall B, editor. PLoS ONE. 2014 Apr 9;9(4):e94358.
8. Ryan AM. A unique mode of action of ultraviolet irradiation in prophage induction. Biochimica et Biophysica Acta. 1962 Jul;60(2):455–7.
9. Lamont I, Brumby AM, Egan JB. UV induction of coliphage 186: prophage induction as an SOS function. Proceedings of the National Academy of Sciences. 1989 Jul 1;86(14):5492–6.
10. Loś JM, Loś M, Wegrzyn G, Wegrzyn A. Differential efficiency of induction of various lambdoid prophages responsible for production of Shiga toxins in response to different induction agents. Microb Pathog. 2009 Dec;47(6):289–98.
11. Alexeeva S, Guerra Martínez JA, Spus M, Smid EJ. Spontaneously induced prophages are abundant in a naturally evolved bacterial starter culture and deliver competitive advantage to the host. BMC Microbiol. 2018 Dec;18(1):120.

12. Santagati M, Iannelli F, Cascone C, Campanile F, Oggioni MR, Stefani S, et al. The Novel Conjugative Transposon Tn1207.3 Carries the Macrolide Efflux Gene mef(A) in Streptococcus pyogenes. Microbial Drug Resistance. 2003 Aug;9(3):243–7.
13. Iannelli F, Santagati M, Santoro F, Oggioni MR, Stefani S, Pozzi G. Nucleotide sequence of conjugative prophage Φ1207.3 (formerly Tn1207.3) carrying the mef(A)/msr(D) genes for efflux resistance to macrolides in Streptococcus pyogenes. Front Microbiol. 2014 Dec 9;5:687–687.
14. Iannelli F, Santoro F, Santagati M, Docquier J-D, Lazzeri E, Pastore G, et al. Type M Resistance to Macrolides Is Due to a Two-Gene Efflux Transport System of the ATP-Binding Cassette (ABC) Superfamily. Front Microbiol. 2018 Jul 31;9:1670.
15. Bernheimer HP. Lysogenic pneumococci and their bacteriophages. Journal of Bacteriology. 1979;138(2):618–24.
16. Santoro F, Romeo A, Pozzi G, Iannelli F. Excision and Circularization of Integrative Conjugative Element Tn5253 of Streptococcus pneumoniae. Front Microbiol. 2018 Jul 31;9:1779.
17. Horton RM, Cai Z, Ho SN, Pease LR. Gene Splicing by Overlap Extension: Tailor-Made Genes Using the Polymerase Chain Reaction. BioTechniques [Internet]. 2013 Mar 1 [cited 2021 Mar 6];54(3). Available from: https://www.future-science.com/doi/10.2144/000114017
18. Iannelli F, Pozzi G. Method for Introducing Specific and Unmarked Mutations Into the Chromosome of Streptococcus pneumoniae. MB. 2004;26(1):81–6.
19. Pearce BJ, Iannelli F, Pozzi G. Construction of new unencapsulated (rough) strains of Streptococcus pneumoniae. Research in Microbiology. 2002;5.
20. McShan WM, Nguyen SV. The Bacteriophages of Streptococcus pyogenes. :30.
21. Iannelli F, Pozzi G. Protocol for conjugal transfer of genetic elements in Streptococcus pneumoniae. In 2007.

Figure 1

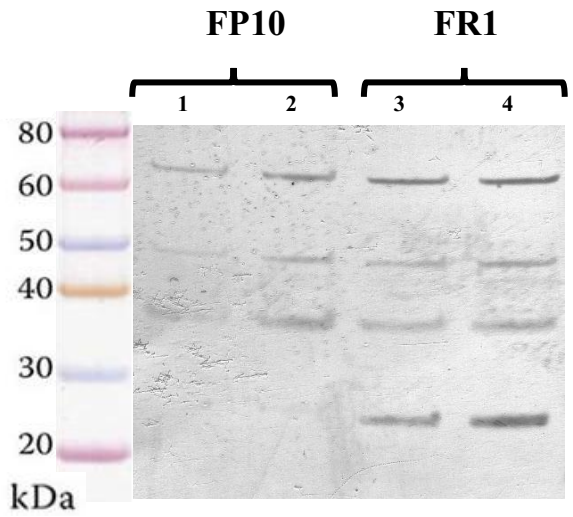

Figure 2

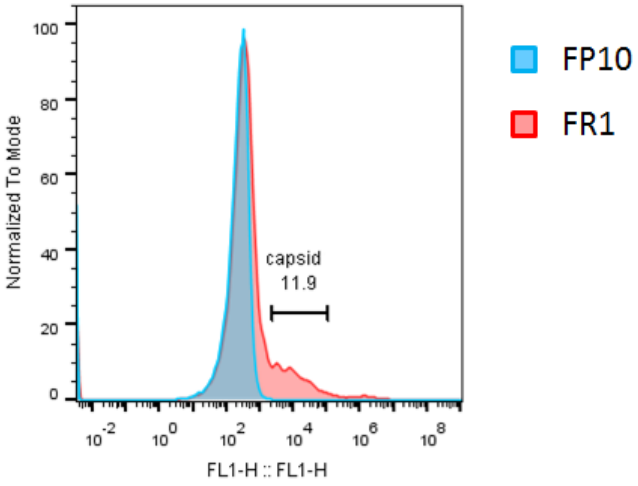

Figure 3

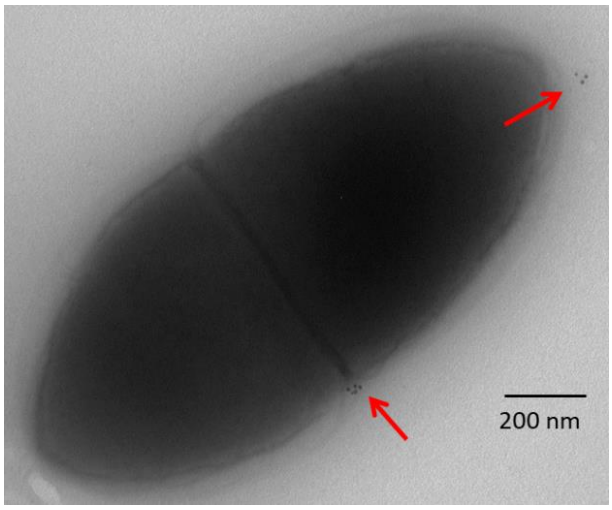

Figure 4

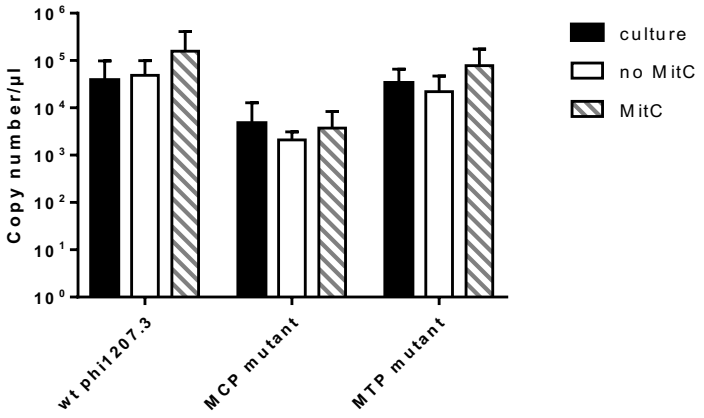

Figure 5

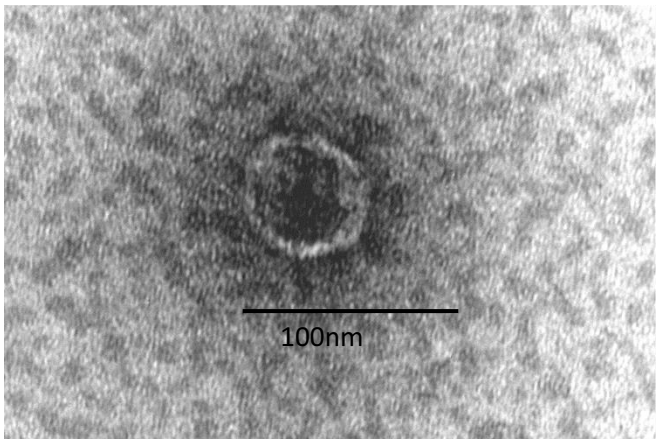

CHAPTER 6

A Mating Procedure for Genetic Transfer of Integrative and Conjugative Elements (ICEs) of Streptococci and Enterococci

Francesco Iannelli, Francesco Santoro, Valeria Fox, Gianni Pozzi

Laboratory of Molecular Microbiology and Biotechnology,

Department of Medical Biotechnologies,

University of Siena, 53100 Siena, Italy

Methods and Protocols 2021, 4(3), 59

methods and protocols

MDPI

Protocol

A Mating Procedure for Genetic Transfer of Integrative and Conjugative Elements (ICEs) of Streptococci and Enterococci

Francesco Iannelli *, Francesco Santoro, Valeria Fox and Gianni Pozzi

Laboratory of Molecular Microbiology and Biotechnology, Department of Medical Biotechnologies, University of Siena, 53100 Siena, Italy; santorof@unisi.it (F.S.); valeria.fox@student.unisi.it (V.F.); gianni.pozzi@unisi.it (G.P.)

* Correspondence: francesco.iannelli@unisi.it

Abstract: DNA sequencing of whole bacterial genomes has revealed that the entire set of mobile genes (mobilome) represents as much as 25% of the bacterial genome. Despite the huge availability of sequence data, the functional analysis of the mobile genetic elements (MGEs) is rarely reported. Therefore, established laboratory protocols are needed to investigate the biology of this important part of the bacterial genome. Conjugation is a mechanism of horizontal gene transfer which allows the exchange of MGEs among strains of the same or different bacterial species. In streptococci and enterococci, integrative and conjugative elements (ICEs) represent a large part of the mobilome. Here, we describe an efficient and easy-to-perform plate mating protocol for in vitro conjugative transfer of ICEs in streptococci (*Streptococcus pneumoniae*, *Streptococcus agalactiae*, *Streptococcus gordonii*, *Streptococcus pyogenes*), *Enterococcus faecalis*, and *Bacillus subtilis*. Conjugative transfer is carried out on solid media and selection of transconjugants is performed with a multilayer plating. This protocol allows the transfer of large genetic elements with a size up to 81 kb, and a transfer frequency up to 6.7×10^{-3} transconjugants/donor cells.

Keywords: horizontal gene transfer; conjugation; MGE; ICE; conjugative transposon; streptococci; enterococci

Citation: Iannelli, F.; Santoro, F.; Fox, V.; Pozzi, G. A Mating Procedure for Genetic Transfer of Integrative and Conjugative Elements (ICEs) of Streptococci and Enterococci. *Methods Protoc.* **2021**, *4*, 59. https://doi.org/10.3390/mps4030059

Academic Editor: Claudio Avignone Rossa

Received: 23 July 2021
Accepted: 26 August 2021
Published: 28 August 2021

1. Introduction

The three major mechanisms of horizontal gene transfer in bacteria are conjugation, transformation, and transduction. Mobile genetic elements (MGEs), including conjugative and integrative elements (ICEs) and prophages, shape the bacterial genome and are responsible for genome evolution [1]. Conjugation enables the genetic exchange of MGEs, which provide a major contribution to the spread of antimicrobial resistance and virulence, by recruiting new resistance and virulence genes and facilitating their dissemination [2]. Genome-wide DNA sequencing disclosed the presence of a large number of uncharacterized MGEs, whose open reading frames are often automatically annotated as conserved genes of unknown function [3]. In fact, the nature of the mobile elements and their transfer mechanisms have been clarified only in few cases [4–7]. ICEs account for the majority of streptococcal and enterococcal MGEs [8]. To elucidate transfer mechanisms and their regulation it is essential to develop an established protocol for efficient conjugal transfer of ICEs also from encapsulated clinical bacterial strains. In this work, we developed a successful plate mating protocol for in vitro transfer of large ICEs with a size up to 81 kb in streptococci (*Streptococcus pneumoniae*, *Streptococcus agalactiae*, *Streptococcus gordonii*, *Streptococcus pyogenes*), *Enterococcus faecalis*, and *Bacillus subtilis*.

2. Materials and Equipment

- Deionized H_2O;
- Tryptic soy broth (TSB), agar technical (BD, Difco, USA);
- Defibrinated horse blood (Liofilchem, Italy);
- Antibiotics, glycerol, ethanol (Sigma-Aldrich, USA);

- Filter 0.2 µm (Minisart, Sartorius, Germany);
- Petri dishes, tubes, serological pipets, microtubes, micropipette tips, cotton swabs, toothpicks, syringes (Sarstedt, Germany);
- Laboratory glassware (Schott, UK);
- Incubators (KW Apparecchi Scientifici, Italy);
- Spectronic GENESYS 200 spectrophotometer (Thermo Scientific, USA);
- Heat block (FALC Instruments, Italy);
- White light transilluminator;
- VAPOUR-Line autoclave (VWR Avantor, USA).

3. Methods

A schematic diagram of the plate mating protocol is reported in Figure 1.

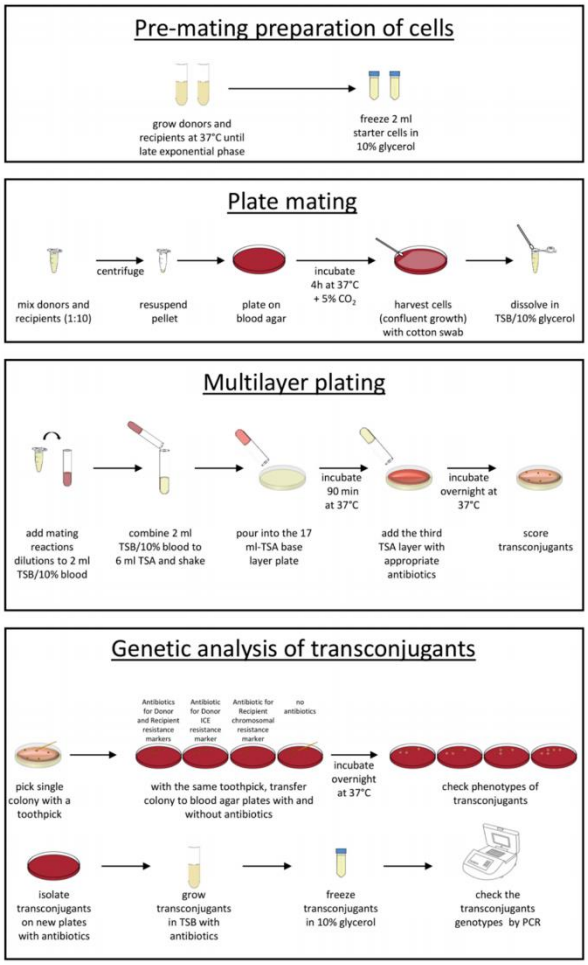

Figure 1. Schematic representation of the plate mating protocol for ICEs conjugal transfer in *streptococci* and *enterococci*.

3.1. Preparation of Media

1. Liquid medium: Dissolve 30 g of TSB dehydrated medium in 1 L of deionized H_2O and autoclave at 121 °C for 15 min (see Note 1). Add the appropriate antibiotics at the following concentrations when required: 3 μg mL^{-1} chloramphenicol, 0.5 μg mL^{-1} erythromycin, 500 μg mL^{-1} kanamycin, 10 μg mL^{-1} novobiocin, 100 μg mL^{-1} spectinomycin, 500 μg mL^{-1} streptomycin, 5 μg mL^{-1} tetracycline, 25 μg mL^{-1} fusidic acid, 25 μg mL^{-1} rifampicin.
2. Solid medium: Add 1.5% agar to TSB liquid medium and autoclave at 121 °C for 15 min. Equilibrate TSA (TSB and agar) at 48 °C for 20 min. Add 5% defibrinated horse blood and the appropriate antibiotics at the concentrations reported in step 1 when required. Mix and pour 25 mL in each Petri dish. Leave to solidify for 20 min, dry at 42 °C for 30 min and store at 4 °C.
3. Antibiotics such as kanamycin, novobiocin, spectinomycin, or streptomycin are resuspended in deionized H_2O, sterilized by filtration with a 0.2 μm filter; chloramphenicol, erythromycin, tetracycline, and fusidic acid are resuspended in absolute ethanol; rifampicin is resuspended in methanol. Stock solutions are as follows: 10 mg mL^{-1} chloramphenicol, 2.5 mg mL^{-1} erythromycin, 100 mg mL^{-1} kanamycin, 10 mg mL^{-1} novobiocin, 50 mg mL^{-1} spectinomycin, 100 mg mL^{-1} streptomycin, 5 mg mL^{-1} tetracycline, 5 mg mL^{-1} fusidic acid, 25 mg mL^{-1} rifampicin. Antibiotics are stored in 1 mL aliquots at −20 °C (see Note 2).
4. Glycerol is diluted two-fold (50%) in TSB.

3.2. Pre-Mating Preparation of Cells

1. Thaw frozen starter cultures at 37 °C.
2. Pre-warm TSB at 37 °C.
3. Dilute frozen cultures 100 fold in TSB containing antibiotics and incubate at 37 °C.
4. Grow donor and recipient cells separately until late exponential phase.
5. Record the OD_{590} on a semi-log paper.
6. Draw the growth curve and determine the duplication time.
7. Freeze 2 mL mating starter cells at OD_{590} = 0.8 (approximately 5×10^8 CFU mL^{-1}) in 10% glycerol (see Note 3).

3.3. Plate Mating

1. Thaw frozen mating starter cultures (see Note 4).
2. Mix 1:10 donor cells (100 μL) and recipient cells (900 μL) in a 1.5 mL microtube (see Note 5).
3. Centrifuge the mixed cells at room temperature for 15 min at 3000 × g.
4. Discard supernatant and resuspend the pelleted cells in 0.1 mL of TSB.
5. Plate mixture on a blood-agar plate and incubate at 37 °C for 4 hours in a 5% CO_2 enriched atmosphere.
6. Harvest cells by scraping from the plate with a cotton swab and dissolve in a 1 mL of TSB/Glycerol 10%.
7. Freeze mating samples at −70 °C (see Note 6).

3.4. Multilayer Plating

1. Prepare TSA medium and equilibrate at 48 °C for 20 min.
2. Pour a 17 mL base layer of TSA in Petri dishes and let the medium solidify.
3. Dispense 2 mL of TSB supplemented with 10% horse blood in 5 mL slip-cap tubes.
4. Put 13 mL slip-cap tubes into a heat block at 48 °C and distribute 6 ml of TSA per tube.
5. Add appropriately diluted mating reactions into the 2 mL-TSB-containing tube (see Note 7).
6. Combine 6 ml of TSA with the 2 mL of TSB blood cells, shake, and pour onto plate.
7. Let the medium solidify, incubate at 37 °C for 90 min (phenotypic expression).
8. Add an 8 ml third layer of TSA containing the appropriate antibiotics (see Note 8).

9. Let the medium solidify, then incubate at 37 °C overnight (see Note 9).
10. Score transconjugant cells, calculate conjugation efficiency as transconjugant per donor cells.

3.5. Genetic Analysis of Transconjugants

1. Fit blood-agar plates on grids of the transilluminator device (see Note 10).
2. Pick single colony isolates from conjugation plates by using sterile toothpicks and transfer to the plates placed on the illuminated grid.
3. Incubate at 37 °C overnight in a 5% CO_2 enriched atmosphere.
4. Check the phenotypes of transconjugants (see Note 11).
5. Isolate transconjugants from the genetic analysis plates on new plates containing the appropriate antibiotic.
6. Incubate at 37 °C overnight in a 5% CO_2 enriched atmosphere.
7. Grow single colony isolates in TSB containing the appropriate antibiotic.
8. Freeze transconjugant starter cultures (in exponential phase, OD_{590} = 0.2–0.3) in 10% glycerol at −70 °C.

4. Notes

1. Other media, such as brain heart infusion (BHI) (Oxoid, UK) for streptococci and enterococci can be used. For *Bacillus subtilis* the Luria–Bertani (LB) medium (BD, Difco) was used.
2. Due to light sensitivity, wrap the microtubes containing novobiocin, tetracycline, and rifampicin antibiotics in aluminum foil. Antibiotics may be stored at −20 °C for extended periods. When preparing antibiotic solutions wear protective clothing, gloves, and eye/face protection.
3. Disposable frozen mating starter cells can be stored at −70°C for extended periods. The use of donor and recipient cells at a concentration of approximately 5 × 10^8 CFU mL^{-1} is mandatory
4. Alternatively, fresh donor and recipient cell cultures may be used.
5. Donor cells (100 µL) and recipient cells (900 µL) are also processed separately with the same procedure and included as controls for the conjugation experiment. The 1/10 donor/recipient cell ratio is mandatory.
6. Mating reactions can be frozen at –70 °C and plated later. Comparable numbers of transconjugants can be obtained from fresh or frozen mating reactions.
7. Dilutions are routinely plated as follows: 10^{-1} and 10^{-2} of the conjugation mixture for transconjugants selection, 10^{-6} and 10^{-7} for donor cells counts, 10^{-7} and 10^{-8} for recipient cells counts.
8. We constructed new *Streptococcus pneumoniae* strains, FP10 and FP11, to be used as standard conjugation recipients to transfer MGEs from the original encapsulated clinical isolates. These strains: (i) lack the capsule, (ii) contain a deletion in the *comC* gene for competence stimulating peptide (CSP) and are impaired in natural competence for genetic transformation, and (iii) harbor the *str-41* (FP10) and the *nov-1* (FP11) point mutations conferring resistance to streptomycin and novobiocin, respectively. The absence of the polysaccharide capsule on the bacterial surface increases the efficiency of ICEs conjugal transfer [9]. The impairment in natural competence for genetic transformation allows us to rule out the contribution of transformation to the genetic exchange during conjugation (F. Iannelli and G. Pozzi, unpublished). The availability of two strains with different resistance markers allows transconjugants selection and to transfer the genetic elements from transconjugants again. Plating of the mating reactions includes: (i) plates containing both antibiotics for the resistance marker of the donor genetic element and for the chromosomal resistance marker of recipient strain; (ii) plates containing antibiotic for the resistance marker of the genetic element of the donor strain; and (iii) plates containing antibiotic for the chromosomal resistance marker of recipient strain. Appropriate antibiotics are added to this 8 ml

TSA layer at the following concentrations: 5 μg mL-1 chloramphenicol, 1 μg mL^{-1} erythromycin, 1000 μg mL^{-1} kanamycin, 10 μg mL^{-1} novobiocin, 400 μg mL^{-1} spectinomycin, 1000 μg mL^{-1} streptomycin, 5 μg mL^{-1} tetracycline, 25 μg mL^{-1} fusidic acid, 25 μg mL^{-1} rifampicin. The multilayer plating allows: (i) a slow diffusion of the antibiotics in the agar layer containing bacteria, (ii) the visualization of the colony's three-dimensional structure, (iii) a better count of the colonies since the plate is transparent and colonies are generally larger than when spread on a plate, and (iv) the prevention of contact with ambient air favoring the growth of fastidious bacteria.

9. Incubation can be extended to 48 h if required.
10. At this stage, carefully check the phenotype of the colonies in order to exclude isolation of spontaneous mutants or colonies which might grow even in the absence of any genotype conferring resistance. We built a transilluminating box apparatus equipped with an inner white light illuminating an upper plexiglass cover. An overhead transparency plotted with petri dish-size grids overlays the plexiglass. Blood-agar plates can be adjusted over the grids so that each plate is divided into a total of 100 sectors [10]. Plates used for the genetic analysis of transconjugants include: (i) a plate containing both antibiotics for the resistance marker of the donor genetic element and for the chromosomal resistance marker of the recipient strain; (ii) a plate containing the antibiotic for the resistance marker of the donor genetic element; (iii) a plate containing the antibiotic for the chromosomal resistance marker of recipient strain; and (iv) a plate containing no antibiotics. In the absence of a transilluminator device, naked eye observation is possible, constructing a grid using a Petri dish lid.
11. Confirm the phenotypes of transconjugants by PCR genotyping using primers for the amplification of the ICE-chromosome junctions and for ICE internal region such as the resistance genes.

5. Results

In this work, we report an established plate mating protocol for the conjugal transfer of large ICEs up to 81 kb in streptococci (*Streptococcus pneumoniae*, *Streptococcus agalactiae*, *Streptococcus gordonii*, *Streptococcus pyogenes*), *Enterococcus faecalis*, and *Bacillus subtilis* (Tables 1 and 2). With this procedure, the transfer of the following genetic elements in the new *S. pneumoniae* recipients was obtained: (i) *S. pneumoniae* ICE Tn*5253* (size 65 kb) carrying the *cat* and *tet*(M) resistance genes [5,11,12], (ii) *S. pneumoniae* ICE Tn*5251* (size 18 kb) carrying the *tet*(M) [11], (iii) ICE*Sp*23FST81-like of *S. pneumoniae* type 23F genome strain ATCC 700669 (size 81 kb) (conjugation frequency 2.3×10^{-6} transconjugants per donor), and (iv) ICE Tn*5253*-like (size 81 kb) of *S. pneumoniae* type 6 genome strain 670–6B (conjugation frequency 2.7×10^{-7} transconjugants per donor). ICE Tn**5253** was successfully transferred from the representative transconjugant FR58 to *S. pneumoniae* strains with different capsular types, *S. pyogenes*, *S. gordonii*, *S. agalactiae*, and transferred back from representative transconjugants of each bacterial species to *S. pneumoniae* (conjugation frequency varying from 4.4×10^{-7} to 6.7×10^{-3} to transconjugants per donor). ICE Tn*5251* is part of the composite *S. pneumoniae* ICE Tn*5253* and uses its highly efficient conjugation machinery to spread among bacterial strains. This conjugation protocol also allows the detection of rare events such as the autonomous transfer of Tn*5251*, as an independent ICE, from the *S. pneumoniae* host to *E. faecalis* [11]. Finally, we applied this protocol to transfer *S. pyogenes* ϕ1207.3 phage (size 53 kb, carrying the *mef* (A)-*msr* (D) macrolide resistance genes [13]), which moves through a mechanism resembling conjugation [14–16]. Conjugal transfer from the original 2812A clinical strain to the FP10 recipient occurred at a frequency of 3.8×10^{-5} transconjugants per donor and from the resulting transconjugant FR119 to *S. pyogenes* SF370 occurred with a frequency of 4.3×10^{-6} transconjugants per donor.

Table 1. ICEs conjugal transfer frequencies obtained with the plate mating protocol in streptococci and enterococci.

Donor Strain (Properties)	ICE (Size)	Recipient Strain (Properties)	Transfer Frequency [a]	Genetic Analysis of Transconjugants(Primer Pairs) [b]				Ref.
				*att*L–*att*Tn	*att*R–*att*Tn)	*tet*(M)	*cat*	
S. pneumoniae FR22 (FP10 transconjugant derivative, laboratory strain)	Tn*5253* (65-kb)	*S. pneumoniae* FP11 (rough laboratory strain)	$1.6 \times 10^{-4} \pm 1.6 \times 10^{-5}$	IF325-IF327	IF328-IF356	IF394-IF564	IF353-IF354	[11]
		S. pneumoniae FP47 (TIGR4 derivative, type 4 clinical strain)	$3.6 \times 10^{-5} \pm 1.7 \times 10^{-6}$	IF325-IF327	IF328-IF356	IF394-IF564	IF353-IF354	[11]
		S. agalactiae H36B (Ib clinical strain)	$3.8 \times 10^{-6} \pm 5.3 \times 10^{-7}$	IF560-IF327	IF328-IF561	IF394-IF564	IF353-IF354	[11]
		S. gordonii GP204 (V288 derivative, laboratory strain)	$2.5 \times 10^{-5} \pm 5.5 \times 10^{-6}$	IF512-IF327	IF328-IF513	IF394-IF564	IF353-IF354	[11]
		S. pyogenes SF370 (M1 clinical strain)	$8.2 \times 10^{-6} \pm 7.5 \times 10^{-7}$	IF509-IF327	IF328-IF510	IF394-IF564	IF353-IF354	[11]
		E. faecalis OG1RF (clinical strain)	$5.4 \times 10^{-6} \pm 5.5 \times 10^{-7}$	IF532-IF327	IF328-IF525	IF394-IF564	IF353-IF354	[11]
		E. faecalis JH2-2 (clinical strain)	$8.6 \times 10^{-7} \pm 8.8 \times 10^{-8}$	IF532-IF327	IF328-IF525	IF394-IF564	IF353-IF354	[11]
S. pneumoniae 670-6B (type 6 clinical strain)	Tn*5253*-like (81-kb)	*S. pneumoniae* FP11	$2.7 \times 10^{-7} \pm 8.1 \times 10^{-8}$	IF325-IF327	IF328-IF356	IF394-IF564	IF353-IF354	This study
S. pneumoniae ATCC700699 (type 23F clinical strain)	ICE*Sp*23FST81 (81-kb)	*S. pneumoniae* FP11	$2.3 \times 10^{-6} \pm 1.0 \times 10^{-6}$	IF345-IF855	IF327-IF347	IF394-IF564	IF353-IF354	This study
S. pneumoniae FR58 (FP11 transconjugant derivative)	Tn*5253* (65-kb)	*S. pneumoniae* FP58 (D39 derivative, type 2 clinical strain)	$1.9 \times 10^{-5} \pm 4.6 \times 10^{-6}$	IF325-IF327	IF328-IF356	IF394-IF564	IF354-IF353	[12]
		S. pneumoniae HB394 (A66 derivative, type 3 clinical strain)	$4.4 \times 10^{-7} \pm 3.6 \times 10^{-8}$	IF325-IF327	IF328-IF356	IF394-IF564	IF354-IF353	[12]
		S. pneumoniae FR55 (SP18-BS74 derivative, type 6 clinical strain)	$1.3 \times 10^{-5} \pm 2.8 \times 10^{-6}$	IF325-IF327	IF328-IF356	IF394-IF564	IF354-IF353	[12]
S. agalactiae FR67 (H36B transconjugant derivative)	Tn*5253* (65-kb)	*S. pneumoniae* FP11	$1.1 \times 10^{-6} \pm 3.5 \times 10^{-7}$	IF325-IF327	IF328-IF356	IF394-IF564	IF354-IF353	[12]
S. gordonii FR43 (GP204 transconjugant derivative)	Tn*5253* (65-kb)	*S. pneumoniae* FP11	$8.3 \times 10^{-7} \pm 2.9 \times 10^{-7}$	IF325-IF327	IF328-IF356	IF394-IF564	IF354-IF353	[12]
S. pyogenes FR40 (SF370 transconjugant derivative)	Tn*5253* (65-kb)	*S. pneumoniae* FP11	$6.7 \times 10^{-3} \pm 1.0 \times 10^{-3}$	IF325-IF327	IF328-IF356	IF394-IF564	IF354-IF353	[12]
S. pneumoniae FR22	Tn*5151* (18-kb)	*S. pneumoniae* FP47	$1.5 \times 10^{-6} \pm 1.2 \times 10^{-8}$			IF394-IF564		[11]
		E. faecalis OG1RF	$5.4 \times 10^{-6} \pm 5.5 \times 10^{-7}$			IF394-IF564		[11]
		E. faecalis JH2-2	$8.6 \times 10^{-7} \pm 8.8 \times 10^{-8}$			IF394-IF564		[11]
S. gordonii FR70 (GP204 transconjugant derivative)	Tn*5151* (18-kb)	S. pneumoniae FP11	$3.1 \times 10^{-7} \pm 1.9 \times 10^{-7}$			IF394-IF564		[11]
S. pyogenes FR71 (SF370 transconjugant derivative)	Tn*5151* (18-kb)	*S. pneumoniae* FP11	$3.3 \times 10^{-5} \pm 1.3 \times 10^{-5}$			IF394-IF564		[11]
E. faecalis FR64 (OG1RF transconjugant derivative)	Tn*5151* (18-kb)	*S. gordonii* GP204	$4.8 \times 10^{-5} \pm 8.5 \times 10^{-6}$			IF394-IF564		[11]
		S. pyogenes SF370	$9.1 \times 10^{-7} \pm 2.8 \times 10^{-7}$			IF394-IF564		[11]
		E. faecalis OG1SS (clinical strain)	$1.3 \times 10^{-6} \pm 3.9 \times 10^{-7}$			IF394-IF564		[11]
		B. subtilis 168 (laboratory strain)	$1.6 \times 10^{-6} \pm 5.1 \times 10^{-7}$			IF394-IF564		[11]
S. pneumoniae FR73 (FP47 transconjugant derivative)	Tn*5151* (18-kb)	*S. pneumoniae* FP22 (rough D39 derivative)	$2.6 \times 10^{-8} \pm 8.9 \times 10^{-9}$			IF394-IF564		[11]
		S. pneumoniae FP23 (rough TIGR4 derivative)	$1.2 \times 10^{-7} \pm 6.1 \times 10^{-8}$			IF394-IF564		[11]
S. pyogenes 2812A (clinical strain)	Φ1207.3 (53-kb)	*S. pneumoniae* FP10	$3.8 \times 10^{-5} \pm 7.6 \times 10^{-6}$	IF281-IF127	IF162-IF282			This study
S. pneumoniae FR119 (FP10 transconjugant derivative)	Φ1207.3 (53-kb)	*S. pyogenes* SR300 (SF370 derivative strain)	$4.3 \times 10^{-6} \pm 1.1 \times 10^{-6}$	IF302-IF127	IF162-IF303			This study

[a] Conjugation frequency is expressed as CFU of transconjugants per CFU of donor. The results are presented as the mean of at least 3 mating experiments. [b] Transconjugants are selected for acquisition of antibiotic resistance and their genotype characterized by PCR. The presence of the *att*L–*att*Tn junction, *att*R–*att*Tn junction, *tet*(M) and *cat* was investigated in the transconjugants carrying Tn*5253*-family elements. Due to the unspecific integration of Tn*5251* into the bacterial chromosome, the presence of *tet*(M) was investigated in the transconjugants carrying the element. Primers sequences are reported in Table 2.

Table 2. PCR oligonucleotide primers for transconjugants genotyping.

Name	Sequence (5′ to 3′)	Target (Bacterial Species)	Direction
IF327	CAATATAGCGTGATGATTGTAAT	5′ end of Tn*5253*, Tn*5253*-like	Reverse
IF328	AGTGAGAATCAAATCAGAGGTT	3′ end of Tn*5253*, Tn*5253*-like	Forward
IF325	ACAAGAACTGTTTGGACATCAT	Tn*5253*, Tn*5253*-like chromosomal integration site (*S. pneumoniae*)	Forward
IF356	GACTAGATAGAGGCAAGCGT		Reverse
IF560	AACGAAACCTATCAGCGGAA	Tn*5253*, Tn*5253*-like chromosomal integration site (*S. agalactiae*)	Forward
IF561	TTTGGGTTTGTCTCCGACGA		Reverse
IF512	TGCTTTAGGAGATGTTGAGTT	Tn*5253*, Tn*5253*-like chromosomal integration site (*S. gordonii*)	Forward
IF513	ACCGCAGACTGTTCTTTAGA		Reverse
IF509	AAGTAGAAATGGCGAAGTGAA	Tn*5253*, Tn*5253*-like chromosomal integration site (*S. pyogenes*)	Forward
IF510	GACTAGAAAGTGGTAAGCGT		Reverse
IF532	GCCTATGGGATTGCTACACC	Tn*5253*, Tn*5253*-like chromosomal integration site (*E. faecalis*)	Forward
IF525	GGTTACGGGAAGAAAGCGGT		Reverse
IF855	ACCAAATTCCTGCCAGAGTTGA	5′ end of ICE*Sp*23FST81	Reverse
IF327	CAATATAGCGTGATGATTGTAAT	3′ end of ICE*Sp*23FST81	Forward
IF345	ATGGTAATCATCTAAAAATGTCAC	ICE*Sp*23FST81chromosomal	Forward
IF347	CACCAGCACTTGTTAAAGAAG	integration site (*S. pneumoniae*)	Reverse
IF394	GCTATAGTATAAGCCATACTT	Tn*5253*-family *tet* (M) resistance gene	Forward
IF564	GAAGTGACTTGTGCTCTGCT		Reverse
IF354	CATTCTCTGGTATTTGGACTC	Tn*5253*-family *cat* resistance gene	Forward
IF353	CTCTCCGTCGCTATTGTAAC		Reverse
IF127	TGTTCTTCATCTACTACGACTG	5′ end of Φ1207.3	Reverse
IF162	TGATGATTATATAAATTGTGAGTT	3′ end of Φ1207.3	Forward
IF281	AGGTGGTAAGGCAGAATC	Φ1207.3 chromosomal	Forward
IF282	GCACCTTTGTTTGAGTCG	integration site (*S. pneumoniae*)	Reverse
IF302	AATAGATGTAGGTGGGCG	Φ1207.3 chromosomal	Forward
IF303	AGCTTTGGCAACCACTTC	integration site (*S. pyogenes*)	Reverse

6. Concluding Remarks

In conclusion, the present conjugation protocol, based on plate mating, represents an efficient, low cost and easy-to-perform procedure to transfer large ICEs with a size up to 81 kb among streptococci and enterococci. This protocol allows compliance with much higher transfer frequencies and the transfer of elements that could not be moved using a classical filter mating protocol. Specifically, we obtained: (i) the autonomous transfer of ICE Tn*5251* element from *S. pneumoniae* to *E. faecalis* (<1.8×10^{-8} transconjugants per donor with the filter mating protocol [17]), and from here among different gram-positive species; (ii) the transfer of the 81 kb ICE*Sp*23FST81 element from the original clinical *S. pneumoniae* type 23 to pneumococcal conjugation recipients (<3.8×10^{-8} transconjugants per donor with the filter mating protocol); and (iii) *S. pyogenes* ϕ1207.3 phage lysogenic transfer to the *S. pneumoniae* FP10 recipient with a 5.4 fold increase compared to that obtained with the filter mating protocol.

Author Contributions: Conceptualization, F.I. and G.P.; investigation, F.I., F.S. and V.F.; methodology, F.I., F.S., V.F. and G.P.; validation, F.I., F.S. and G.P.; writing—original draft preparation, F.I. and G.P.; writing—review and editing, F.I., F.S., V.F. and G.P.; visualization, F.I., F.S., V.F. and G.P.; supervision, F.I. and G.P.; project administration, F.I. and G.P.; resources, F.I. and G.P.; funding acquisition, G.P. All authors have read and agreed to the published version of the manuscript.

Funding: This research was funded by the Italian Ministry of Education, University and Research (MIUR-Italy) under grant number 20177J5Y3P (call "Progetti di Ricerca di Rilevante Interesse Nazionale—Bando 2017").

Institutional Review Board Statement: Not applicable.

Informed Consent Statement: Not applicable.

Data Availability Statement: Not applicable.

Conflicts of Interest: The authors declare no conflict of interest.

References

1. Burrus, V.; Waldor, M.K. Shaping bacterial genomes with integrative and conjugative elements. *Res. Microbiol.* **2004**, *155*, 376–386. [CrossRef] [PubMed]
2. Frost, L.; Leplae, R.; Summers, A.; Toussaint, A. Mobile genetic elements: The agents of open source evolution. *Nat. Rev. Genet.* **2005**, *3*, 722–732. [CrossRef] [PubMed]
3. Santoro, F.; Iannelli, F.; Pozzi, G. Genomics and Genetics of Streptococcus pneumoniae. *Microbiol. Spectr.* **2019**, *7*. [CrossRef] [PubMed]
4. Johnson, C.M.; Grossman, A.D. Integrative and Conjugative Elements (ICEs): What They Do and How They Work. *Annu. Rev. Genet.* **2015**, *49*, 577–601. [CrossRef] [PubMed]
5. Santoro, F.; Romeo, A.; Pozzi, G.; Iannelli, F. Excision and Circularization of Integrative Conjugative Element Tn5253 of Streptococcus pneumoniae. *Front. Microbiol.* **2018**, *9*, 1779. [CrossRef] [PubMed]
6. Santoro, F.; Vianna, M.E.; Roberts, A.P. Variation on a theme; an overview of the Tn916/Tn1545 family of mobile genetic elements in the oral and nasopharyngeal streptococci. *Front. Microbiol.* **2014**, *5*, 535. [CrossRef]
7. Burrus, V.; Marrero, J.; Waldor, M.K. The current ICE age: Biology and evolution of SXT-related integrating conjugative elements. *Plasmid* **2006**, *55*, 173–183. [CrossRef] [PubMed]
8. Ambroset, C.; Coluzzi, C.; Guédon, G.; Devignes, M.-D.; Loux, V.; Lacroix, T.; Payot, S.; Leblond-Bourget, N. New Insights into the Classification and Integration Specificity of Streptococcus Integrative Conjugative Elements through Extensive Genome Exploration. *Front. Microbiol.* **2016**, *6*, 1483. Available online: http://journal.frontiersin.org/Article/10.3389/fmicb.2015.01483/abstract (accessed on 21 July 2021). [CrossRef] [PubMed]
9. Dahmane, N.; Robert, E.; Deschamps, J.; Meylheuc, T.; Delorme, C.; Briandet, R.; Leblond-Bourget, N.; Guédon, E.; Payot, S. Impact of Cell Surface Molecules on Conjugative Transfer of the Integrative and Conjugative Element ICE St3 of Streptococcus thermophilus. *Appl. Environ. Microbiol.* **2018**, *84*. [CrossRef] [PubMed]
10. Iannelli, F.; Pozzi, G. Method for Introducing Specific and Unmarked Mutations into the Chromosome of Streptococcus pneumoniae. *Mol. Biotechnol.* **2004**, *26*, 81–86. [CrossRef]
11. Santoro, F.; Oggioni, M.R.; Pozzi, G.; Iannelli, F. Nucleotide sequence and functional analysis of the tet (M)-carrying conjugative transposon Tn5251 of Streptococcus pneumoniae: Tn5251 of *Streptococcus pneumoniae*. *FEMS Microbiol. Lett.* **2010**, *308*, 150–158. [CrossRef] [PubMed]

12. Iannelli, F.; Santoro, F.; Oggioni, M.R.; Pozzi, G. Nucleotide sequence analysis of integrative conjugative element Tn5253 of Strep-tococcus pneumoniae. *Antimicrob. Agents Chemother.* **2014**, *58*, 1235–1239. [CrossRef] [PubMed]
13. Iannelli, F.; Santoro, F.; Santagati, M.; Docquier, J.-D.; Lazzeri, E.; Pastore, G.; Cassone, M.; Oggioni, M.R.; Rossolini, G.M.; Stefani, S.; et al. Type M Resistance to Macrolides Is Due to a Two-Gene Efflux Transport System of the ATP-Binding Cassette (ABC) Superfamily. *Front. Microbiol.* **2018**, *9*, 1670. [CrossRef] [PubMed]
14. Iannelli, F.; Santagati, M.; Santoro, F.; Oggioni, M.R.; Stefani, S.; Pozzi, G. Nucleotide sequence of conjugative prophage Φ1207.3 (formerly Tn1207.3) carrying the mef(A)/msr(D) genes for efflux resistance to macrolides in Streptococcus pyogenes. *Front. Microbiol.* **2014**, *5*, 687. [CrossRef] [PubMed]
15. Pozzi, G.; Iannelli, F.; Oggioni, M.R.; Santagati, M.; Stefani, S. Genetic Elements Carrying Macrolide Efflux Genes in Streptococci. *Curr. Drug Target Infect. Disord.* **2004**, *4*, 203–206. [CrossRef] [PubMed]
16. Santagati, M.; Iannelli, F.; Cascone, C.; Campanile, F.; Oggioni, M.R.; Stefani, S.; Pozzi, G. The Novel Conjugative Transposon Tn1207.3 Carries the Macrolide Efflux Gene mef(A) in *Streptococcus pyogenes*. *Microb. Drug Resist.* **2003**, *9*, 243–247. [CrossRef] [PubMed]
17. Provvedi, R.; Manganelli, R.; Pozzi, G. Characterization of conjugative transposon Tn5251 of Streptococcus pneumoniae. *FEMS Microbiol. Lett.* **1996**, *135*, 231–236. [CrossRef] [PubMed]

CHAPTER 7

Complete Genome Sequence of the *Streptococcus pneumoniae* strain Rx1, a Hex Mismatch Repair-deficient standard transformation recipient

Anna Maria Cuppone, Lorenzo Colombini, Valeria Fox, David Pinzauti, Francesco Santoro, Gianni Pozzi and Francesco Iannelli

Laboratory of Molecular Microbiology and Biotechnology,

Department of Medical Biotechnologies,

University of Siena, 53100 Siena, Italy

Accepted for publication on Microbiology Resource Announcements

Abstract

The complete genome sequence of the *Streptococcus pneumoniae* strain Rx1, a Hex Mismatch Repair-deficient standard transformation recipient, is obtained combining Nanopore and Illumina sequencing technologies. The genome consists of 2.03-Mb circular chromosome, with 2,054 open reading frames, and a GC content of 39.72%.

Announcement

Streptococcus pneumoniae is a human pathogen and the most important model organism for studying bacterial genetics and genomics. Widely used laboratory strains include type 2 Avery's strain D39 and its derivatives Rx1 and R6, standard transformation recipients[1,2]. We characterized the complete genome sequence of Rx1, a highly transformable and Hex Mismatch Repair System-deficient strain. To track genomic changes that gave rise to Rx1 we also sequenced the genome of its unencapsulated parental strain R36A (Table 1). Strains, obtained from the Guild's laboratory collection[3], were grown in Tryptic Soy Broth at 37°C for 4h until an OD_{590}=0.8. Pneumococcal cells were harvested by centrifugation (5,000 x*g* for 30 minutes at 4°C), the cell pellet was dry vortexed and lysed in 0.1% DOC, 0.008% SDS. High-molecular-weight DNA was purified three times with 1 volume of Chloroform:Isoamyl-alcohol (24:1,v:v), precipitated in 0.6 volumes of ice-cold isopropanol and spooled on a glass rod. DNA was resuspended in saline-sodium citrate (SSC)/10 buffer, then adjusted to SSC 1X and maintained at 4°C. DNA solution was homogenized using a rotator mixer. Oxford Nanopore MinION and Illumina HiSeq 2500 instruments were used for DNA sequencing. DNA was not sheared; size selection was obtained with 0.8 volumes of AMPure XP beads (Beckman Coulter). Nanopore sequencing library was prepared using the SQK-LSK108 kit following Manufacturer's instructions (Oxford Nanopore Technologies) and the sample was sequenced using an R9.4 flow cell (FLO-MIN106). Post-sequencing high-accuracy basecalling and adapter trimming of raw Nanopore reads was performed using Guppy v4.0.11 (https://community.nanoporetech.com/downloads) with configuration "dna_r9.4.1_450bps_hac"

and basecalled reads were analysed with NanoPlot v1.18.2[4]. Illumina sequencing was performed at MicrobesNG (University of Birmingham) using Nextera XT library preparation kit (Illumina Inc.) followed by paired-end sequencing. Illumina reads were trimmed using Trimmomatic v0.30[5] and analysed with FastQC v0.11.5 (http://www.bioinformatics.babraham.ac.uk/projects/fastqc). Nanopore and Illumina sequencing generated 3,892 long reads (26,780,859 bp, N50=18.3 kbp) and 86,582 read pairs (2x250 bp), respectively, for Rx1, whereas for R36A 4,771 long reads (27,433,219 bp, N50=16.9 kbp) and 278,462 read pairs were obtained. Sequence coverage was 31.6x for Rx1 and 67.0x for R36A. A hybrid assembly of Nanopore and Illumina reads was obtained using Unicycler v0.4.712[6]. Assembly completeness and quality were assessed using Bandage v.0.8.1[7] and Ideel (https://github.com/mw55309/ideel), respectively. Annotation was performed with the NCBI Prokaryotic Genome Annotation Pipeline (PGAP) v5.1[8]. Default parameters were used for all tools unless otherwise specified. Rx1 genome consists of a 2,030,186-bp single circular chromosome containing 2,054 open reading frames (ORFs), of which 1,813 have a predicted function. The 2,039,955-bp circular chromosome of R36A contains 2,059 ORFs, of which 1,834 with a putative function. Both genomes have: i) a GC content of 39.72%, ii) 58 tRNA genes, 3 rRNA operons, and 3 structural RNAs, iii) a 36.6-kb PPI1 pathogenicity island[9], iv) prophages remnants, v) remnants of the integrative and conjugative element Tn*5253*[10-12]. Rx1 and R36A capsule loci are schematized in Fig.1. Rx1 harbors type I restriction-modification system SpnD39III variant C, while R36A variant D[13]. In Rx1 g.168,614C>A, g.1,979,527G>A, and g. 1,629,603delA nucleotide changes introduce a premature termination codon in *hexB*, *pspc3.1*, and *dpnC*, respectively.

Data availability

The complete genome sequences of R36A and Rx1 are assigned GenBank accession no. CP079922 and CP079923, respectively. The sequencing project is assigned NCBI BioProject accession no. PRJNA748391. Nanopore and Illumina sequencing reads are accessible under Sequence Read

Archive accession no. SRR15216323 and SRR15216322 for R36A, SRR15216380 and SRR15216379 for Rx1.

Acknowledgments

This was supported by the Italian Ministry of Education, University and Research (MIUR-Italy) under grant number 20177J5Y3P (call "Progetti di Ricerca di Rilevante Interesse Nazionale – Bando 2017"). Illumina genome sequencing was provided by MicrobesNG (http://www.microbesng.uk).

Table 1. Genealogy of *S. pneumoniae* Rx1 strain

Strain	Description[a]	Relevant properties[b]	Genome GenBank acc. no.[a]
D39	Avery's strain, clinical isolate [1916], type 2, virulent[3,14-18]	pDP1$^+$, Hex$^+$, *Dpn*I$^+$, *comC1-comD1*, *pspC3.1*	CP000410.1 [2007][28]
R36	D39 passaged 36x in anti-type 2 serum [1944], rough, avirulent[3,16,17]	pDP1$^+$, Hex$^+$, *Dpn*I$^+$, *comC1-comD1*, *pspC3.1*	not available
R36A	Highly transformable R36 colony morphology variant [1944], rough, avirulent[3,15,18,29]	pDP1$^-$, Hex$^+$, *Dpn*I$^+$, *comC1-comD1*, *pspC3.1*	CP079922 [2021] this study
R6	Highly transformable R36A single colony isolate [1962], rough, avirulent[3,30,31]	pDP1$^-$, **Hex$^+$**, *Dpn*I$^+$, *comC1-comD1*, *pspC3.1*	AE007317.1 [2001][32]
A66	Avery's strain, clinical isolate [1949], type 3, virulent[18,29]	Hex$^+$, *Dpn*I, *comC2-comD2*, *pspC11.4*	LN847353.1 [2015][33]
SIII-N	R36A transformed with A66 DNA [1949], type 3, virulent[15,18,29,34]	*comC1-comD1*, *pspC3.1*	not available
Rx	Spontaneous rough derivative of R36A [1959], reduced type 3 capsule production, avirulent[3,18,35,36]	pDP1$^-$, Hex$^-$ (HexB$^-$), *comC1-comD1*, *pspC3.1*	not available
Rx1	Highly transformable derivative of Rx [1959], reduced type 3 capsule production (Ugd mutant), avirulent [3,37]	pDP1$^-$, **Hex$^-$** (HexB$^-$), *Dpn*I$^-$ (DpnC$^-$), *comC1-comD1*, *pspC3.1*$'$	CP079923 [2021] this study

[a] The year of the first strain description (except for D39 isolation year) or of the sequence release is reported in square brackets.

[b] pDP1 is a 3,161-bp cryptic plasmid[19]. Hex is the DNA Mismatch Repair System encoded by *hexA* and *hexB*[20]. *Dpn*I is a restriction system composed by the *Dpn*I/DpnC endonuclease and DpnD[21]. *comC-comD* competence genes encode the CSP and its ComD receptor[22-25]. *pspC* encodes the virulence surface protein PspC[26,27].

FIGURE LEGEND

Figure 1. *S. pneumoniae* capsule locus. Rx1 harbors a type 3 capsule locus acquired by A66 DNA through a double crossover between IS*630*-*Spn*I and *aliA*. At the 3' end, recombination produced the insertion of a IS*L3* transposase and a 950-bp deletion of the *aliA* 5' end, as in the A66 capsule locus. IS*1548* identifies: i) a 5' fragment, common to all serotypes[38], that contains *wzg* and *wzh* pseudogenes, *wzd* and *wze* genes and is not involved in type 3 capsular synthesis[39], ii) a 3' fragment containing *ugd*/*cap3D*/*cap3A* UDP-glucose dehydrogenase gene, *wchE*/*cps3S*/*cap3B* synthase gene, *galU*/*cps3U*/*cap3C* and *pgm*/*cps3M*/*cap3D* genes involved in the UDP-glucose biosynthesis[32,35,39]. Nucleotide change g.317,495C>T in *ugd*/*cps3A*/*cps3D* (indicated by an asterisk) causes p.R320C in the UDP-glucose dehydrogenase UDP binding domain. The type 2 capsule locus of R36A harbors a 7,505-bp deletion involving the 3' end of *wzg*/*cps2A*, 7 genes (namely, *wzh*/*cps2B*, *wzd*/*cps2C*, *wze*/*cps2D*, *wchA*/*cps2E*, *wchF*/*cps2T*, *wchG*/*cps2F*, *wchH*/*cps2G*), and the 5' end of *wzy*/*cps2H* [40]. Deletion event left an inverted 25-bp fragment (reported as an open box) belonging to the lost *wzg*/*cps2A* 3' end.

References

1. Pearce BJ, Iannelli F, Pozzi G. 2002. Construction of new unencapsulated (rough) strains of *Streptococcus pneumoniae*. *Research in Microbiology*. 153(4):243-247. doi:10.1016/S0923-2508(02)01312-8
2. Santoro F, Iannelli F, Pozzi G. 2019. Genomics and genetics of *Streptococcus pneumoniae*. Fischetti VA, Novick RP, Ferretti JJ, Portnoy DA, Braunstein M, Rood JI, eds. *Microbiol Spectr*. 7(3). doi:10.1128/microbiolspec.GPP3-0025-2018
3. Smith MD, Guild WR. 1979. A plasmid in *Streptococcus pneumoniae*. *J Bacteriol*. 137(2):735-739. doi:10.1128/jb.137.2.735-739.1979
4. De Coster W, D'Hert S, Schultz DT, Cruts M, Van Broeckhoven C. 2018. NanoPack: visualizing and processing long-read sequencing data. *Bioinformatics*. 34(15):2666-2669. doi:10.1093/bioinformatics/bty149
5. Bolger AM, Lohse M, Usadel B. 2014. Trimmomatic: a flexible trimmer for Illumina sequence data. *Bioinformatics*. 30(15):2114-2120. doi:10.1093/bioinformatics/btu170
6. Wick RR, Judd LM, Gorrie CL, Holt KE. 2017. Unicycler: Resolving bacterial genome assemblies from short and long sequencing reads. Phillippy AM, ed. *PLoS Comput Biol*. 13(6):e1005595. doi:10.1371/journal.pcbi.1005595
7. Wick RR, Schultz MB, Zobel J, Holt KE. 2015. Bandage: interactive visualization of *de novo* genome assemblies. *Bioinformatics*. 31(20):3350–3352. doi: 10.1093/bioinformatics/btv383.
8. Tatusova T, DiCuccio M, Badretdin A, et al. 2016. NCBI prokaryotic genome annotation pipeline. *Nucleic Acids Res*. 44(14):6614-6624. doi:10.1093/nar/gkw569
9. Brown JS, Gilliland SM, Spratt BG, Holden DW. 2004. A locus contained within a variable region of pneumococcal pathogenicity island 1 contributes to virulence in mice. *Infect Immun*. 72(3):1587-1593. doi:10.1128/IAI.72.3.1587-1593.2004
10. Santoro F, Oggioni MR, Pozzi G, Iannelli F. 2010. Nucleotide sequence and functional analysis of the tet (M)-carrying conjugative transposon Tn*5251* of *Streptococcus pneumoniae*: Tn*5251* of *Streptococcus pneumonia*e. *FEMS Microbiology Letters*. Published online April 28, 2010:no-no. doi:10.1111/j.1574-6968.2010.02002.x
11. Iannelli F, Santoro F, Oggioni MR, Pozzi G. 2014. Nucleotide sequence analysis of integrative conjugative element Tn*5253* of *Streptococcus pneumoniae*. *Antimicrobial Agents and Chemotherapy*. 58(2):5.
12. Santoro F, Romeo A, Pozzi G, Iannelli F. 2018. Excision and circularization of integrative conjugative element Tn*5253* of *Streptococcus pneumoniae*. *Front Microbiol*. 9:1779. doi:10.3389/fmicb.2018.01779

13. Manso AS, Chai MH, Atack JM, et al. 2014. A random six-phase switch regulates pneumococcal virulence via global epigenetic changes. *Nat Commun*. 5(1):5055. doi:10.1038/ncomms6055
14. Griffith F. 1928. The significance of pneumococcal types. *J Hyg (Lond)*. 27(2):113-159. doi:10.1017/s0022172400031879
15. Avery OT, Macleod CM, McCarty M. 1944. Studies on the chemical nature of the substance inducing transformation of pneumococcal types : induction of transformation by a desoxyribonucleic acid fraction isolated from pneumococcus type III. *J Exp Med*. 79(2):137-158. doi:10.1084/jem.79.2.137
16. Macleod CM, Krauss MR. 1947. Stepwise intratype transformation of pneumococcus from R to S by way of a variant intermediate in capsular polysaccharide production. *J Exp Med*. 86(6):439-452. doi:10.1084/jem.86.6.439
17. Austrian R. 1953. Morphologic variation in pneumococcus. I. An analysis of the bases for morphologic variation in pneumococcus and description of a hitherto undefined morphologic variant. *J Exp Med*. 98(1):21-34. doi:10.1084/jem.98.1.21
18. Ravin AW. 1959. Reciprocal capsular transformations of pneumococci. 77:14.
19. Oggioni MR, Iannelli F, Pozzi G. 1999. Characterization of cryptic plasmids pDP1 and pSMB1 of *Streptococcus pneumoniae*. *Plasmid*. 41(1):70-72. doi:10.1006/plas.1998.1364
20. Claverys JP, Lacks SA. 1986. Heteroduplex deoxyribonucleic acid base mismatch repair in bacteria. *Microbiol Rev*. 50:33.
21. Lacks SA, Springhorn SS, Laboratory N. 1986. Genetic basis of the complemental DpnI and DpnII restriction systems of *S. pneumoniae*: an intercellular cassette mechanism. Published online 1986:8.
22. Havarstein LS, Coomaraswamy G, Morrison DA. 1995. An unmodified heptadecapeptide pheromone induces competence for genetic transformation in *Streptococcus pneumoniae*. *Proceedings of the National Academy of Sciences*. 92(24):11140-11144. doi:10.1073/pnas.92.24.11140
23. Pozzi G, Masala L, Iannelli F, et al. 1996. Competence for genetic transformation in encapsulated strains of *Streptococcus pneumoniae*: two allelic variants of the peptide pheromone. *Journal of bacteriology*. 178(20):6087-6090. doi:10.1128/JB.178.20.6087-6090.1996
24. Pestova EV, Håvarstein LS, Morrison DA. 1996. Regulation of competence for genetic transformation in *Streptococcus pneumoniae* by an auto-induced peptide pheromone and a two-component regulatory system. *Molecular Microbiology*. 21(4):853-862. doi:10.1046/j.1365-

2958.1996.501417.x

25. Iannelli F, Oggioni MR, Pozzi G. 2005. Sensor domain of histidine kinase ComD confers competence pherotype specificity in *Streptoccoccus pneumoniae*. *FEMS Microbiology Letters*. 252(2):321-326. doi:10.1016/j.femsle.2005.09.008
26. Iannelli F, Oggioni MR, Pozzi G. 2002. Allelic variation in the highly polymorphic locus *pspC* of *Streptococcus pneumoniae*. *Gene*. 284(1-2):63-71. doi:10.1016/S0378-1119(01)00896-4
27. Iannelli F, Chiavolini D, Ricci S, Oggioni MR, Pozzi G. 2004. Pneumococcal surface protein C contributes to sepsis caused by *Streptococcus pneumoniae* in mice. *Infect Immun*. 72(5):3077-3080. doi:10.1128/IAI.72.5.3077-3080.2004
28. Lanie JA, Ng W-L, Kazmierczak KM, et al. 2007. Genome sequence of Avery's virulent serotype 2 strain D39 of *Streptococcus pneumoniae* and comparison with that of unencapsulated laboratory strain R6. *J Bacteriol*. 189(1):38-51. doi:10.1128/JB.01148-06
29. Taylor HE. 1949. Additive effects of certain transforming agents from some variants of pneumococcus. *J Exp Med*. 89(4):399-424. doi:10.1084/jem.89.4.399
30. Ottolenghi E, Hotchkiss RD. 1962. Release of genetic transforming agent from pneumococcal cultures during growth and disintegration. *Journal of Experimental Medicine*. 116(4):491-519. doi:10.1084/jem.116.4.491
31. Tomasz A, Hotchkiss RD. 1964. Regulation of the transformability of pneumococcal cultures by macromolecular cell products. *Proc Natl Acad Sci U S A*. 51(3):480-487. doi:10.1073/pnas.51.3.480
32. Hoskins J, Alborn WE, Arnold J, et al. 2001. Genome of the bacterium *Streptococcus pneumoniae* strain R6. *J Bacteriol*. 183(19):5709-5717. doi:10.1128/JB.183.19.5709-5717.2001
33. Hahn C, Harrison EM, Parkhill J, Holmes MA, Paterson GK. 2015. Draft genome sequence of the *Streptococcus pneumoniae* Avery strain A66. *Genome Announc*. 3(3). doi:10.1128/genomeA.00697-15
34. Austrian R, Bernheimer HP, Smith EE, Mills GT. 1959. Simultaneous production of two capsular polysaccharides by pneumococcus. II. The genetic and biochemical bases of binary capsulation. *J Exp Med*. 110(4):585-602. doi:10.1084/jem.110.4.585
35. Prudhomme M, Martin B, Mejean V, Claverys JP. 1989. Nucleotide sequence of the *Streptococcus pneumoniae hexB* mismatch repair gene: homology of HexB to MutL of *Salmonella typhimurium* and to PMS1 of *Saccharomyces cerevisiae*. *J Bacteriol*. 171(10):5332-5338. doi:10.1128/jb.171.10.5332-5338.1989
36. Dillard JP, Vandersea MW, Yother J. 1995. Characterization of the cassette containing genes for type 3 capsular polysaccharide biosynthesis in *Streptococcus pneumoniae*. *Journal of*

Experimental Medicine. 181(3):973-983. doi:10.1084/jem.181.3.973

37. Guild WR, Shoemaker NB. 1974. Intracellular competition for a mismatch recognition system and marker-specific rescue of transforming DNA from inactivation by ultraviolet irradiation. *Molec Gen Genet*. 128(4):291-300. doi:10.1007/BF00268517
38. Bentley SD, Aanensen DM, Mavroidi A, et al. 2006. Genetic analysis of the capsular biosynthetic locus from all 90 pneumococcal serotypes. Frasier CM, ed. *PLoS Genet*. 2(3):e31. doi:10.1371/journal.pgen.0020031
39. Arrecubieta C, Garcia E, López R. 1995. Sequence and transcriptional analysis of a DNA region involved in the production of capsular polysaccharide in *Streptococcus pneumoniae* type 3. *Gene*. 167(1-2):1-7. doi:10.1016/0378-1119(95)00657-5
40. Iannelli F, Pearce BJ, Pozzi G. 1999. The type 2 capsule locus of *Streptococcus pneumoniae*. *J Bacteriol*. 181(8):2652-2654. doi:10.1128/JB.181.8.2652-2654.1999

Figure 1

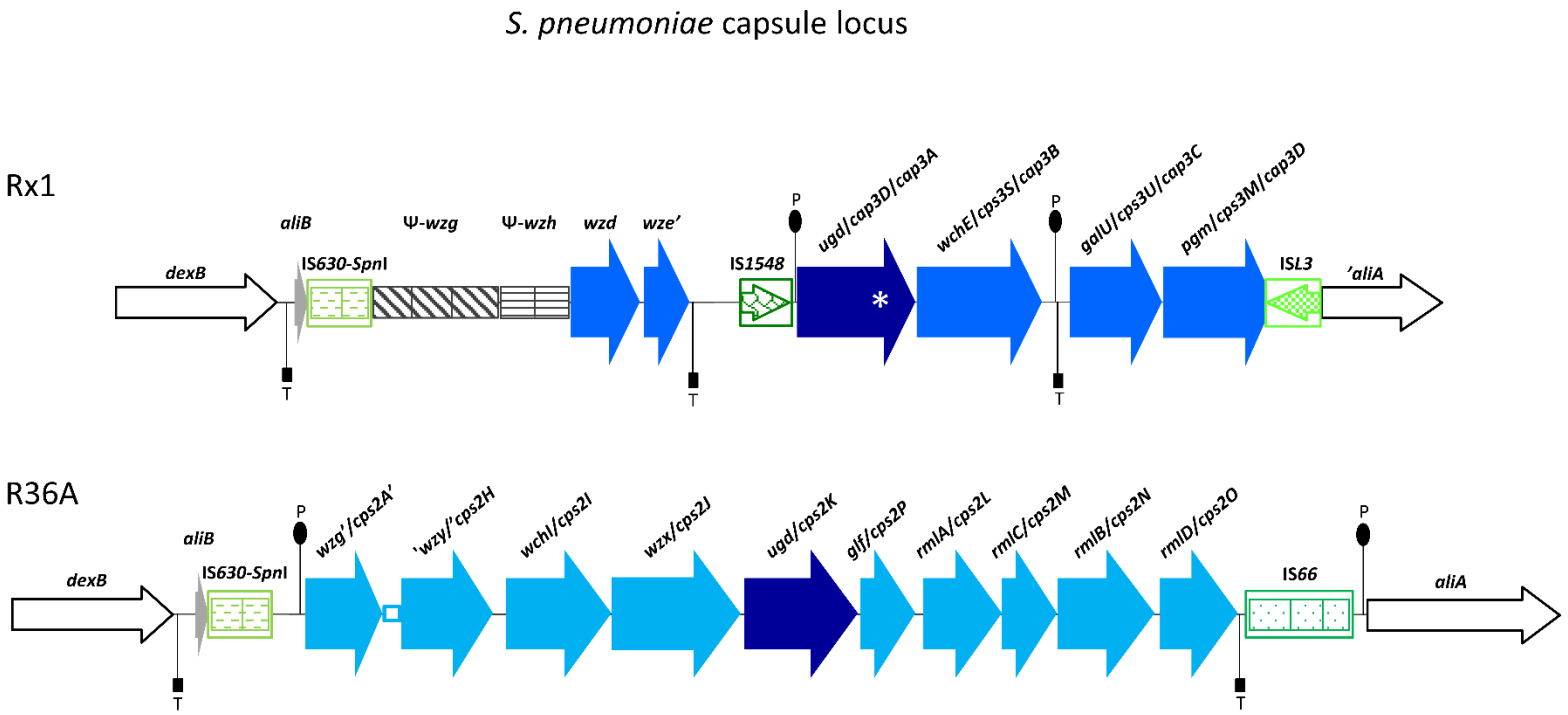
S. pneumoniae capsule locus
Rx1
dexB
aliB
IS630-SpnI
Ψ-wzg
Ψ-wzh
wzd
wze'
IS1548
P
ugd/cap3D/cap3A
wchE/cps3S/cap3B
galU/cps3U/cap3C
pgm/cps3M/cap3D
ISL3
'aliA
T
R36A
dexB
aliB
IS630-SpnI
wzg'/cps2A'
'wzy/''cps2H
wchI/cps2I
wzx/cps2J
ugd/cps2K
glf/cps2P
rmlA/cps2L
rmlC/cps2M
rmlB/cps2N
rmlD/cps2O
IS66
aliA

CHAPTER 8

Predicted transmembrane proteins with homology to Mef(A) are not responsible for complementing *mef*(A) deletion in the *mef*(A)-*msr*(D) macrolide efflux system in *Streptococcus pneumoniae*

Valeria Fox, Francesco Santoro, Gianni Pozzi and Francesco Iannelli

Laboratory of Molecular Microbiology and Biotechnology,

Department of Medical Biotechnologies,

University of Siena, 53100 Siena, Italy

Submitted to BMC Research Notes

Abstract

Objectives: In streptococci, the type M resistance to macrolides is due to the *mef*(A)-*msr*(D) efflux transport system of the ATP-Binding cassette (ABC) superfamily, where it is proposed that *mef*(A) codes for the transmembrane channel and *msr*(D) for the two ATP-binding domains. Phage ϕ1207.3 of *Streptococcus pyogenes*, carrying the *mef*(A)-*msr*(D) gene pair, is able to transfer the macrolide efflux phenotype to *Streptococcus pneumoniae*. Deletion of *mef*(A) in pneumococcal ϕ1207.3-carrying strains did not affect erythromycin efflux. In order to identify candidate genes likely involved in complementation of *mef(*A) deletion, the Mef(A) amino acid sequence was used as probe for database searching.

Results: *In silico* analysis identified 3 putative candidates in the *S. pneumoniae* R6 genome, namely *spr0971*, *spr1023* and *spr1932*. Isogenic deletion mutants of each candidate gene were constructed and used in erythromycin sensitivity assays to investigate their contribution to *mef*(A) complementation. Since no change in erythromycin sensitivity was observed compared to the parental strain, we produced double and triple mutants to assess the potential synergic activity of the selected genes. Also these mutants did not complement the *mef*(A) function.

Keywords: *mef*(A), *msr*(D), macrolide efflux, *Streptococcus pyogenes*, *Streptococcus pneumoniae*, ABC-transporter, ϕ1207.3, prophage

Introduction

Macrolide resistance in streptococci is usually associated with two major mechanisms: (i) target-site modification, mediated by the erythromycin ribosomal methylase (*erm*) family genes responsible for 23S rRNA methylation; (ii) active drug efflux, mediated by the *mef* family genes which confer the M phenotype, characterized by low level resistance to 14- and 15-membered macrolides [1–6]. The two *mef* major allelic variants, *mef*(A) and *mef*(E), were originally described in *Streptococcus pyogenes* and in *Streptococcus pneumoniae*, respectively [7,8]. These variants are highly homologous and are also found in other streptococcal species, gram-positive and gram-negative genera [3,5,9–12] (for an updated list see the Dr. Marylin Roberts's website https://faculty.washington.edu/marilynr). The *mef* alleles are associated to different chromosomal genetic elements. In *S. pneumoniae*, we found Tn*1207.1*, a 7,244-bp non-conjugative element carrying *mef*(A), whereas the 5,532-bp pneumococcal genetic element (mega) was found to carry *mef*(E) [13–17]. In *S. pyogenes*, we described the 52,491-bp prophage Φ1207.3 carrying *mef*(A) whose left 7,244-bp sequence is identical to Tn*1207.1* [18–20]. In clinical isolates of *S. pyogenes* other *mef*(A)-carrying prophages were found, including Φ10394.4, Φm46.1 and its variant VP_00501.1 [21–23]. In the *mef*-carrying genetic elements, the *msr*(D) gene was always associated to and co-transcribed with the *mef* gene and contributes to macrolide efflux resistance [23–28]. In our previous work, genome database search showed that in 33 out of 37 genomes, *mef*(A) was associated in tandem to *msr*(D), while bioinformatic analysis showed that the Mef(A) protein was predicted to form six transmembrane helices and the Msr(D) protein to have two Nucleotide Binding Domains (NBDs) typical of ATP-binding transporters [27]. We hypothesized that *mef(*A) and *msr*(D) constitute a two-gene ATP-Binding Cassette efflux transport system, where *mef*(A) encodes the transmembrane channel, and *msr(*D) the two ATP-binding domains. A functional analysis of the relative contribution of *mef*(A) and *msr*(D) to macrolide resistance supported this hypothesis, showing that deletion of *msr*(D) abolishes erythromycin resistance, whereas deletion of *mef*(A) causes only a two-fold reduction of MIC value [27]. It is likely that in absence of Mef(A),

Msr(D) utilizes an alternative transmembrane channel for macrolide efflux. In the present work, a pneumococcal genome homology search was used to investigate the presence of transmembrane proteins homologous to Mef(A), which could complement the Mef(A) function. Three genes encoding transmembrane proteins were identified and their role as alternative Msr(D) cognate transmembrane channel was investigated through site specific mutagenesis and functional studies.

Main text

Methods

Bacterial strains, growth and mating condition

All pneumococcal strains used in this work and their relevant properties are reported in Table 1. Bacterial strains were grow grown in Tryptic Soy Broth (TSB) or Tryptic Soy Agar supplemented with 3% defibrinated horse blood [29]. Transfer of Φ1207.3 or Φ1207.3Δ*mef*(A) from strains FR183 and FP40 to the deletion mutants was obtained through a mating protocol as already reported [30]. Briefly, donor and recipient cells were grown separately in TSB in the presence of the appropriate antibiotics. Upon reaching the end of exponential phase, cells were mixed at a donor-recipient 1:10 ratio, centrifuged, and pellet was plated on TSA plates supplemented with 5% blood. Plates were incubated at 37°C in the presence of 5% CO_2 for 4 hours and cells were recovered with a cotton swab and resuspended in TSB. To select for recombinants, cell suspension was plated following a multilayer plating procedure [30]**.**

Bioinformatic analysis

Homology searches of the pneumococcal genome R6 available at the National Center for Biotechnology Information (https://www.ncbi.nlm.nih.gov/genome/microbes/) was performed using Microbial BLAST with the Megablast algorithm (https://blast.ncbi.nlm.nih.gov/Blast.cgi?PROGRAM=blastp&PAGE_TYPE=BlastSearch&BLAST_SPEC=MicrobialGenomes&LINK_LOC=blasttab&LAST_PAGE=blastp). Default parameters were used and only alignments with significant e-values were considered. Protein sequence analysis was carried out with the softwares TMpred and Phyre2 [31–34]

Gene SOEing PCR mutagenesis

Isogenic deletion mutants were obtained transforming *S. pneumoniae* Rx1 derivative recipients with mutagenic constructs assembled by Gene Splicing by Overlap Extension [29]. The oligonucleotide primers used for mutagenesis, sequencing and PCR selection of the recombinants strain are reported in Table S1. Deletion of *spr0971* coding sequence (CDS) was obtained with a mutagenic construct containing the *ami/aad9* spectinomycin resistance cassette (894 bp) [35] flanked by the upstream (601 bp) and downstream (459 bp) *spr*0971 flanking fragments, respectively. The *spr1023* CDS was deleted with a mutagenic construct containing the *ami/aphIII* kanamycin resistance cassette (1033 bp) [36] joined to the left (696 bp) and right (658 bp) *spr1023* flanking fragments. The *spr1932* mutagenic construct contained the kanamycin resistance cassette flanked by the upstream (724 bp) and downstream (694 bp) *spr1932* flanking fragments. The mutagenic construct for *spr1023* in-frame deletion was obtained assembling the DNA fragments located upstream (749 bp) and downstream (773 bp) of *spr1023* CDS. Linear PCR constructs were used directly as donor DNA in transformation experiments. Recombinant strains were selected for acquisition of spectinomycin or kanamycin resistance, while deletion of *spr1023* was selected by selective PCR analysis [29]. The correct integration of constructs was confirmed by PCR and sequencing.

Minimal inhibitory concentration (MIC) determination

The minimal inhibitory concentration (MIC) was assessed by microdilution method, according to the Clinical and Laboratory Standards Institute guideline (CLSI, 2020) as already reported [27]. Briefly, bacteria were grown in TSB until reaching the exponential phase (OD_{590}=0.3, corresponding to approximately 10^8 CFU/ml), then culture aliquots were taken and frozen at -70 °C in 10% glycerol. Frozen cultures were then thawed, diluted 1:100 in TSB (10^6 CFU/ml) and 100 µl were added to a 96-wells microplate containing 100 µl of serial twofold dilutions of erythromycin, reaching a final concentration of 5 x 10^5 CFU/ml in each well. Plates were incubated at 37°C and visually analyzed after 18 hours. Bacterial growth was assessed using the microplate ELISA reader VERSAmax (Molecular Devices). The *S. pneumoniae* ATCC49619 strain was used as a quality

control. MIC assays were performed in quintuplicate with at least two technical replicates per experiment.

Results

Identification and sequence analysis of a candidate genes encoding a Mef(A) homologous protein

The 405-aa Mef(A) sequence (GenBank accession no. AAT72347) was used as a query to conduct a BLAST homology search of *S. pneumoniae* R6 genome. Homology analysis revealed the presence of three genes coding for proteins with a significant homology (e-value < 0.001) to Mef(A): (i) *spr0971* (GenBank accession number NP_358565.1); (ii) *spr1023* (GenBank accession number NP_358617.1); (iii) *spr*1932 (GenBank accession number NP_359523.1). The *spr0971* gene, annotated as "ABC transporter membrane-spanning permease - macrolide efflux", codes for a 403 aa protein displaying 23% identity to Mef(A). The *spr1023* gene, annotated as "macrolide ABC transporter permease", codes for a 392 aa protein with 24% identity to Mef(A). The *spr1932* gene, annotated as "hypothetical protein", codes for a 415 aa protein with 21% identity to Mef(A). Analysis of the transmembrane domains of all predicted proteins predicted the presence of up to 12 transmembrane helices.

Investigation of the role of the candidate genes on Mef(A) complementation

To define if the selected candidate genes could complement the *mef*(A) function, we constructed three isogenic deletion mutants in *S. pneumoniae* DP1004 background (Table 1). The 1209 bp *spr0971* CDS was deleted and replaced by the 894-bp *ami/aad9* cassette, whereas the 1176 bp *spr1023* and the 1245 bp *spr1932* CDSs were deleted by allelic replacement with the 1033-bp *ami/aphIII* cassette. These mutants were used as recipients to obtain derivative strains harboring the recombinant Φ1207.3Δ*mef*(A). Sensitivity to erythromycin of the isogenic mutants was assessed by determining the minimal inhibitory concentration (MIC). In our previous study, we reported that Φ1207.3Δ*mef*(A)-carrying strain FP40 has an erythromycin MIC of 4 µg/ml, consistent with the presence of an alternative transmembrane channel able to complement the *mef*(A) function (Iannelli

et al 2018). Deletion of *spr0971, spr1023* and *spr1932*, did not affect erythromycin sensitivity (Figure 1 and Table 2). Then, to investigate if the Mef(A) complementation is due to a synergic action of these genes, we constructed double deletion mutants. The *spr0971-spr1023* and *spr0971-spr1932* double deletion mutants were obtained transforming strain FR323 (*spr0971*ΔSpe) with the *spr1023* and *spr1932* kanamycin mutagenic constructs, respectively, while the *spr1023-spr1932* double mutant was obtained by transforming the strain FR325 (*spr1932*ΔKm) with a mutagenic construct designed to produce *spr1023* in frame deletion. Deletion of *spr1023* and *spr1932*, did not affect erythromycin sensitivity, whereas the *spr0971-spr1023* and *spr0971-spr1932* deletions produce a two-fold increase of erythromycin MIC (8 μg/ml). Finally, a triple *spr0971-spr1023-spr1932* mutant was constructed using the *spr1023-spr1932* double mutant FR337 as recipient and the *spr0971* spectinomycin mutagenic construct as donor DNA. No change in erythromycin sensitivity (MIC=4 μg/ml) was observed also for the triple mutant. As control strains we used: i) the parental strain DP1004; ii) strain FR183 carrying the Φ1207.3 phage; iii) strain FP40 carrying the Φ1207.3Δ*mef*(A) recombinant phage; iv) deletion mutants without Φ1207.3; v) deletion mutants carrying Φ1207.3.

Conclusions

Our previous findings and those of other research groups [23–28] reported that the macrolide efflux in Streptococci relies on the presence of the *mef(*A)-*msr*(D) operon. Based on bioinformatic analysis of the Mef(A) and Msr(D) proteins and their functional characterization, we proposed that *mef(*A) and *msr*(D) constitute a two-gene ATP-Binding Cassette efflux transport system, where *mef*(A) encodes the transmembrane channel, and *msr*(D) the two ATP-binding domains. Since deletion of *msr*(D) abolishes erythromycin resistance, whereas deletion of *mef*(A) causes only a two-fold reduction of MIC value, we hypothesized that in absence of Mef(A), Msr(D) recruits an alternative transmembrane partner. In this work, to determine if the *mef*(A) deletion is complemented by pneumococcal chromosomal genes, we investigated the presence of genes encoding transmembrane proteins homologous to Mef(A). Homology search identified three candidate genes, namely

spr0971, *spr1023*, *spr1932*. Isogenic single, double and triple deletion mutants were constructed and the single and synergic contribution of these genes to *mef*(A) complementation was assessed by erythromycin sensitivity assays. The expected decrease of erythromycin MIC, due to the absence of a putative alternative Mef(A) channel, was not observed, suggesting that these genes are not involved in the complementation of *mef*(A) deletion. For the two *spr0971-spr1023* and *spr0971-spr1932* double mutants, we observed a two-fold increase of the erythromycin MIC, which was not seen in the triple mutant. These results are unexpected, as the MIC value in absence of *mef*(A) and other alternative transmembrane channels would be predicted to decrease. The same increase was observed also following the deletion of a fourth gene, *spr0875* (data not shown). This gene, which encodes a protein homologous to Mef(A), was previously characterized and associated to the efflux of other compounds including fusidic acid and sodium dodecyl sulfate [37,38]. For this reason and because its deletion resulted in the increase of erythromycin MIC value, we excluded it from further investigations. We hypothesise that this increase could be due a possible "unspecific" permease activity which allows erythromycin entrance in the bacterial cell through one or more of the pores encoded by these genes. In conclusion the quest to identify the alternative Msr(D) cognate transmembrane channel remains open.

Limitations

Investigation of putative candidate genes, responsible for complementing *mef*(A) deletion in the *mef*(A)-*msr*(D) macrolide efflux system in *S. pneumoniae*, was performed using a targeted approach based on the homology to Mef(A). Nonetheless, it is possible that the proteins involved in this complementation may not display significant homology to Mef(A). A genome-wide approach based on the creation and screening of a library of random mariner transposon mutants [39,40], allowing for random mutagenesis of the whole pneumococcal genome, could be used to investigate the possible effect of other chromosomal genes in *mef*(A) complementation.

Declarations

Ethics approval and consent to participate

Not applicable

Consent for publication

Not applicable

Availability of data and materials

All data generated or analysed during this study are included in this published article

Competing interests

The authors declare that they have no competing interests

Funding

This research was funded by the Italian Ministry of Education, University and Research (MIUR-Italy) under grant number 20177J5Y3P (call "Progetti di Ricerca di Rilevante Interesse Nazionale – Bando 2017")

Author Contributions

V.F., F.S., G.P., F.I. conceived and designed the study; V.F. carried out the experiments; V.F., F.S., F.I. performed data analysis; F.S., F.I., G.P. supervised the work; V.F. and F.I. drafted the first version of the manuscript; F.S. reviewed the manuscript; G.P. received funds for the study. All authors read and approved the final manuscript.

Acknowledgements

Not applicable

Table 1. Bacterial strains

Strain	Properties[a]	References
Rx1	Unencapsulated D39 *S. pneumoniae* derivative	[36,41]
DP1004	Rx1 derivative, *str-41*, Sm^R	[29,42]
FR183	DP1004 derivative, carrying φ1207.3, Sm^R, Em^R	[27]
FP40	FR183 derivative, carrying φ1207.3Δ*mef*(A), Sm^R, Em^R, Cm^R	[27]
FR323	DP1004 derivative, *spr0971*ΔSpe, Sm^R, Spe^R	This study
FR324	DP1004 derivative, *spr1023*ΔKm, Sm^R, Km^R	This study
FR325	DP1004 derivative, *spr1932*ΔKm, Sm^R, Km^R	This study
FR358	FR323 derivative, carrying φ1207.3, Sm^R, Em^R, Spe^R	This study
FR359	FR324 derivative, carrying φ1207.3, Sm^R, Em^R, Spe^R	This study
FR360	FR325 derivative, carrying φ1207.3, Sm^R, Em^R, Spe^R	This study
FR355	FR323 derivative, carrying φ1207.3Δ*mef*(A), Sm^R ,Em^R, Cm^R, Spe^R	This study
FR356	FR324 derivative, carrying φ1207.3Δ*mef*(A), Sm^R, Em^R, Cm^R, Spe^R	This study
FR357	FR325 derivative, carrying φ1207.3Δ*mef*(A), Sm^R, Em^R, Cm^R, Spe^R	This study
FR335	FR323 derivative, *spr0971*ΔSpe, *spr1023*ΔKm, Sm^R, Spe^R, Km^R	This study
FR336	FR323 derivative, *spr0971*ΔSpe, *spr1932*ΔKm, Sm^R, Spe^R, Km^R	This study
FR337	FR325 derivative, *spr1932*ΔKm, Δ*spr1023* (*in-frame*), Sm^R, Km^R	This study
FR344	FR335 derivative, carrying φ1207.3, Sm^R, Em^R, Spe^R, Km^R	This study
FR345	FR336 derivative, carrying φ1207.3, Sm^R, Em^R, Spe^R, Km^R	This study
FR349	FR337 derivative, carrying φ1207.3, Sm^R, Em^R, Km^R	This study
FR346	FR335 derivative, carrying φ1207.3Δ*mef*(A), Sm^R, Em^R, Cm^R, Spe^R, Km^R	This study
FR347	FR336 derivative, carrying φ1207.3Δ*mef*(A), Sm^R, Em^R, Cm^R, Spe^R, Km^R	This study
FR348	FR337 derivative, carrying φ1207.3Δ*mef*(A), Sm^R, Em^R, Cm^R, Km^R	This study
FR338	FR337 derivative, *spr*1932ΔKm, Δ*spr*1023 (*in-frame*), *spr*0971ΔSpe, Sm^R, Km^R, Spe^R	This study
FR351	FR338 derivative, carrying φ1207.3, Sm^R, Em^R, Km^R, Spe^R	This study
FR350	FR338 derivative, carrying φ1207.3Δ*mef*(A), Sm^R, Em^R, Cm^R, Km^R, Spe^R	This study

[a] *str-41* indicates a point mutation conferring resistance to streptomycin. Sm, streptomycin; Em, erythromycin Cm, chloramphenicol, Spe, spectinomycin; Km, kanamycin

Table 2. Erythromycin sensitivity

Strain	Genotype					Phenotype[b]	Erythromycin MIC (µg/ml)
	chromosome			Φ1207.3[a]			
	spr0971	*spr1023*	*spr1932*	*mef*(A)	*msr(D)*		
DP1004	+	+	+	np	np	Sensitive	0.06
FR183	+	+	+	+	+	Resistant	8
FP40	+	+	+	-	+	Resistant	4
FR323	-	+	+	np	np	Sensitive	0.06
FR324	+	-	+	np	np	Sensitive	0.06
FR325	+	+	-	np	np	Sensitive	0.06
FR358	-	+	+	+	+	Resistant	8
FR359	+	-	+	+	+	Resistant	8
FR360	+	+	-	+	+	Resistant	8
FR355	-	+	+	-	+	Resistant	4
FR356	+	-	+	-	+	Resistant	4
FR357	+	+	-	-	+	Resistant	4
FR335	-	-	+	np	np	Sensitive	0.06
FR336	-	+	-	np	np	Sensitive	0.06
FR337	+	-	-	np	np	Sensitive	0.06
FR344	-	-	+	+	+	Resistant	8
FR345	-	+	-	+	+	Resistant	8
FR349	+	-	-	+	+	Resistant	8
FR346	-	-	+	-	+	Resistant	8
FR347	-	+	-	-	+	Resistant	8
FR348	+	-	-	-	+	Resistant	4
FR338	-	-	-	np	np	Sensitive	0.06
FR351	-	-	-	+	+	Resistant	8
FR350	-	-	-	-	+	Resistant	4

[a] np: Φ1207.3 phage not present

[b] MIC interpretative standards: sensitive ≤ 0.25 µg/ml, intermediate = 0.5 µg/ml, and resistant ≥ 1 µg/ml.

FIGURE LEGEND

Figure 1. Schematic representation of genotype and phenotype of *S. pneumoniae* isogenic deletion mutants. Macrolide efflux in Streptococci is associated to the *mef*(A)-*msr*(D) macrolide efflux system, with Mef(A) acting as the transmembrane channel and Msr(D) as the cytoplasmatic ATP-binding protein. *mef*(A) deletion is probably complemented by other genes. The *spr0971*, *spr1023*, *spr1932* genes are predicted to encode transmembrane proteins homologous to Mef(A). To define if their gene products act as the alternative Msr(D) cognate transmembrane channel, isogenic deletion mutants, carrying the recombinant Φ1207.3Δ*mef*(A) phage, were constructed. Single, double and triple mutants were obtained by PCR gene SOEing and transformation. Genes are reported as arrows, while the cross indicates gene deletions. Spr0971, Spr1023 and Spr1932 proteins are reported as not scaled boxes and the 12 transmembrane domains as bars.

References

1. Weisblum B. Erythromycin resistance by ribosome modification. Antimicrob Agents Chemother. 1995 Mar;39(3):577–85.
2. Sutcliffe J, Grebe T, Tait-Kamradt A, Wondrack L. Detection of erythromycin-resistant determinants by PCR. Antimicrob Agents Chemother. 1996 Nov;40(11):2562–6.
3. Roberts MC, Sutcliffe J, Courvalin P, Jensen LB, Rood J, Seppala H. Nomenclature for Macrolide and Macrolide-Lincosamide-Streptogramin B Resistance Determinants. Antimicrob Agents Chemother. 1999 Dec 1;43(12):2823–30.
4. Leclercq R, Courvalin P. Resistance to Macrolides and Related Antibiotics in Streptococcus pneumoniae. Antimicrob Agents Chemother. 2002 Sep;46(9):2727–34.
5. Roberts MC. Update on macrolide-lincosamide-streptogramin, ketolide, and oxazolidinone resistance genes: MLSKO genes. FEMS Microbiol Lett. 2008 Apr 9;282(2):147–59.
6. Fyfe C, Grossman TH, Kerstein K, Sutcliffe J. Resistance to Macrolide Antibiotics in Public Health Pathogens. Cold Spring Harb Perspect Med. 2016 Oct;6(10):a025395.
7. Clancy J, Petitpas J, Dib-Hajj F, Yuan W, Cronan M, Kamath AV, Bergeron J, Retsema JA. Molecular cloning and functional analysis of a novel macrolide-resistance determinant, *mefA* , from *Streptococcus pyogenes* . Mol Microbiol. 1996 Dec;22(5):867–79.
8. Tait-Kamradt A, Clancy J, Cronan M, Dib-Hajj F, Wondrack L, Yuan W, Sutcliffe J. mefE is necessary for the erythromycin-resistant M phenotype in Streptococcus pneumoniae. Antimicrob Agents Chemother. 1997 Oct;41(10):2251–5.
9. Luna VA, Coates P, Eady EA, Cove JH, Nguyen TTH, Roberts MC. A variety of Gram-positive bacteria carry mobile mef genes. J Antimicrob Chemother. 1999 Jan;44(1):19–25.
10. Luna VA, Heiken M, Judge K, Ulep C, Van Kirk N, Luis H, Bernardo M, Leitao J, Roberts MC. Distribution of *mef* (A) in Gram-Positive Bacteria from Healthy Portuguese Children. Antimicrob Agents Chemother. 2002 Aug;46(8):2513–7.
11. Roberts MC, Soge OO, No DB. Characterization of macrolide resistance genes in Haemophilus influenzae isolated from children with cystic fibrosis. J Antimicrob Chemother. 2011 Jan 1;66(1):100–4.
12. Klaassen CHW, Mouton JW. Molecular Detection of the Macrolide Efflux Gene: To Discriminate or Not To Discriminate between *mef* (A) and *mef* (E). Antimicrob Agents Chemother. 2005 Apr;49(4):1271–8.
13. Santagati M, Iannelli F, Oggioni MR, Stefani S, Pozzi G. Characterization of a Genetic Element Carrying the Macrolide Efflux Gene mef(A) in Streptococcus pneumoniae. Antimicrob Agents Chemother. 2000 Sep 1;44(9):2585–7.

14. Gay K, Stephens DS. Structure and Dissemination of a Chromosomal Insertion Element Encoding Macrolide Efflux in *Streptococcus pneumoniae*. J Infect Dis. 2001 Jul;184(1):56–65.
15. Del Grosso M, Iannelli F, Messina C, Santagati M, Petrosillo N, Stefani S, Pozzi G, Pantosti A. Macrolide Efflux Genes mef(A) and mef(E) Are Carried by Different Genetic Elements in Streptococcus pneumoniae. J Clin Microbiol. 2002 Mar 1;40(3):774–8.
16. Del Grosso M, Scotto d'Abusco A, Iannelli F, Pozzi G, Pantosti A. Tn2009, a Tn916-Like Element Containing mef(E) in Streptococcus pneumoniae. Antimicrob Agents Chemother. 2004 Jun;48(6):2037–42.
17. Del Grosso M, Camilli R, Iannelli F, Pozzi G, Pantosti A. The mef(E)-Carrying Genetic Element (mega) of Streptococcus pneumoniae: Insertion Sites and Association with Other Genetic Elements. Antimicrob Agents Chemother. 2006 Oct;50(10):3361–6.
18. Santagati M, Iannelli F, Cascone C, Campanile F, Oggioni MR, Stefani S, Pozzi G. The Novel Conjugative Transposon Tn1207.3 Carries the Macrolide Efflux Gene mef(A) in Streptococcus pyogenes. Microb Drug Resist. 2003 Aug;9(3):243–7.
19. Pozzi G, Iannelli F, Oggioni M, Santagati M, Stefani S. Genetic Elements Carrying Macrolide Efflux Genes in Streptococci. Curr Drug Target -Infect Disord. 2004 Sep 1;4(3):203–6.
20. Iannelli F, Santagati M, Santoro F, Oggioni MR, Stefani S, Pozzi G. Nucleotide sequence of conjugative prophage Φ1207.3 (formerly Tn1207.3) carrying the mef(A)/msr(D) genes for efflux resistance to macrolides in Streptococcus pyogenes. Front Microbiol. 2014 Dec 9;5:687–687.
21. Banks DJ, Porcella SF, Barbian KD, Martin JM, Musser JM. Structure and Distribution of an Unusual Chimeric Genetic Element Encoding Macrolide Resistance in Phylogenetically Diverse Clones of Group A *Streptococcus*. J Infect Dis. 2003 Dec 15;188(12):1898–908.
22. Brenciani A, Bacciaglia A, Vignaroli C, Pugnaloni A, Varaldo PE, Giovanetti E. Φm46.1, the Main *Streptococcus pyogenes* Element Carrying *mef* (A) and *tet* (O) Genes. Antimicrob Agents Chemother. 2010 Jan;54(1):221–9.
23. Vitali LA, Di Luca MC, Prenna M, Petrelli D. Correlation between genetic features of the mef (A)- msr (D) locus and erythromycin resistance in Streptococcus pyogenes. Diagn Microbiol Infect Dis. 2016 Jan;84(1):57–62.
24. Ambrose KD, Nisbet R, Stephens DS. Macrolide Efflux in *Streptococcus pneumoniae* Is Mediated by a Dual Efflux Pump (*mel* and *mef*) and Is Erythromycin Inducible. Antimicrob Agents Chemother. 2005 Oct;49(10):4203–9.

25. Nunez-Samudio V, Chesneau O. Functional interplay between the ATP binding cassette Msr(D) protein and the membrane facilitator superfamily Mef(E) transporter for macrolide resistance in Escherichia coli. Res Microbiol. 2013 Apr;164(3):226–35.
26. Zhang Y, Tatsuno I, Okada R, Hata N, Matsumoto M, Isaka M, Isobe K, Hasegawa T. Predominant role of msr(D) over mef(A) in macrolide resistance in Streptococcus pyogenes. Microbiology. 2016 Jan 1;162(1):46–52.
27. Iannelli F, Santoro F, Santagati M, Docquier J-D, Lazzeri E, Pastore G, Cassone M, Oggioni MR, Rossolini GM, Stefani S, Pozzi G. Type M Resistance to Macrolides Is Due to a Two-Gene Efflux Transport System of the ATP-Binding Cassette (ABC) Superfamily. Front Microbiol. 2018 Jul 31;9:1670.
28. Tatsuno I, Isaka M, Masuno K, Hata N, Matsumoto M, Hasegawa T. Functional Predominance of *msr* (D), Which Is More Effective as *mef(* A)-Associated Than *mef(* E)-Associated, Over *mef* (A)/ *mef* (E) in Macrolide Resistance in *Streptococcus pyogenes*. Microb Drug Resist. 2018 Oct;24(8):1089–97.
29. Iannelli F, Pozzi G. Method for Introducing Specific and Unmarked Mutations Into the Chromosome of Streptococcus pneumoniae. Mol Biotechnol. 2004;26(1):81–6.
30. Iannelli F, Santoro F, Fox V, Pozzi G. A Mating Procedure for Genetic Transfer of Integrative and Conjugative Elements (ICEs) of Streptococci and Enterococci. Methods Protoc. 2021 Aug 28;4(3):59.
31. Ikeda M, Arai M, Okuno T, Shimizu T. TMPDB: a database of experimentally-characterized transmembrane topologies. Nucleic Acids Res. 2003 Jan 1;31(1):406–9.
32. Santoro F, Oggioni MR, Pozzi G, Iannelli F. Nucleotide sequence and functional analysis of the tet (M)-carrying conjugative transposon Tn5251 of Streptococcus pneumoniae: Tn5251 of Streptococcus pneumoniae. FEMS Microbiol Lett. 2010 Apr 28;no-no.
33. Iannelli F, Santoro F, Oggioni MR, Pozzi G. Nucleotide sequence analysis of integrative conjugative element Tn5253 of Streptococcus pneumoniae. Antimicrob Agents Chemother. 2013/12/02 ed. 2014;58(2):1235–9.
34. Kelley LA, Mezulis S, Yates CM, Wass MN, Sternberg MJE. The Phyre2 web portal for protein modeling, prediction and analysis. Nat Protoc. 2015 Jun;10(6):845–58.
35. Santoro F, Romeo A, Pozzi G, Iannelli F. Excision and Circularization of Integrative Conjugative Element Tn5253 of Streptococcus pneumoniae. Front Microbiol. 2018 Jul 31;9:1779.
36. Pearce BJ, Iannelli F, Pozzi G. Construction of new unencapsulated (rough) strains of Streptococcus pneumoniae. Res Microbiol. 2002;5.

37. Gill MJ, Brenwald NP, Wise R. Identification of an Efflux Pump Gene, *pmrA* , Associated with Fluoroquinolone Resistance in *Streptococcus pneumoniae*. Antimicrob Agents Chemother. 1999 Jan;43(1):187–9.
38. Tocci N, Iannelli F, Bidossi A, Ciusa ML, Decorosi F, Viti C, Pozzi G, Ricci S, Oggioni MR. Functional Analysis of Pneumococcal Drug Efflux Pumps Associates the MATE DinF Transporter with Quinolone Susceptibility. Antimicrob Agents Chemother. 2013 Jan;57(1):248–53.
39. Akerley BJ, Rubin EJ, Camilli A, Lampe DJ, Robertson HM, Mekalanos JJ. Systematic identification of essential genes by in vitro mariner mutagenesis. Proc Natl Acad Sci. 1998 Jul 21;95(15):8927–32.
40. Lampe DJ, Akerley BJ, Rubin EJ, Mekalanos JJ, Robertson HM. Hyperactive transposase mutants of the Himar1 mariner transposon. Proc Natl Acad Sci. 1999 Sep 28;96(20):11428–33.
41. Smith MD, Guild WR. A Plasmid in Streptococcus pneumoniae. 1979;137:5.
42. Salles C, Créancier L, Claverys JP, Méjean V. The high level streptomycin resistance gene from Streptococcus pneumoniae is a homologue of the ribosomal protein S12 gene from Escherichia coli. Nucleic Acids Res. 1992 Nov 25;20(22):6103–6103.

Figure 1

Strain	Genotype			Erythromycin MIC (µg/ml)
	spr0971	*spr1023*	*spr1932*	
FP40	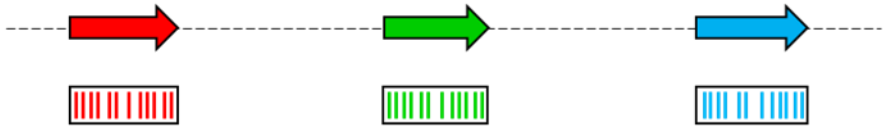			4
FR355				4
FR356				4
FR357				4
FR346				8
FR347				8
FR348				4
FR350				4

CHAPTER 9

Chromosomal integration of Tn*5253* occurs downstream of a conserved 11-bp sequence of the *rbgA* gene in *Streptococcus pneumoniae* and in all the other known hosts of this integrative conjugative element (ICE)

Francesco Santoro, Valeria Fox, Alessandra Romeo, Elisa Lazzeri, Gianni Pozzi and Francesco Iannelli

Laboratory of Molecular Microbiology and Biotechnology,

Department of Medical Biotechnologies,

University of Siena, 53100 Siena, Italy

Submitted to Mobile DNA

ABSTRACT

Background

Tn*5253*, a composite Integrative Conjugative Element (ICE) of *Streptococcus pneumoniae* carrying *tet*(M) and *cat* resistance determinants, was found (i) to integrate at specific 83-bp target site (*att*B), (ii) to produce circular forms joined by a 84-bp sequence (*att*Tn), and (iii) to restore the chromosomal integration site. The purpose of the present study is to functionally characterize the *att*B in *S. pneumoniae* strains with different genetic backgrounds and in other bacterial species, and to investigate the presence of the Tn*5253 att*B site into bacterial genomes.

Results

Analysis of representative Tn*5253*-carryng transconjugants obtained in *S. pneumoniae* strains with different genetic backgrounds and in other bacterial species, namely *Streptococcus agalactiae*, *Streptococcus gordonii*, *Streptococcus pyogenes*, and *Enterococcus faecalis*, confirmed that: (i) Tn*5253* integrates in *rbgA* of *S. pneumoniae* and in orthologous *rbgA* genes of other bacterial species, (ii) Tn*5253* produced circular forms containing the *att*Tn site at a concentration ranging between 2.0 x 10^{-5} to 1.2 x 10^{-2} copies per chromosome depending on bacterial species and strain, (iii) reconstitution of *att*B sites occurred at 3.7 x 10^{-5} to 1.7 x 10^{-2} copies per chromosome.

A database search of complete Microbial Genomes using Tn*5253 att*B as a probe showed that (i) thirteen *att*B variants, ranging from 41 to 84 nucleotides in length, were present in the 85 complete pneumococcal genomes, (ii) in other bacterial species *att*B was located in orthologous *rbgA* genes and its size ranged between 14 and 82 nucleotides, (iii) 11 nucleotides are conserved among the different bacterial species and can be considered the core of the target site.

Conclusions

A functional characterization of the Tn*5253 att*B insertion site integrated by a genomic sequence analysis contributed to elucidating the potential of Tn*5253* horizontal gene transfer among different bacterial species.

INTRODUCTION

The acquisition of new genetic material by horizontal gene transfer (HGT) significantly drives bacterial genome evolution and is mediated by Mobile Genetic Elements (MGEs). The term "mobilome" is used to indicate the entire set of MGEs of the microbiome[1]. MGEs are responsible for the spread of resistance and virulence genes in the microbial communities [2–4]. Thus, to study the acquisition and dissemination of antibiotic determinants in a bacterial population, the characterization of mobilome is crucial[5]. Even though new metagenomic approaches, both whole and targeted[1,6,7] have been implemented, a functional study of MGEs is still required[8,9]. Integrative and Conjugative Elements (ICEs) are MGEs commonly found in bacteria where they can constitute up to 25% of the genome[5,10–14]. One of the most studied ICE of gram-positive bacteria is Tn*916*, a conjugative transposon originally found in *Enterococcus faecalis* which carries the *tet*(M) tetracycline resistance gene and is considered the prototype of the Tn*916*-Tn*1545* family of ICEs[15–19]. Conjugative transposons of the Tn*916*-Tn*1545* family can insert at multiple insertion sites in the chromosome [20], while other ICEs, like Tn*5253*, SXT, Tn*5397*, and ICE*St1*, insert at a single specific site[21–26]. We previously characterized Tn*5253*, a 64,528-bp composite ICE of *Streptococcus pneumoniae*, containing the ICE Tn*5251* of the Tn*916*-Tn*1545* family and the Ω*cat*(pC194) element carrying *tet*(M) and *cat* resistance determinants, respectively[27–29]. Tn*5253* was found integrated at 83-bp specific target site (*att*B) located in the essential gene *rbgA* of the *S. pneumoniae* chromosome[26,28,30]. The ICE was shown to excise from the pneumococcal chromosome with production of i) circular forms in which the ends of the element were joined by a 84-bp sequence (*att*Tn) and ii) a reconstituted chromosomal *att*B. Tn*5253*, once integrated into the chromosome, was flanked by the *att*L site, identical to *att*B, and the *att*R site, identical to *att*Tn. Pneumococcal mobilome analysis showed the frequent presence of Tn*5253*-like elements in multidrug-resistant *S. pneumoniae* strains and the maintenance of the element in all derivative isolates[31–34]. In this work, in order to contribute to mobilome characterization, we first

conducted a functional characterization of the *Tn5253* integration site, by analyzing *att*B in Tn*5253*-carrying transconjugants obtained in *S. pneumoniae* strains with different genetic backgrounds and in other bacterial species. We then investigated the presence of the Tn*5253 att*B site into the complete microbial genomes available in public databases.

RESULTS AND DISCUSSION

Tn*5253* attachment sites and circularization in different pneumococcal transconjugants

Representative Tn*5253*-carrying transconjugants were obtained in *S. pneumoniae* with different genetic backgrounds, namely TIGR4, A66 and SP18-BS74[28] (Table 1). DNA sequence analysis of Tn*5253*-chromosome junction fragments showed that: (i) Tn*5253* integration occurred at a specific target site (*att*B) located in *rbgA* gene of the pneumococcal chromosome [26], (ii) *att*L was identical to *att*B and (iii) *att*R was identical to *att*Tn, as already described for D39 derivative strains[26], and that (iv) *att*B sites among these pneumococcal strains were not identical, with their size varying from 41 (in SP18-BS74) to 83 nucleotides (in TIGR4 and A66) . We also analysed the nucleotide sequence of Tn*5253* junctions in BM6001 and DP1322, in which Tn*5253* was transferred by transformation of a crude lysate from BM6001[35]. *att*L of BM6001 was found to belong to a 84 bp-long variant, different from the one of DP1322, which derived from Tn*5253* integration via homologous recombination between DNA sequences beyond Tn*5253 att* sites.

Tn*5253* was found to excise from pneumococcal chromosome with consequent production of circular forms, containing the *att*Tn site, and reconstitution of *att*B site[26]. To investigate if different pneumococcal genetic backgrounds influence the excision and circularization of Tn*5253*, qPCR on cell lysates was used to quantify the excision of Tn*5253* and *att*B reconstitution in liquid pneumococcal cultures (Table 1). Interestingly, the transconjugant FR56, derived from SP18-BS74, produced Tn*5253* circular forms and reconstituted *att*B site at very high frequency (1.2×10^{-2} and 1.9×10^{-3} copies per chromosome, respectively), however these results did not correlate with the conjugation frequency, which was 6.1×10^{-6}, indicating that the frequency of circularization is not

the only limiting factor of the conjugation process. Neither circular forms nor reconstituted *att*B of Tn*5253* could be detected in the TIGR4 background (<3.6 x 10^{-5} and to <3.5 x 10^{-4}, respectively), correlating with the absence of conjugal transfer (<9.9 x 10^{-8}).

Tn*5253 att* sites and circularization in *Streptococcus* and *Enterococcus*

We also characterized Tn*5253* circular forms and insertion site in the transconjugants obtained when *S. agalactiae* H36B, *S. gordonii* V288, *S. pyogenes* SF370, *E. faecalis* OG1SS and JH2-2 strains were used as conjugation recipients (Table 1). As found in *S. pneumoniae*, *att*L was identical to *att*B regardless the bacterial strain harbouring the element and *att*R was identical to *att*Tn in all bacterial species tested. Tn*5253* produced circular forms at a similar frequency in *S. agalactiae* (2.9 x 10^{-5} copies per chromosome) and in *S. pyogenes* (3.0 x 10^{-5} copies per chromosome), while no circular forms were detected in *S. gordonii* (<2.7 x 10^{-6} copies per chromosome). Reconstituted *att*B sites were found in all streptococci tested at a frequency ranging between 1.5 x 10^{-5} (in *S. gordonii*) to 3.0 x 10^{-4} (in *S. agalactiae*) copies per chromosome (Table 1). In *E. faecalis*, Tn*5253* excision and circularization are strain dependent: a representative transconjugant obtained in OG1SS background produced circular forms and reconstituted *att*B sites at 1.4 x 10^{-4} and 6.8 x 10^{-3} copies per chromosome, respectively; a transconjugant obtained in JH2-2 background produced reconstituted *att*B site at a frequency of 1.7 x 10^{-2} copies per chromosome but did not produce circular forms (<2.7 x 10^{-7}). Both in *S. pneumoniae* and other bacterial species, length of the target site corresponds to length of the duplication after Tn*5253* integration. Conjugation frequency was lower than circularization frequency in all the tested strains except in *S. pyogenes* FR68 and in *S. gordonii* FR43. Many other factors are likely to be important in the conjugation process such as the expression of a capsular polysaccharide[36], the cell wall thickness, the surface charges, and the ability of the conjugation pore to establish a stable contact between cells from different species.

Genomic sequence analysis of Tn*5253 att*B site

The database of 58,138 complete Microbial genomes (accessed in August 2021) was interrogated by using as a query the 83-bp *att*B. Thirteen allelic variants of *att*B, ranging from 41 to 84 nucleotides in length, were identified in the 85 complete pneumococcal genomes (Figure 1A). The 83-bp *att*B was labeled variant 1, as it is the most frequent variant, carried by 38 genome strains (44.7% of total), including D39, its derivative strain R6, and the classical type 3 Avery's strain A66. Variant 2 is carried by TIGR4 and other 8 genome strains (10.6%) and contains two nucleotide substitutions. Variant 13 is harboured by G54 and other 9 genome strains (11.7%) and contains only the last 41 nucleotides of variant 1. In addition, SP18-BS74, whose draft genome is available in GenBank (accession no. NZ_ABAE01000001.1), also harbours variant 13. In thirteen pneumococcal genomes, carrying the *att*B variants 1, 2, 7, 11 and 12, Tn*5253*-like elements were integrated into the pneumococcal chromosome resulting in the duplication of the *att*B site. Furthermore, homology search identified 15 additional *att*B variants in other bacterial species, including *Streptococcus agalactiae*, *Streptococcus gordonii*, *Streptococcus pyogenes*, and *Enterococcus faecalis*. Tn*5253 att*B was located in orthologous *rbgA* genes and its size ranged between 14 nucleotides of *Enterococcus faecalis* to 82 nucleotides of *Streptococcus pseudopneumoniae* (Figure 1B). Alignment of the *att*B sequences obtained from the different bacterial species shows that 11 nucleotides, namely the last nucleotides of the *S. pneumoniae* variant 1, are conserved among all species and can be considered the core of the target site. Only in one genome, namely *Streptococcus mitis* SVGS_061, a Tn*5253*-like element was integrated into chromosome producing *att*B duplication.

CONCLUSIONS

Mobile Genetic Element, comprising Integrative Conjugative Elements (ICEs), are important drivers of bacterial evolution and adaptation[2,3]. ICEs are responsible for the shaping of the bacterial genome[11] and for the spread of antibiotic resistance and virulence genes in the microbial communities, representing an important aspect in clinical settings[3,5]. Depending on the type of

ICE, integration in the bacterial chromosome can occur at different sites, like in the case of the Tn*916* family[15–19], or at specific site, like in the case of the Tn*5253*[26]. Identification, through genomic and metagenomic studies, and functional characterization of the insertion sites and mechanisms underlying the transfer of these elements, in different bacterial species, is pivotal in mobilome studies[8,9]. In the present paper we conducted a functional characterization of Tn*5253* *att*B site in *S. pneumoniae* and other streptococcal and enterococcal species and found that: (i) during conjugal transfer, Tn*5253* integrated in *S. pneumoniae rbgA* gene or in the orthologous *rbgA* genes of the other bacterial species, (ii) Tn*5253* produced circular forms containing the *att*Tn site and the frequency was species- and strain-dependent, (iii) reconstitution of *att*B site was species- and strain-dependent. Through a DNA homology search conducted in the complete microbial genome database, we also found that: (i) thirteen allelic variants of the Tn*5253* *att*B site were present in the complete *S. pneumoniae* genomes and their size ranged from 41 to 84 nucleotides, (ii) in other streptococcal and enterococcal species, Tn*5253* *att*B is located in orthologous *rbgA* genes with a size ranging between 14 to 82 nucleotides, (iii) 11 nucleotides are conserved among the different bacterial species and can be considered the core of the target site. Since we demonstrated that the 41 nucleotides of *S. pneumoniae att*B variant 13 (in SP18-BS74) and the 14 nucleotides of *E. faecalis att*B allow the chromosomal integration of Tn*5253*, it is likely that the 11-nucleotide core target site is sufficient for the integration of Tn*5253*-family elements. This site is located within an essential bacterial gene and acts as a hotspot for the integration of novel genes, including antibiotic resistance determinants. In conclusion, even if a huge number of bacterial genomes is available, an *in-silico* analysis and a functional characterization of the mobilome is reported only in few cases. In this work, a functional characterization of the Tn*5253* *att*B insertion site integrated by genomic sequence analysis contributed to elucidating the potential of Tn*5253* horizontal gene transfer among different bacterial species.

MATERIALS AND METHODS

Bacterial strains, growth, and mating conditions.

Bacterial strains and their relevant properties are reported in Table 1. Both streptococcal and enterococcal strains were grown in tryptic soy broth or tryptic soy agar (Difco) supplemented, where appropriate, with antibiotics. Plate mating conjugation experiments were performed as previously described[37]. Briefly, donor and recipient cells were grown until the end of exponential phase and mixed at a 1:10 ratio, then were collected by centrifugation, plated and incubated for 4 h. Cells were harvested by scraping the plates and recombinant strains were selected by a multilayer plating procedure in presence of the appropriate antibiotics. Transconjugant FR39 was obtained from a mating experiment where FP58[29] was the donor of Tn*5253* and HB565, a streptomycin resistance derivative of type 3 Avery strain A66[14,38,39], was the recipient.

Bacterial lysate preparation.

Bacterial cultures (1 ml) were harvested in exponential phase (OD_{590} about 0.2, roughly corresponding to 5 x 10^8 CFU/ml) and centrifuged at 11,000 x *g* for 2 minutes. Pneumococcal lysates were obtained by using lysis solution (0.1% DOC, 0.008% SDS) as already reported[26]. Streptococcal and enterococcal cell pellets were resuspended in 90 µl protoplasting buffer (25% sucrose, 100 mM Tris pH 7.2, 5 mM EDTA), then lysozyme (for *E. faecalis*) or mutanolysin (for *S. agalactiae*, *S. gordonii* and *S. pyogenes*) was added at a final concentration of 1 mg/ml or 20 µg/ml respectively and mixtures were incubated at 37°C for 1 hour. Protoplasts were centrifuged at 3,000 x *g* for 15 minutes, resuspended in 100 µl of dH_2O, heated at 85°C for 5 minutes and kept on ice until use.

PCR, sequencing and sequence analysis.

PCR experiments and DNA sequencing of PCR amplicons were carried out following an already described protocol[28,29]. DNA sequence analysis was performed with standard softwares.

Quantitative Real time PCR

A LightCycler 1.5 apparatus (Roche) and the KAPA SYBR FAST qPCR kit Master Mix Universal (2X) (Kapa Biosystems) were used for Real Time PCR experiments according to the protocol

extensively described[26]. Quantification of Tn*5253* circular intermediates and reconstituted pneumococcal *att*B was obtained with the primer pairs IF327/IF328 and IF496/IF356, respectively[26]. Reconstituted *att*B site was quantified in *S. agalactiae* with the primer pair IF560/IF561 which amplified a 353 bp fragment, in *S. gordonii* with IF544/IF545 which amplified a 396 bp fragment, in *S. pyogenes* with IF509/IF510 which amplified a 249 bp fragment, in *E. faecalis* with IF525/IF532 which amplified a 480 bp fragment (Table 2). A standard curve for the *gyrB* gene was used to standardize results and melting curve analysis was performed to differentiate the amplified products from primer dimers as reported[26].

Microbial database interrogation

To overcome difficulties in bacterial database exploration, we built a stand-alone database containing only genomes of interest to be searched with BLAST software.

Data obtained from the stand-alone database were confirmed by using the Microbial Nucleotide BLAST (https://blast.ncbi.nlm.nih.gov/Blast.cgi?PAGE_TYPE=BlastSearch&BLAST_SPEC =MicrobialGenomes), selecting the complete genomes database.

DECLARATIONS

Ethics approval and consent to participate

Not applicable

Consent for publication

Not applicable

Availability of data and materials

All data generated or analyzed during this study are included in this published article

Competing interests

The authors declare that they have no competing interests

Funding

This work was supported by the Italian Ministry of Education, University and Research (MIUR-Italy) under grant number 20177J5Y3P (call “Progetti di Ricerca di Rilevante Interesse Nazionale – Bando 2017”).

Authors' contributions

FS, GP, FI conceived and designed the study, FS, VF, AR, EL carried out the experiments, FS, VF, GP, FI performed data analysis, FS, FI drafted the first version of the manuscript, FS, VF, GP, FI drafted subsequent versions of the manuscript, GP received funds for the study. All authors read and approved the final manuscript.

Acknowledgements

Not applicable

Table 1. Real Time PCR quantification of Tn*5253* circular form and reconstituted *att*B in Tn*5253*-carrying transconjugants.

Strain (reference)	Relevant properties of parental strain[a]	Circular Forms	Reconstituted *att*B sites	Conjugation Frequency[b]
FR39 (This study)	HB565, *S. pneumoniae* A66 derivative, serotype 3, *str-1*, Sm^R	$2.0 \times 10^{-5} \pm 1.9 \times 10^{-5}$	$<6.9 \times 10^{-6}$	4.4×10^{-7}
FR54 [28]	FP47, *S. pneumoniae* TIGR4 derivative, serotype 4, *nov-1*, Nov^R	$<3.6 \times 10^{-5}$	$<3.5 \times 10^{-4}$	$<9.9 \times 10^{-8}$
FR56 [28]	FR55, *S. pneumoniae* SP18-BS74 derivative, serotype 18C, Sm^R	$1.2 \times 10^{-2} \pm 7.5 \times 10^{-5}$	$1.9 \times 10^{-3} \pm 1.0 \times 10^{-4}$	6.1×10^{-6}
FR49 [29]	OG1SS, *E. faecalis*, Spe^R Sm^R	$1.4 \times 10^{-4} \pm 9.2 \times 10^{-5}$	$6.8 \times 10^{-3} \pm 1.0 \times 10^{-4}$	$<1.8 \times 10^{-8}$
FR50 [29]	JH2-2, *E. faecalis*, Fus^R Rif^R	$<2.7 \times 10^{-7}$	$1.7 \times 10^{-2} \pm 1.3 \times 10^{-3}$	$<2.7 \times 10^{-8}$
FR67 [29]	H36B, *S. agalactiae*, serotype Ib	$2.9 \times 10^{-5} \pm 8.7 \times 10^{-6}$	$3.0 \times 10^{-4} \pm 1.0 \times 10^{-4}$	1.1×10^{-6}
FR68 [29]	SF370, *S. pyogenes*, serotype M1	$3.0 \times 10^{-5} \pm 1.0 \times 10^{-5}$	$3.7 \times 10^{-5} \pm 6.2 \times 10^{-6}$	9.5×10^{-4}
FR43 [29]	GP204, *S. gordonii* Challis V288 derivative, *str-204*, Sm^R	$6.5 \times 10^{-5} \pm 4.4 \times 10^{-5}$	$7.9 \times 10^{-5} \pm 1.2 \times 10^{-5}$	8.3×10^{-7}

[a]*nov-1* indicates point mutations conferring resistance to novobiocin, while *str-41 and str-204* to streptomycin. Sm, streptomycin; Nov, novobiocin; Spe, spectinomycin; Fus, fusidic acid; Rif, rifampicin; [b]Frequency refers to mating experiments where *S. pneumoniae* FP10 or FP11[29] were the recipients, conjugation frequencies of strains FR49, FR50, FR67 and FR43 were reported in Iannelli et al. 2014[28]; conjugation frequency is expressed as the number of transconjugant per donor; each result is the mean of at least three mating experiments

Table 2. Oligonucleotide primers.

Name	Sequence (5'to 3')	GenBank ID: nucleotides
Streptococcus agalactiae		
IF560	AAC GAA ACC TAT CAG CGG AA	AAJS01000088: 6,047-6,028
IF561	TTT GGG TTT GTC TCC GAC GA	AAJS01000088: 5,695-5,714
IF927	ACA AGC GAG AAG GTC AAG AAG TT	AAJS01000029: 4,775-4,797
IF928	GTG TCA AGG CAG TAC GAA ATC	AAJS01000029: 5,012-5,032
Streptococcus gordonii		
IF512	TGC TTT AGG AGA TGT TGA GTT	CP000725: 1,253,207-1,253,187
IF513	ACC GCA GAC TGT TCT TTA GA	CP000725: 1,252,812-1,252,831
IF544	CAG ATG GAG AAA TGG AAG AT	CP000725: 1,483,666- 1,483,647
IF545	GCT GTA CGG AAA CCT TGC TC	CP000725: 1,483,531-1,483,550
Streptococcus pyogenes		
IF509	AAG TAG AAA TGG CGA AGT GAA	AE004092: 953,960-953,980
IF510	GAC TAG AAA GTG GTA AGC GT	AE004092: 954,208-954,189
IF306	AAG GTT TGA CGG CGG TAA	AE004092: 582,657-582,674
IF307	ACG AGC AAC TTG TGG GTT	AE004092: 582,814-582,797
Enterococcus faecalis		
IF525	GGT TAC GGG AAG AAA GCG GT	CP002621: 1,430,659-1,430,678
IF532	GCC TAT GGG ATT GCT ACA CC	CP002621: 1,431,138-1,431,119
IF943	ACC AAG AAT ATC GTC GTG GT	CP002621: 5,120-5,139
IF944	AAT TGA AAT GTG TAA GCC TCG	CP002621: 5,310-5,290

FIGURE LEGEND

FIG. 1. Sequence alignment of Tn*5253 att*B in A) *S. pneumoniae* genomes, B) other bacterial species genomes.

A) In *S. pneumoniae* genomes, 13 allelic variants of *att*B were found, ranging from 41 to 84 nucleotides in length. Variant 1 is the most frequent variant, carried by 38 genome strains (44.7% of total), including D39, R6 and A66. Variant 2 is carried by TIGR4 and other 8 genome strains (10.6%). Variant 13 is harboured by G54 and other 9 genome strains (11.7%). Variants 5 and 7 are carried by 7 strains (8.2%), variant 4 by 5 strains (5.8%), variants 6 and 9 by 2 strains (2.4%). The remaining 5 variants (3, 8, 10, 11 and 12) were found in only in one strain.

B) In other bacterial species, *att*B size varied from 14 to 82 nucleotides. Since inside the same bacterial species, different strains can harbour different variants (up to 7 in *S. equi*), sequence of the most representative variant was shown. For both alignments, the D39 *att*B variant 1 was used as reference. Within the sequences, identical nucleotides are indicated by periods. For better alignment dashes are inserted. Variant names are indicated on the left and the representative pneumococcal strains or bacterial species are reported in parentheses, while lengths of attachment sites are indicated on the right.

REFERENCES

1. Carr VR, Shkoporov A, Hill C, Mullany P, Moyes DL. Probing the Mobilome: Discoveries in the Dynamic Microbiome. Trends Microbiol. 2021 Feb;29(2):158–70.
2. Ghaly TM, Gillings MR. Mobile DNAs as Ecologically and Evolutionarily Independent Units of Life. Trends Microbiol. 2018 Nov;26(11):904–12.
3. Partridge SR, Kwong SM, Firth N, Jensen SO. Mobile Genetic Elements Associated with Antimicrobial Resistance. Clin Microbiol Rev. 2018;31(4).
4. Gyles C, Boerlin P. Horizontally Transferred Genetic Elements and Their Role in Pathogenesis of Bacterial Disease. Vet Pathol. 2014 Mar 1;51(2):328–40.
5. Botelho J, Schulenburg H. The Role of Integrative and Conjugative Elements in Antibiotic Resistance Evolution. Trends Microbiol. 2021 Jan;29(1):8–18.
6. Jørgensen TS, Kiil AS, Hansen MA, Sørensen SJ, Hansen LH. Current strategies for mobilome research. Front Microbiol. 2015 Jan 22;5:750–750.
7. Lee K, Kim D-W, Cha C-J. Overview of bioinformatic methods for analysis of antibiotic resistome from genome and metagenome data. J Microbiol. 2021 Mar;59(3):270–80.
8. Saak CC, Dinh CB, Dutton RJ. Experimental approaches to tracking mobile genetic elements in microbial communities. FEMS Microbiol Rev. 2020 Sep 1;44(5):606–30.
9. Bellanger X, Payot S, Leblond-Bourget N, Guédon G. Conjugative and mobilizable genomic islands in bacteria: evolution and diversity. FEMS Microbiol Rev. 2014 Jul;38(4):720–60.
10. Paulsen IT. Role of Mobile DNA in the Evolution of Vancomycin-Resistant Enterococcus faecalis. Science. 2003 Mar 28;299(5615):2071–4.
11. Burrus V, Waldor MK. Shaping bacterial genomes with integrative and conjugative elements. Res Microbiol. 2004 Jun;155(5):376–86.
12. Wozniak RAF, Waldor MK. Integrative and conjugative elements: mosaic mobile genetic elements enabling dynamic lateral gene flow. Nat Rev Microbiol. 2010 Aug;8(8):552–63.
13. Johnson CM, Grossman AD. Integrative and Conjugative Elements (ICEs): What They Do and How They Work. Annu Rev Genet. 2015;49:577–601.
14. Santoro F, Iannelli F, Pozzi G. Genomics and Genetics of Streptococcus pneumoniae. Microbiol Spectr. 2019 May;7(3).
15. Franke AE, Clewell DB. Evidence for a chromosome-borne resistance transposon (Tn916) in Streptococcus faecalis that is capable of ‘conjugal’ transfer in the absence of a conjugative plasmid. J Bacteriol. 1981 Jan;145(1):494–502.

16. Rice LB. Tn *916* Family Conjugative Transposons and Dissemination of Antimicrobial Resistance Determinants. Antimicrob Agents Chemother. 1998 Aug;42(8):1871–7.
17. Roberts AP, Mullany P. A modular master on the move: the Tn916 family of mobile genetic elements. Trends Microbiol. 2009 Jun;17(6):251–8.
18. Mullany P, Williams R, Langridge GC, Turner DJ, Whalan R, Clayton C, et al. Behavior and Target Site Selection of Conjugative Transposon Tn *916* in Two Different Strains of Toxigenic Clostridium difficile. Appl Environ Microbiol. 2012 Apr;78(7):2147–53.
19. Santoro F, Vianna ME, Roberts AP. Variation on a theme; an overview of the Tn916/Tn1545 family of mobile genetic elements in the oral and nasopharyngeal streptococci. Front Microbiol. 2014;5:535.
20. Gawron-Burke C, Clewell DB. A transposon in Streptococcus faecalis with fertility properties. Nature. 1982 Nov 1;300(5889):281–4.
21. Hochhut B, Waldor MK. Site-specific integration of the conjugal Vibrio cholerae SXT element into prfC. Mol Microbiol. 1999 Apr;32(1):99–110.
22. Burrus V, Roussel Y, Decaris B, Guédon G. Characterization of a Novel Integrative Element, ICE *St1* , in the Lactic Acid Bacterium *Streptococcus thermophilus*. Appl Environ Microbiol. 2000 Apr;66(4):1749–53.
23. Burrus V, Pavlovic G, Decaris B, Guédon G. The ICESt1 element of Streptococcus thermophilus belongs to a large family of integrative and conjugative elements that exchange modules and change their specificity of integration. Plasmid. 2002 Sep;48(2):77–97.
24. Burrus V, Waldor MK. Control of SXT Integration and Excision. J Bacteriol. 2003 Sep;185(17):5045–54.
25. Wang H, Smith MCM, Mullany P. The Conjugative Transposon Tn *5397* Has a Strong Preference for Integration into Its *Clostridium difficile* Target Site. J Bacteriol. 2006 Jul;188(13):4871–8.
26. Santoro F, Romeo A, Pozzi G, Iannelli F. Excision and Circularization of Integrative Conjugative Element Tn5253 of Streptococcus pneumoniae. Front Microbiol. 2018 Jul 31;9:1779.
27. Provvedi R, Manganelli R, Pozzi G. Characterization of conjugative transposon Tn5251 of Streptococcus pneumoniae. FEMS Microbiol Lett. 1996 Jan 15;135(2–3):231–6.
28. Iannelli F, Santoro F, Oggioni MR, Pozzi G. Nucleotide sequence analysis of integrative conjugative element Tn5253 of Streptococcus pneumoniae. Antimicrob Agents Chemother. 2013/12/02 ed. 2014;58(2):1235–9.

29. Santoro F, Oggioni MR, Pozzi G, Iannelli F. Nucleotide sequence and functional analysis of the tet (M)-carrying conjugative transposon Tn5251 of Streptococcus pneumoniae: Tn5251 of Streptococcus pneumoniae. FEMS Microbiol Lett. 308(2):150–8.
30. Vijayakumar, Ayalew. Nucleotide sequence analysis of the termini and chromosomal locus involved in site-specific integration of the streptococcal conjugative transposon Tn5252. J Bacteriol. 1993;175(9). /
31. Croucher NJ, Walker D, Romero P, Lennard N, Paterson GK, Bason NC, et al. Role of conjugative elements in the evolution of the multidrug-resistant pandemic clone Streptococcus pneumoniaeSpain23F ST81. J Bacteriol. 2009 Mar;191(5):1480–9.
32. Henderson-Begg SK, Roberts AP, Hall LMC. Diversity of putative Tn5253-like elements in Streptococcus pneumoniae. Int J Antimicrob Agents. 2009 Apr;33(4):364–7.
33. Mingoia M, Tili E, Manso E, Varaldo PE, Montanari MP. Heterogeneity of Tn5253-like composite elements in clinical Streptococcus pneumoniae isolates. Antimicrob Agents Chemother. 2011 Apr;55(4):1453–9.
34. Croucher NJ, Harris SR, Fraser C, Quail MA, Burton J, van der Linden M, et al. Rapid pneumococcal evolution in response to clinical interventions. Science. 2011 Jan 28;331(6016):430–4.
35. Smith MD, Hazum S, Guild WR. Homology among tet determinants in conjugative elements of streptococci. J Bacteriol. 1981 Oct;148(1):232–40.
36. Dahmane N, Robert E, Deschamps J, Meylheuc T, Delorme C, Briandet R, et al. Impact of Cell Surface Molecules on Conjugative Transfer of the Integrative and Conjugative Element ICE *St3* of Streptococcus thermophilus. Appl Environ Microbiol. 2018;84(5).
37. Iannelli F, Santoro F, Fox V, Pozzi G. A Mating Procedure for Genetic Transfer of Integrative and Conjugative Elements (ICEs) of Streptococci and Enterococci. Methods Protoc. 2021 Sep;4(3):59.
38. Iannelli F, Chiavolini D, Ricci S, Oggioni MR, Pozzi G. Pneumococcal Surface Protein C Contributes to Sepsis Caused by *Streptococcus pneumoniae* in Mice. Infect Immun. 2004 May;72(5):3077–80.
39. Pearce BJ, Iannelli F, Pozzi G. Construction of new unencapsulated (rough) strains of Streptococcus pneumoniae. Res Microbiol. 2002;5.

Figure 1

A) Tn*5253 att*B variants in *S. pneumoniae*

B) Tn*5253 att*B variants in streptococci and enterococci

CHAPTER 10

Complete Genome Sequence of two *Mycobacterium chimaera* strains 850 and 852, isolated from an Heater-cooling units (HCUs) water reservoir

David Pinzauti, Stefano De Giorgi, Valeria Fox, Francesco Santoro, Francesco Iannelli, Susanna Ricci, Gianni Pozzi

Laboratory of Molecular Microbiology and Biotechnology,

Department of Medical Biotechnologies,

University of Siena, 53100 Siena, Italy

Manuscript in preparation

Abstract

Two *Mycobacterium chimaera* strains, 850 and 852, were isolated from heater-cooler units at the Hospital of Siena (Italy). Here we present their complete 6.28-Mb (1 chromosome plus 5 plasmids) and 6.45-Mb (1 chromosome and 5 plasmids) genomes, assembled using Nanopore and Illumina sequencing technologies for strain 850 and 852, respectively.

Announcement

Mycobacterium chimaera is a non-tuberculous mycobacterium belonging to the *Mycobacterium avium* complex (MAC)[1–3]. In recent years, *M. chimaera* infections in cardiothoracic surgery patients were related to the use of heater-cooler units (HCUs)[4–6]. Here we report the complete genomes of two *M. chimaera* strains, 850 and 852, isolated in 2017 at the hospital Le Scotte of Siena (Italy) during routine analysis of the HCU water reservoirs. The complete genome sequences of 850 and 852, were determined by combining Illumina and Nanopore sequencing technologies.

Strains were grown at 37°C on solid 7H11 medium (BD) for 5 days. Colonies were scraped from plate and resuspended in 7H9 medium. DNA extraction was performed as previously described[7]. Briefly, clumps were disrupted by vortexing for 1 minute with 20 glass beads (Ø 3mm, Sigma) and bacteria were inactivated for 3 hours at 85°C. Samples were centrifuged (4,000 x *g* for 20 minutes) and resuspended in 5 ml GTE buffer (50 mM Glucose, 25 mM Tris-HCl pH=8, 10 mM EDTA) with 10 mg/ml lysozyme and 0.4 g glass beads (Ø 150-212 µm, Sigma), vortexed for 2 minutes (Vortex Genie 2, Scientific Industries) and incubated at 37°C for 1 hour. Cells were lysed 1 hour at 55°C in 2% SDS and 1 mg/ml proteinase K. After the addition of NaCl and CTAB, the solution was incubated 10 minutes at 65°C, DNA was purified twice with an equal volume of chloroform:isoamyl alcohol (24:1, v:v), precipitated in 2 volumes of ethanol and resuspended in saline.

Three µg of DNA were size selected using 0.5x AMPure XP beads (Beckman Coulter).

Nanopore sequencing libraries were prepared using the SQK-LSK108 kit following Manufacturer's instructions (Oxford Nanopore Technologies, ONT). Sequencing run was managed by a GridION x5 device, enabling Guppy v5.0.12 (ONT) live basecalling (High Accuracy mode, quality threshold >9). Sequencing results were analysed with NanoPlot v1.38.0[8]. Illumina sequencing was performed at MicrobesNG (University of Birmingham) using NexteraXT library preparation kit followed by paired-end sequencing on an Illumina HiSeq 2500. Sequencing yields are reported in Table 1. Nanopore reads were filtered using Filtlong (v0.2.0) (https://github.com/rrwick/Filtlong) to exclude reads smaller than 1,000 bases (--min_length 1,000) and the worst 5% of reads (--keep_percent 95). Illumina reads were trimmed using Trimmomatic v0.30[9]. Genomes were *de novo* assembled with Flye v2.8.3[10] and polished with Medaka v1.4.1 (https://github.com/nanoporetech/medaka). A final Illumina-based polishing was performed with Pilon v1.2.4[11]. The genome of *M. chimaera* 852 was manually closed using Mauve v2.4.0[12] and Bandage v0.8.1[13] tools. Assembly quality was evaluated using Ideel (https://github.com/mw55309/ideel), and the genomes annotated with NCBI Prokaryotic Genome Annotation Pipeline (PGAP) v5.1[14]. Tools were run using default parameters, if not otherwise specified.

The genome of *M. chimaera* 850 consists of a 6,076,815-bp circular chromosome and 5 plasmids, while strain 852 consists of a 5,971,317-bp circular chromosome and 5 complete plasmids. Results are summarized in Table 1. Figure 1 represents similarities between the two genomes. A unique 300-kbp in length plasmid was reconstructed for M. chimaera 852 strain, harboring 26 supplementary tRNA genes. The *M. chimaera* 850 genome contains an Integrative Conjugative Element (ICE) which is absent in strain 852. This 147-kbp long element has 62.2% GC content and encodes for 168 ORFs, including a 94-kb operon putatively involved in degradation of polycyclic aromatic hydrocarbons.

Data availability

The complete genome sequences of 850 and 852 are assigned GenBank accession no. CP084592-97 and CP084586-91, respectively. The sequencing project is assigned NCBI BioProject accession no. PRJNA767558. Nanopore and Illumina sequencing reads are accessible under Sequence Read Archive accession no. SRR16127352 and SRR16127351 for 850, SRR16127350 and SRR16127349 for 852, respectively.

Acknowledgments

This was supported by the Italian Ministry of Education, University and Research (MIUR-Italy) under grant number 20177J5Y3P (call "Progetti di Ricerca di Rilevante Interesse Nazionale – Bando 2017"). The GridION x-5 was acquired through the "Excellence Departments" grant from MIUR to the Department of Medical Biotechnologies, University of Siena. Illumina genome sequencing was provided by MicrobesNG (http://www.microbesng.com) which is supported by the BBSRC (grant number BB/L024209/1).

Table1: *Mycobacterium chimaera* 850 and 852 whole genome sequencing results

Characteristics:		***Mycobacterium chimaera* 850**	***Mycobacterium chimaera* 852**
No. of reads (Illumina 2x250 bp)		1,572,298	974,771
No. of nucleotides (Illumina 2x250 bp)		335,350,687	213,336,547
No. of reads (Nanopore)		107,279	180,586
No. of nucleotides (Nanopore)		476,310,676	737,333,218
Read length N50 (Nanopore)		6,764	6,113
Chromosome Length (nt)		6,076,815	5,971,317
GC content (%)		67.6	67.73
No. of predicted CDS		5671	5564
No. of tRNAs		55	83*
Plasmid length (CDS/GC%)	1	97,267 (104/65.98%)	322,178 (473/64.57%)
	2	39,887 (32/65.0%)	95,688 (101/65.94%)
	3	32,137 (29/64.85)	26,921 (33/65.77%)
	4	21,123 (22/65.11%)	21,123 (22/65.11%)
	5	13,457 (18/65.77%)	15,917 (18/65.26%)
GenBank Accession Number		CP084592-97	CP084586-91
SRA Accession Number		SRR16127352, SRR16127351	SRR16127350, SRR16127349

*= 55 tRNAs chromosomally encoded and 28 tRNAs encoded by plasmid 1

FIGURE LEGEND

Figure 1. Similarities between *M. chimaera* 850 and 852 chromosomes.

Comparison between *M. chimaera* 850 and 852 (red ring) chromosomes. *M. chimaera* 850 chromosome was used as backbone of the image (black label). *M. chimaera* 852 homologous regions were reported at different % similarities, depending on red intensity regions (upper image legend features). GC Skew (green/purple) is reported. The image was generated using BRIG (BLAST Ring Image Generator, v. 0.95[15]).

References

1. Tortoli E, Rindi L, Garcia MJ, Chiaradonna P, Dei R, Garzelli C, Kroppenstedt RM, Lari N, Mattei R, Mariottini A, Mazzarelli G, Murcia MI, Nanetti A, Piccoli P, Scarparo C. Proposal to elevate the genetic variant MAC-A, included in the Mycobacterium avium complex, to species rank as Mycobacterium chimaera sp. nov. International Journal of Systematic and Evolutionary Microbiology. 2004 Jul 1;54(4):1277–85.
2. Gardy JL. Mycobacterium chimaera : unraveling a mystery through genomics. The Lancet Infectious Diseases. 2017 Oct;17(10):1004–5.
3. Henry R. Etymologia: Mycobacterium chimaera. Emerg Infect Dis. 2017 Mar;23(3):499–499.
4. Kohler P, Kuster SP, Bloemberg G, Schulthess B, Frank M, Tanner FC, Rössle M, Böni C, Falk V, Wilhelm MJ, Sommerstein R, Achermann Y, Ten Oever J, Debast SB, Wolfhagen MJHM, Brandon Bravo Bruinsma GJ, Vos MC, Bogers A, Serr A, Beyersdorf F, Sax H, Böttger EC, Weber R, van Ingen J, Wagner D, Hasse B. Healthcare-associated prosthetic heart valve, aortic vascular graft, and disseminated Mycobacterium chimaera infections subsequent to open heart surgery. Eur Heart J. 2015 Oct 21;36(40):2745–53.
5. Sax H, Bloemberg G, Hasse B, Sommerstein R, Kohler P, Achermann Y, Rössle M, Falk V, Kuster SP, Böttger EC, Weber R. Prolonged Outbreak of Mycobacterium chimaera Infection After Open-Chest Heart Surgery. Clinical Infectious Diseases. 2015 Jul 1;61(1):67–75.
6. Riccardi N, Monticelli J, Antonello RM, Luzzati R, Gabrielli M, Ferrarese M, Codecasa L, Di Bella S, Giacobbe DR. Mycobacterium chimaera infections: An update. Journal of Infection and Chemotherapy. 2020 Mar;26(3):199–205.
7. Santoro F, Guerrini V, Lazzeri E, Iannelli F, Pozzi G. Genomic polymorphisms in a Laboratory Isolate of Mycobacterium tuberculosis Reference Strain H37Rv (ATCC27294). New Microbiol. 2017 Jan;40(1):62–9.
8. De Coster W, D'Hert S, Schultz DT, Cruts M, Van Broeckhoven C. NanoPack: visualizing and processing long-read sequencing data. Berger B, editor. Bioinformatics. 2018 Aug 1;34(15):2666–9.
9. Bolger AM, Lohse M, Usadel B. Trimmomatic: a flexible trimmer for Illumina sequence data. Bioinformatics. 2014 Aug 1;30(15):2114–20.
10. Kolmogorov M, Yuan J, Lin Y, Pevzner PA. Assembly of long, error-prone reads using repeat graphs. Nat Biotechnol. 2019 May;37(5):540–6.
11. Walker BJ, Abeel T, Shea T, Priest M, Abouelliel A, Sakthikumar S, Cuomo CA, Zeng Q, Wortman J, Young SK, Earl AM. Pilon: an integrated tool for comprehensive microbial variant detection and genome assembly improvement. PLoS One. 2014;9(11):e112963.
12. Darling ACE. Mauve: Multiple Alignment of Conserved Genomic Sequence With Rearrangements. Genome Research. 2004 Jun 14;14(7):1394–403.
13. Wick RR, Schultz MB, Zobel J, Holt KE. Bandage: interactive visualization of *de novo* genome assemblies: Fig. 1. Bioinformatics. 2015 Oct 15;31(20):3350–2.
14. Tatusova T, DiCuccio M, Badretdin A, Chetvernin V, Nawrocki EP, Zaslavsky L, Lomsadze A, Pruitt KD, Borodovsky M, Ostell J. NCBI prokaryotic genome annotation pipeline. Nucleic Acids Res. 2016 Aug 19;44(14):6614–24.
15. Alikhan N-F, Petty NK, Ben Zakour NL, Beatson SA. BLAST Ring Image Generator (BRIG): simple prokaryote genome comparisons. BMC Genomics. 2011 Dec;12(1):402.

Figure 1.

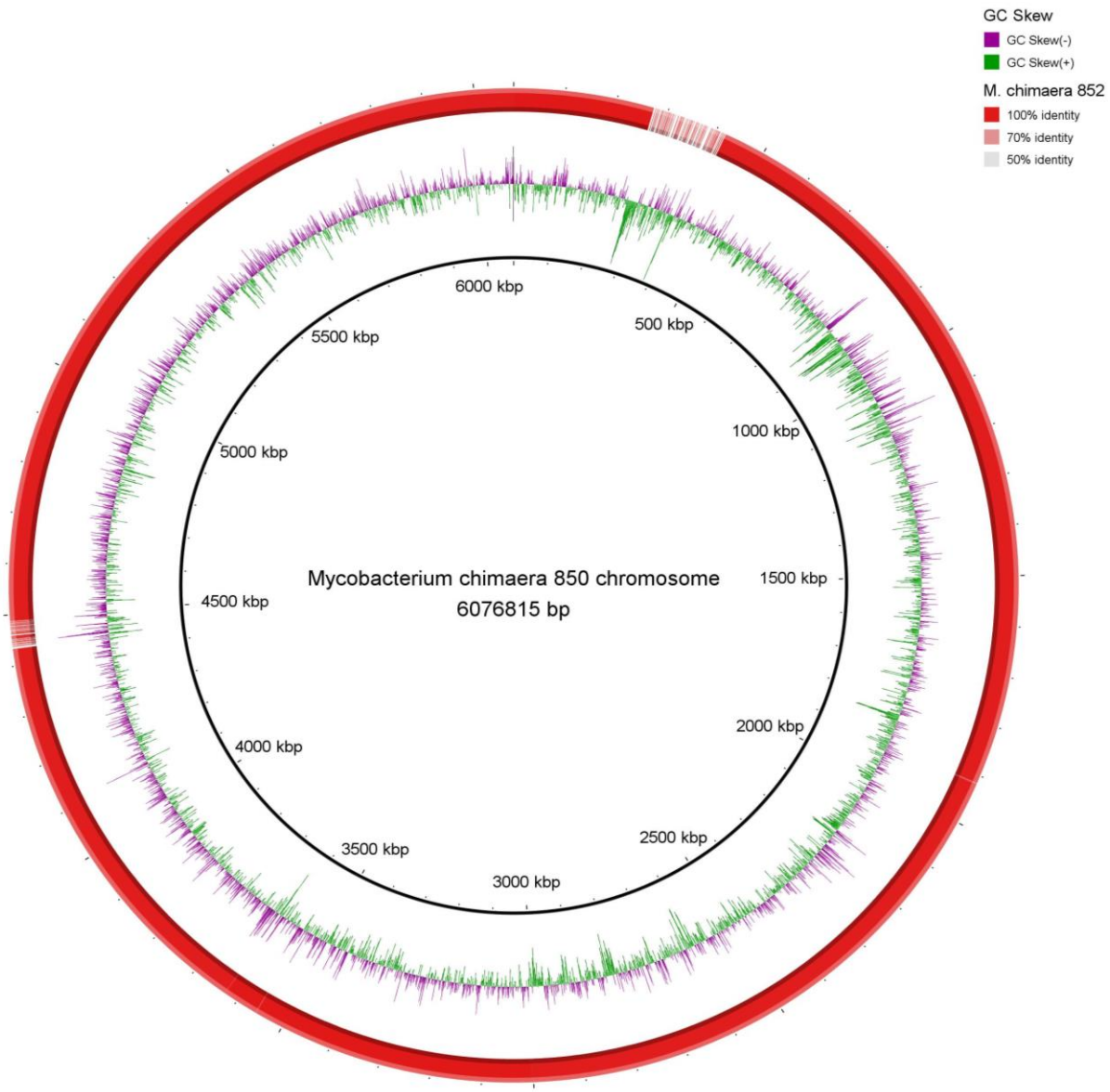
GC Skew
GC Skew(-)
GC Skew(+)
M. chimaera 852
100% identity
70% identity
50% identity
6000 kbp
500 kbp
1000 kbp
1500 kbp
2000 kbp
2500 kbp
3000 kbp
3500 kbp
4000 kbp
4500 kbp
5000 kbp
5500 kbp
Mycobacterium chimaera 850 chromosome
6076815 bp

CHAPTER 11 - General conclusions

Despite their essential role in prokaryotic evolution and biology, the knowledge of Mobile Genetic Elements is still scarce. The study of the MGEs is necessary to better understand their role in bacterial physiology, virulence and antimicrobial resistance spread in the bacterial community.

In this thesis, I studied mobile genetic elements and their involvement in different processes, including the response to stress conditions, the spread of antimicrobial resistance determinants and the metabolism of compounds. The main focus was on the characterization of *S. pyogenes* φ1207.3 prophage. It was demonstrated that the presence of the prophage in the *S. pneumoniae* chromosome not only leads to antibiotic resistance but is responsible for the activation of an SOS-like response, resulting in increased survival and in the temporary activation of a hypermutable phenotype. Transmission Electron Microscopy study of φ1207.3 revealed that is a functional bacteriophage of the Siphoviridae family, able to produce mature phage particles and able to transfer to other streptococcal species through a mechanism resembling conjugation. φ1207.3 phage particles are present on the bacterial surface 1000-times higher than in the bacterial supernatant, supporting the hypothesis that the transfer occurs through a mechanism similar to conjugation, dependent on cell-to-cell contact. I set up and implemented a mating protocol, which represents an efficient low cost and easy-to-perform procedure to transfer large mobile genetic elements. Compared to the classical filter mating protocol, this procedure allowed for higher transfer frequencies and the transfer of elements that could not be moved with the standard protocols. Furthermore, the chromosomal integration site of the pneumococcal ICE Tn*5253*, was carried out in *S. pneumoniae* strains of different backgrounds and in other streptococcal and enterococcal species. The clarification of the transfer and integration of Tn*5253* is of pivotal importance, as it contributes to the elucidation of the potential of Tn*5253* horizontal gene transfer among different bacterial species. Finally, I determined the whole genome sequence of *S. pneumoniae* Rx1 strain, a common laboratory strain devoid of the Mismatch Repair System, and of its parental strain R36A to track genome evolution. The genome

sequence of two *Mycobacterium chimaera* strains was also determined. One of these strains was found to carry an ICE, which contains genes putatively implicated in the catabolism of polycyclic aromatic hydrocarbons, important environmental pollutants. Further analysis and engineering of this ICE will be needed to assess its possible role as a valid strategy for bioremediation processes.

APPENDIX - Scientific Curriculum Vitae

- **Education and work experience**
  - October 2018 - present : **PhD student** in the XXXIV cycle of doctoral program in Medical Biotechnology by the Medical Biotechnologies Department of the University of Siena. Research activities on Mobile Genetic Elements in the laboratory of Molecular Microbiology and Medical Biotechnologies
  - January - April 2020 : **Visiting PhD student** by the Departamento de Microbiología, Facultad de Medicina, Universidad de Sevilla, Sevilla, Spain. Research activity under the project entitled 'Evaluation of the impact of *S. pyogenes* prophage φ1207.3 on SOS-response and genome evolution'
  - October 2017 - September 2018 : **Research fellowship** by the Laboratory of Molecular Microbiology and Medical Biotechnologies (LAMMB), Department of Medical Biotechnologies, University of Siena. Research activities within the project named 'Identification of disease and immunity biomarkers through transcriptome analysis'
  - September 2015 - July 2017 : **Master's degree** in Medical Biotechnologies (courses held in English): Department of Medical Biotechnologies of the University of Siena. Thesis title 'Immune detection of bacteriophage Φ1207.3 Major Capsid Protein', 110/110 cum laude
  - September 2011 - February 2015 : **Bachelor's degree** in Biotechnology: Centre for integrative biology (CIBIO) of the University of Trento. Thesis title 'Diffusion of carbapenemase-producing bacteria in Trentino region: epidemiology and phenotypic and genotyping methods of detection', 101/110

- **Training courses**

- May 2019 : '**ALMALE** - (2018DU0092) Tuscan Start-Up Academy 4.0' - University of Siena, organized by Regione Toscana. Introductory training course on Machine Learning algorithms.
- October 2018 : '**Fluorescence microscopy** – FluoMicro@ICGEB' - ICGEB Trieste. Course on fluorescence microscopy and live imaging technologies

- **Additional information**

  -(2019-2021) I have collaborated in the teaching activities of the "Advanced bacterial genetics" course held during the first year of the Master course in Medical Biotechnologies at the University of Siena.

  - I have supervised several students during their lab internship and was thesis co-advisor for Bachelor course in Biotechnology, Master course in Medical Biotechnologies and Master course in Biology.

- **Languages**
  - **Italian:** native
  - **English:** excellent knowledge (written and spoken). 2011, Certificate in Advanced English (CAE) Cambridge University – European level **C1**
  - **German:** good (written) and sufficient (spoken) knowledge. 2011, Goethe Zertifikat, Goethe Institut – European level B1
  - **Spanish:** sufficient knowledge (written and spoken)

- **List of pubblications**
  - A Mating Procedure for Genetic Transfer of Integrative and Conjugative Elements (ICEs) of Streptococci and Enterococci. Methods Protoc. 2021, 4, 59. https://doi.org/10.3390/mps4030059 Iannelli, F., Santoro, F., **Fox, V.,** Pozzi, G.

- Disbalancing Envelope Stress Responses as a Strategy for Sensitization of Escherichia coli to Antimicrobial Agents. Front Microbiol. 2021 Apr 7;12:653479. doi: 10.3389/fmicb.2021.653479. PMID: 33897667; PMCID: PMC8058218. Recacha E., **Fox V.**, Díaz-Díaz S., García-Duque A., Docobo-Pérez F., Pascual Á., Rodríguez-Martínez J.M.

- **Conferences**
  - 2021, 49° Congresso Nazionale SIM (Società Italiana di Microbiologia), virtual conference. The *mef*(A)/*msr*(D)-carrying prophage φ1207.3 encodes an SOS-like system responsible for both increased survival and antibiotic resistance mutation rates in *Streptococcus pneumoniae.* Fox V., Santoro F., Díaz-Díaz S., Iannelli F., Rodríguez Martínez J.M.,Pozzi G. **Poster**
  - 2021, 31st ECCMID (European Congress of Clinical Microbiology and Infectious Diseases), virtual conference. The *mef*(A)/*msr*(D)-carrying prophage φ1207.3 encodes an SOS-like system induced by UV-C light and responsible for increased survival and antibiotic resistance mutation rates in *Streptococcus pneumoniae.* Fox V., Santoro F., Díaz-Díaz S., Iannelli F., Rodríguez Martínez J.M.,Pozzi G. **Poster**
  - 2019, 47° Congresso Nazionale SIM (Società Italiana di Microbiologia), Roma. Construction and characterization of Major Capsid Protein and Major Tail Protein deletion mutants of *Streptococcus pyogenes* phi1207.3 phage. Fox V., Pastore G., Iannelli F., Santoro F., Pozzi G. **Poster**
  - 2019, XXXIII Congresso SIMGBM (Società italiana di Microbiologia Generale e Biotecnologie Microbiche), Firenze. Construction and characterization of Major Capsid Protein and Major Tail Protein deletion mutants of phage φ1207.3. Fox V., Pastore G., Iannelli F., Santoro F., Pozzi G. **Poster**

- 2018, 28th ECCMID (European Congress of Clinical Microbiology and Infectious Diseases), Madrid. The genetic element Φ1207.3 carrying macrolide efflux genes *mef(*A) and *msr*(D) in *Streptococcus pyogenes* is the first example of a functional bacteriophage transferring drug resistance among Streptococci. Santoro F., Pastore G., **Fox V**., Iannelli F., Pozzi G. **Poster**

- **Awards**
  - 2021, best poster within the topic 'Resistenza agli antimicrobici, sorveglianza e test di sensibilità' at the 49° Congresso Nazionale SIM (Società Italiana di Microbiologia) - Miglior poster sessione
  - 2021, travel grant at the 31st ECCMID (European Congress of Clinical Microbiology and Infectious Diseases)